

Caledonian deformation in the Oslo Region, updating the regional tectonic model

A MSc thesis in Geoscience
11th December 2015

Joost van den Broek



Supervised by:

Prof. Dr. Roy H. Gabrielsen (University of Oslo)

Prof. Dr. Dimitrios Sokoutis (Univeristy of Utrecht)

Dr. Bjørn Larsen (Det Norkse oljeselskap ASA)



Universiteit Utrecht



UiO • **University of Oslo**



DET NORSKE

Cover: Panoramic view of the Ringerike district above Sundvollen, Norway.
Photograph by Martijn Vlieg (2014)

Abstract

Tectonically the Oslo Region is part of the Osen-Røa nappe which is the most external part of the Scandinavian Caledonides. The region extends roughly 100 km north and south of the city of Oslo, Norway, and contains a roughly 2000 m thick Lower Paleozoic sedimentary of shales and limestones. The proportion of competent units increases up stratigraphy culminating in the very competent Ringerike Group. Contrasting structural styles due present in the stratigraphy lead to discrepancies in shortening experienced by the Cambrian to Lower-Ordovician strata and the Middle-Ordovician to Silurian sediments. A layer parallel detachment to account for this discrepancy was postulated by Morley (1987a).

The entire region is underlain by the Osen-Røa basal thrust which, is constricted to the Alum Shale Formation. This study focusses on structures of this Osen-Røa thrust in the Hønefoss area. A detailed description of structures and southward directed transport direction of the Osen-Røa basal thrust in the Hønefoss area are presented. Combining and analysing the structural data gathered in the Hønefoss area with previously published structural data, a very homogeneous regional transport direction towards the SE is found.

In order to gain insight into the mechanical parameters controlling the localization of deformation, stress transfer up stratigraphy and their influence on structural style analogue models where utilized. Results are mainly applied to large thrust splaying from the Osen-Røa thrust which cut the entire stratigraphic succession. It is concluded, based on modelling results, that the structural style of such large faults is controlled by effective lateral competence contrasts.

By using data from various sources, the regional tectonic model initially presented by Bruton et al. (2010) is updated to include a layer parallel detachment in the Ordovician strata and involvement of basement in the Osen-Røa basal thrust.

Acknowledgements

The completion of this MSc. thesis would not have been possible were it not for the help and guidance from many people.

First of all, I would like to express my deep gratitude to Prof. Roy Gabrielsen for the subject of this thesis, his continuous support, guidance and patience, both in the field and during the writing process. I benefited greatly from his knowledge and enthusiasm.

I would also like express my deep gratitude my field partners, Martijn Vlieg, Martijn Weekenstroo and Arne Verdonk, for their cooperation during the analogue modelling study and their very pleasant company and invaluable help during the fieldwork and afterwards. The realization of this thesis would not have been possible without them.

Supervision and guidance in the field by Bjørn Larsen was also very much appreciated and this research benefited greatly from his vast field experience and extensive knowledge on geology of the Oslo Region. Many thanks also to Det Norske oljeselskap ASA for providing the financial support which made the fieldwork possible

Various forms of support from the many people at the Tectonics group at Utrecht University was greatly appreciated. Specifically, many thanks are expressed to Dimitrios Sokoutis for his help during the analogue modelling study and the writing process.

Finally, I would like to express my deep gratitude to Lisa de Ruiter for her support and patience during the writing period and her critical but very constructive review of this manuscript.

Joost van den Broek

Utrecht, December 2015

Table of content

1	Introduction	5
1.1	Tectonic setting of the Scandinavian Caledonides and the Oslo Region	6
1.2	Lithostratigraphy in the study area	13
2	The Hønefoss area, a field perspective	16
2.1	Field methodology.....	16
2.2	Field observations	17
2.2.1	Viul locality	17
2.2.2	Road section, south of Klækken	26
2.2.3	Ringkollen section.....	28
3	Analogue modelling.....	32
3.1	Outstanding issues in the Oslo region.....	32
3.2	Analogue modelling methodology	33
3.2.1	Aim and limitations.....	33
3.2.2	Experimental setup and procedure	34
3.2.3	Materials and scaling.....	35
3.2.4	Variation of parameters	38
3.2.5	Construction and strength profiles.....	38
3.3	Modelling results.....	38
3.3.1	Model 1 (Figure 3.4)	39
3.3.2	Model 2 (Figure 3.5)	40
3.3.3	Model 3 (Figure 3.6)	41
3.3.4	Model 4 (Figure 3.7)	42
3.3.5	Model 5 (Figure 3.8)	43
3.3.6	Summary of modelling results.....	44
3.4	Initial discussion of modelling results – similarities with nature	45
4	Discussion	48
4.1	The Osen-Røa thrust.....	49
4.2	Regional synthesis	51
4.2.1	Structural data.....	51
4.2.2	Regional tectonic model.....	54
4.3	Influence of lateral and stratigraphical shortening variations on structural style.....	57
4.3.1	Insights from analogue models	57
4.3.2	Variable deformation style in the field.....	59
4.4	Updating the existing tectonic model	62
5	Conclusions	64
6	References	65
	Appendix A	
	Appendix B	

1 Introduction

Stretching over 1800 km in length, covering most of Norway from Finnmark to Stavanger as well as north western Finland and western Sweden, the Scandinavian Caledonides is the major orogen in Scandinavia. It is the result of the oblique collision between Baltica and Laurentia during Paleozoic times. The tecto-metamorphic history of the allochthonous napes of internal of the Scandinavian Caledonides have been the focus of many researchers for some time. However, the more outlying areas have not been studied this extensively. Just as any orogen, the Caledonian orogen created foreland basins due to loading of the lithosphere. As the basin is filled in with sediments, subsequent deformation of the Caledonian orogen spread outward reaching the foreland basins creating a thin skinned fold and thrust belt in the Paleozoic sediments. One of these Caledonian foreland basins is located in the Oslo Region, stretching about 100 km north and south of the city Oslo, Norway (Figure 1.1). It is located in a 40-70 km wide, downfaulted, Permian graben which protected the Paleozoic sediments now exposed on the shoulders of this graben.

The Oslo Region is a classical area in terms of research, with studies taking place as early as the 19th century (Brøgger, 1882; Kjerulf, 1879, 1873, 1855; Murchison, 1847). Kjerulf recognised contractional deformation in the form of faults ('mirror planes') and associated folding. Brøgger (1882) linked the Oslo Region to the Caledonian deformation, correlated folds and thrusts and deduced a transport direction towards the SSE. After these initial studies Størmer (1934) conducted excellent research in the Oslo Region providing a basis for modern structural studies conducted in the 1980s, during this time the Oslo Region was placed in the context of the Caledonian Orogen (Bockelie and Nystuen, 1985; Harper and Owen, 1983; Morley, 1987a, 1987b, 1986a, 1986b; Nystuen, 1983, 1981; Ramberg and

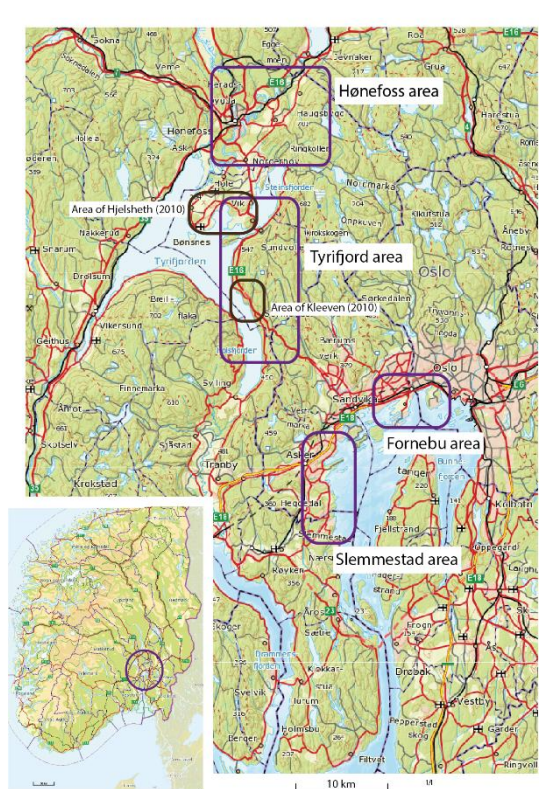


Figure 1.1: Map of the Oslo Region displaying the various districts which have been recently investigated by several authors. The field observations presented in this study are from the Hønefoss area in the north. Inset map shows the position of the Oslo Region with respect to southern Norway.

Bockelie, 1981). In 2010, a paper by (Bruton et al., 2010) provided a detailed overview of the Oslo Region, presented new data and updated the regional tectonic model (Figure 1.6). Thus, although recently research into the Oslo Region has been done, sufficiently detailed structural data and descriptions are still lacking. In order to address this deficiency, a project focusing on the entire Oslo region has been carried out. Three other authors, Vlieg (2015), Weekenstroo (2015) and Verdonk, (2015) have investigated the Tyrifjord, Slemmestad and Bygdoy areas) respectively (Figure 1.1). The overall aim of this project is to provide a better description of the Caledonian deformation in the Oslo region in terms of structural style and deformation history. Vlieg (2015) focusses on the significance of observed backthrusting as well as strain intensity variations. His area is closely linked to the focus area of this study as his northern boundary is the southern boundary of this study. The study near the city of Slemmestad, carried out by Weekenstroo (2015) is focused on the differences in structural style by investigating transport

directions and strain intensity variations. Verdonk (2015) studied the area near the village of Bygdoy and focusses on the structural style of the strata, their mechanical parameters and the role of different generations of veining in light of the Caledonian deformation. Both of the latter studies are carried out closer to the deformation front near the edge of the Caledonian foreland basin.

This study focusses on the Caledonian deformation of the Oslo Region with an initial focus on the Hønefoss area. Specifically, the Osen-Røa basal thrust system itself and faults splaying of the basal thrust system will be investigated. This will be done by providing a detailed description on the structural style and analysis of observed transport directions. An analogue modelling study is also done to gain insight into the mechanical parameters controlling the localisation of deformation, stress transfer and up stratigraphy and their influence on the structural style. Combining these observations with data and observations made from other recent studies and using the tectonic model from Burton et al. (2010) as a framework, a regional tectonic model will be constructed. This model will then be utilised to provide insights into lateral and stratigraphical variations in structural style and amount of shortening observed. Finally, by utilizing all gathered data the regional tectonic model of Bruton et al. (2010) will be updated with new insights.

1.1 Tectonic setting of the Scandinavian Caledonides and the Oslo Region

During Cambrian times, Baltica, which included the terranes which would make up the Scandinavian Caledonides, together with most of the landmass on the planet, was located on the southern hemisphere (Figure 1.2). Only the northern part of China is thought to have been north of the equator (Cocks and Torsvik, 2005, 2002). Models for the plate tectonic evolution of Baltica and Laurentia during these times are somewhat controversial. (Torsvik and Rehnström, 2001) propose a model where Baltica was inverted with the present day northern margin facing the south pole. During Ordovician and Silurian times, a rapid northward drift (4-7 cm/yr) and a counter clockwise rotation of a total of $\sim 160^\circ$ is proposed. However, such a large rotation of a continent should have left evidence. But there is no indication of an ocean opening or closing anywhere near Baltica at that time. Combined with the

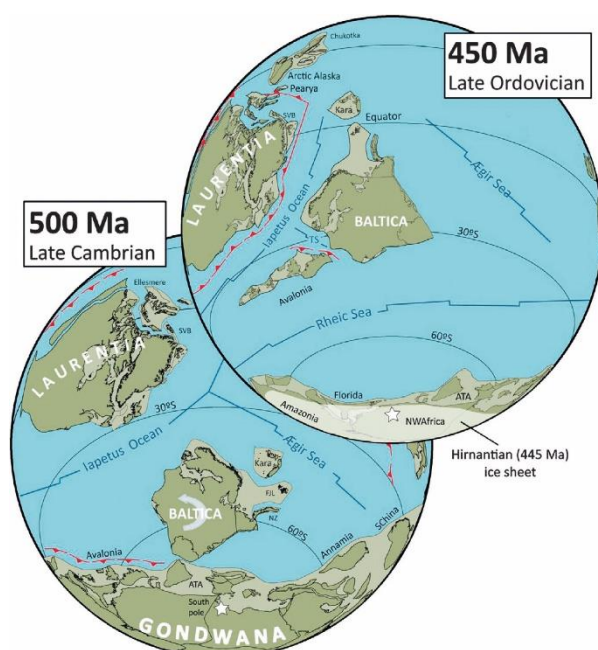


Figure 1.2: Plate tectonic setting of Baltica in the Late Cambrian (bottom left) and Late Ordovician (upper right). Figure from Torsvik et al. (2012).

fact that reliable paleomagnetic data for this time is limited, the model by (Torsvik and Rehnström, 2001) is still considered to be controversial and shall not be accepted as the plate tectonic model for this thesis.

However, regardless of how the continents have been translated during Cambrian – Silurian times, the fact of the matter is that the Iapetus Ocean closed during Silurian times, resulting in the formation and subsequent translation and deformation of the nappes of the Caledonian orogeny (Hossack and Cooper, 1986; Roberts, 2003). Final nappe movement in the core of the orogen ceased around Silurian to Early Devonian time (Roberts, 2003), but deformation in the foreland is likely to have continued (Bockelie and Nystuen, 1985; Hossack and Cooper, 1986). The obliquity of the convergence resulted in a

significant amount of orogen parallel shear as well as thrust sheets with an oblique movement sense (Hossack and Cooper, 1986).

As a result of this convergence, passive margin and shelf sediments of the Baltoscandian margin, as well as oceanic and arc terrains derived from the Iapetus Ocean were transported eastward and emplaced on the Fennoscandian Shield (Archaean and Proterozoic crystalline rocks; Roberts, 2003). This led to the characteristic tectonostratigraphy consisting of Lower, Middle, Upper and Uppermost Allochthons (Figure 1.3). These nappes were involved in translations of up to several hundreds of kilometres (Roberts, 2003; Roberts and Gee, 1985). Below the Lower Allochthon, black and grey shales of Middle to Upper Cambrian age were activated as a decollement surface (Roberts and Gee, 1985). These sediments, together with some involved basement, form the para-autochthonous tectonic unit in the Caledonian system (Figure 1.3).

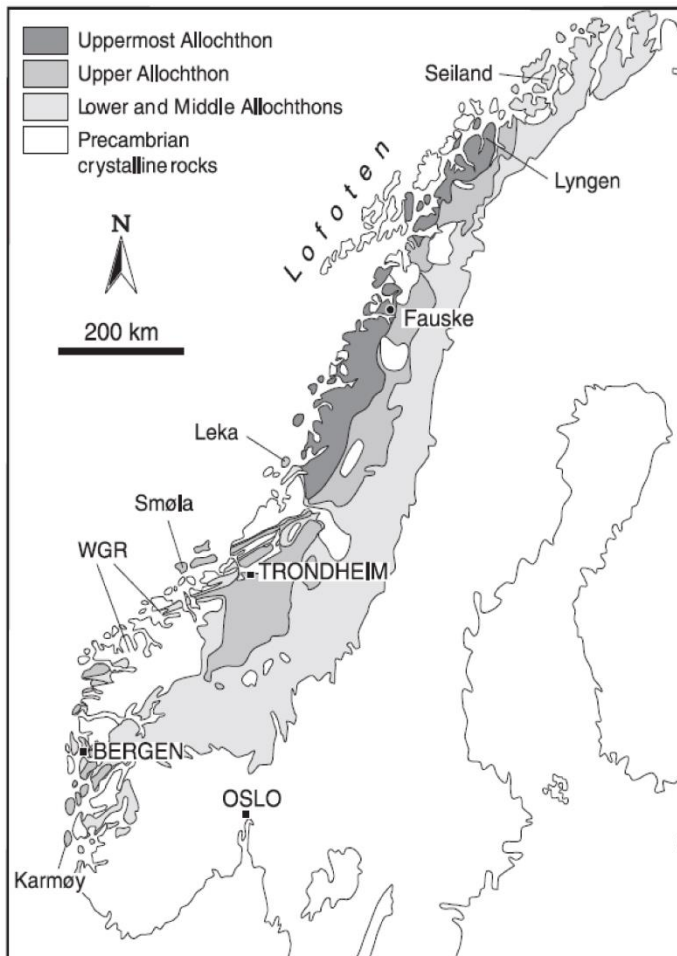


Figure 1.3: Simplified tectonostratigraphic map displaying the various nappes of the Scandinavian Caledonian Orogen. Figure from Roberts (2003).

At present there are four main orogenic phases recognised in the Norwegian part of the Caledonian orogen, the *Finnmarkian*, *Trondheim*, *Taconian* and *Scandian* events. They are followed by a phase of late stage orogenic collapse, partly associated with orogen-parallel sinistral shear (Roberts, 2003). The *Scandian* event is the result of oblique collision of Baltica and Laurentia, taking place roughly during Silurian times, involved all principal Allochthons and is responsible for their present day distribution (Gee, 1975). Timing of the event varies spatially due to the diachroneity arising from the oblique convergence. Deformation at one locality was likely very intense and short lived (Terry et al., 2000). Late-stage extensional deformation as a result of gravitational collapse of the Caledonian orogen and can be divided into two phases. The first phase took place during Early to Mid-Devonian times (Roberts, 2003 and references therein), when major low angle detachments with a top to W or SW sense of shear and ductile, sinistral shear along vertical faults extended the Caledonian orogen (Roberts, 2003). During this extension, the foreland and lower crust were still being affected by contractional deformation (Fossen and Dallmeyer, 1998; Fossen and Dunlap, 1998) (Figure 1.4). During Late Devonian to

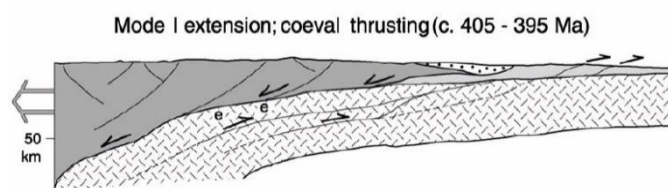


Figure 1.4: Simplified WNW - ESE profile depicting the initial stage of orogenic collapse and backsliding (Mode I extension of Fossen), with coeval Devonian molasses sedimentation (dotted ornament) and contractional deformation at depth and farther east in the

Carboniferous, there was extensional reactivation in the brittle regime as well as open folding with a roughly E-W trend. For more details regarding the principal orogenic events responsible for the formation of the Scandinavian Caledonides the reader is referred to Roberts (2003) and references therein.

The Oslo region

Consisting of a region of roughly 10.000 km², the Oslo region, in geological terms, extends some 115 km north and south of the city of Oslo and varies in width from 40-70 km (Figure 1.1) (Bruton et al., 2010). Stratigraphically, the Oslo region contains a lower Palaeozoic sedimentary succession of roughly 2000 to locally 4000 m thick (Bockelie and Nystuen, 1985; Bruton et al., 2010; Larsen and Olausen, 2005) which is exposed on the shoulders of the overlying volcanics which have a Carboniferous to Permian age. Marine conditions prevailed in the area until Late-Ordovician to Silurian times, when the growing Caledonides led to an increased clastic input from the (present day) north. As such, basin infill can be, schematically, divided into four major events (Larsen and Olausen, 2005):

- A shallow southward transgressing sea, from Early to Middle Cambrian.
- Typical epicontinental sea environment (low sedimentation rate) from Late Cambrian to Middle Ordovician.
- Shallow marine warm water carbonates and the onset of foreland basin sediments (silt- and sandstones) from Late-Ordovician to Middle Silurian.
- Basin fill by alluvial foreland sediments during late Silurian.

From this sequence it becomes clear that the sedimentary evolution over time was that of an epicontinental sea (slowly) evolving into a foreland basin of the Caledonian Orogeny (Larsen and Olausen, 2005).

Structurally the Oslo Region is situated in the lower allochthon nappe of the Caledonian orogen, in the Osen part of the Osen-Røa nappe complex (Nystuen, 1981) and has been affected by the *Scandian* deformation phase (Nystuen, 1981). Estimates of the total distance of nappe displacement over the Osen-Røa thrust vary between 100 km (Morley, 1986a) to 200 to 400 km (Nystuen, 1981) and is still a matter of conjecture in literature. It is clear however, that deformation continued after main nappe movement ceased, as evidenced by contractional deformation in Devonian times (Larsen and Olausen, 2005; Størmer, 1934). Subsequent large scale deformation of the Oslo region during the Late Carboniferous to Early Permian was the result of lithospheric stretching above the Tornquist fault zone. It is related to the final phase of the Variscan orogeny. The resulting rift is asymmetric with a polarity switch along a large strike slip fault located near Sundvollen. In the south, there is an east dipping half graben (Vestvold Graben), whereas in the north the half graben is dipping towards the west (Akershus Graben). The prolonged phase of extensional faulting and volcanism resulted in the emplacement of and intrusion of large volumes of multiple types of igneous rocks with varying compositions, all related to this rifting phase (Larsen et al., 2008). Volcanic activity ceased in the Early Triassic with the emplacement of major batholiths.

Traditionally the Caledonian thrust front is placed in Mjøsa (Figure 1.5) along a line separating the 'old' Osen-Røa nappe to the north from the folded Cambro-Silurian sequence to the south (Morley, 1986a; Nystuen, 1981) and the Cambro-Silurian sequence was thus considered a para-autochthonous unit. However, studies by (Oftedahl, 1943) and (Morley, 1986a; Oftedahl, 1943) realised that the thrust front has to be located at the limit of deformed strata in the Oslo Region. This extended the Caledonian deformation front to include the lower Paleozoic succession in the Oslo Region and the thrust front

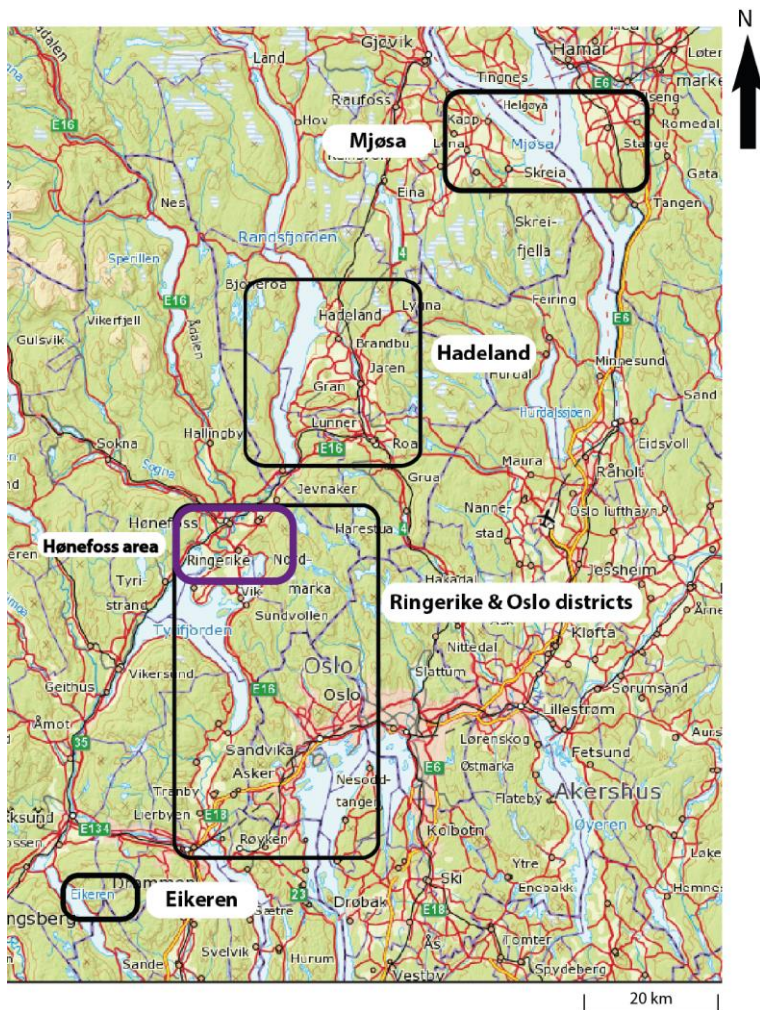


Figure 1.5: Map displaying the geographical relationships between various districts in relation to the Oslo Region. Position with respect to Norway can be inferred from Figure 1.1.

today is positioned in a buried thrust front north of Langesund (Bruton et al., 2010; Morley, 1987a, 1986a). Based on these conclusion, Morley (1986a) argued that the term ‘para-autochthonous’ to describe the structures in the Oslo Region is to be discontinued.

The region is situated in the external frontal zone of the Caledonian nappe system and the structures in the Oslo Region are characteristic of such a system. The region contains a pronounced basal thrust system, the Osen-Røa thrust, over which the entire region is displaced and from which faults and ramps splay up stratigraphy (Bruton et al., 2010; Morley, 1986b; Nystuen, 1983). In the northern Mjøsa district the Osen-Røa thrust is situated in Cambrian shales and phyllites and sometimes on basement or quartzites (Nystuen, 1983). Towards the south of the Mjøsa district it cuts up stratigraphically

into the Alum Shale Formation. The Osen-Røa thrust is then consequently positioned in the Alum Shale where it forms the ductile decollement of the Oslo Region (Bruton et al., 2010; Morley, 1986a, 1986b; Nystuen, 1983). Structural styles of the overlying strata are variable both laterally from north to south and stratigraphically (Morley, 1987a). Cambrian to Lower-Ordovician strata is deformed by closely space imbricates in the north and triangle, pop-up and imbricate zones in the south whereas Mid-Ordovician to Silurian rocks are mostly deformed by buckle folding and display significantly less lateral variation in structural style (Morley, 1987a). Morley (1986a; 1987a) postulated that these different structural styles are due to an increase in the proportion of competent units when going up stratigraphy and that the stratigraphy thus has strong control on the vertical changes in deformation style. Lateral changes in deformation style for the Cambrian to Lower-Ordovician are explained by Morley (1987a) to be related to a lateral increase in competent Lower-Ordovician beds. It is also observed in the Asker-Slemmestad area, where a section displaying Silurian strata in the north and Cambrian Alum Shales in the south, shows clear variations in structural style (Figure 3.12) (Weekenstroo, 2015).

These contrasting structural styles of the Cambrian to Lower-Ordovician and the Mid-Ordovician to Silurian strata are also observed in Hadeland (Figure 1.5) (Morley, 1987b) and in the Ringerike district (Harper and Owen, 1983). In the Ringerike district the style change is very clear across the Klækken

fault where it changes from closely spaced imbricate thrust slices north of the Klækken fault to weakly deformed folds and minor faulting (Morley, 1987a; Harper and Owen, 1983). Also, the amount of shortening markedly decreases on a local level to 20% whereas north of the Klækken fault it is about 50% (Figure 4.9) (Morley, 1987a). The Klækken fault splays from the Osen-Røa thrust and cuts up through the entire stratigraphy having experienced at least 5 km of horizontal displacement (Harper and Owen, 1983; Morley, 1987a; Størmer, 1934).

These stratigraphical contrasting in structural styles also result in a discrepancy in the amount of shortening between the Cambrian to Lower-Ordovician and the Middle-Ordovician to Silurian strata (Table 4.1) (Morley, 1987a). In order to accommodate for this, Morley (1987a; 1986a) postulated that the remainder of the shortening was taken up by a single or multiple layer parallel detachments present somewhere in a weak part of the Ordovician sequence. The decline in the Silurian sequence is only visible in the southern part of the Oslo Region. This led Morley (1987a) to conclude that the roughly 30 km to the north of the thrust front have been deformed as single units.

The general transport direction in the Oslo Region has been determined to be SE to S directed with local variation with top to the ENE and top to the NW-WNW directed transport (Bruton et al., 2010; Hjelseth, 2010; Kleven, 2010; Morley, 1987b; Vlieg, 2015; Weekenstroom, 2015). Exact mechanisms for most of these local variations in transport direction are unclear at this time. However, the top to NW-WNW directed thrusting is found to be related to backthrusting. Recent studies have determined that this backthrusting, especially in the Silurian strata of the Tyrifjord area, is much more dominant than previously thought (Hjelseth, 2010; Kleven, 2010; Vlieg, 2015).

Hjelseth (2010) studied the structures in the lower Silurian east of Sundvollen with a focus on this backthrusting (Figure 1.1). The study found four separate deformation phases; the first phase is associated with bedding-parallel shortening. The second phase is linked to tight to isoclinal disharmonic folding with upright axial planes. Foreland directed thrust faults and large, open folds with hundred meter wavelengths are associated with the third deformation phase. Phase four is dominated by low angle back-thrusting and fault-propagation-folds. A transport direction for the faults of N-NNW found in the southern part of the area and WNW-NW in the northern part (Hjelseth, 2010). It is observed that these back-thrusts are the most dominant form of faulting in outcrops. A general gentle style of deformation in the upper part of the Cambro-Silurian stratigraphy, characterised by large open folding is observed and consistent with earlier work (Morley, 1987a). Hjelseth links all of the four different deformation phases to the Scandian deformation phase of Roberts (2003) due to the presence of the structures in Lower Silurian strata.

Situated in the Tyrifjord area, the area studied by Kleven (2010) is partly overlapping with the study area of Vlieg (2015) (Figure 1.1). This study focused on geometry and kinematics of the Caledonian structural development of the Silurian section at Sønstrud, Holsfjorden, Ringerike. A special emphasis was placed on backthrusting (Kleven, 2010). The study posts the hypothesis that regionally significant out-of-sequence backthrusting occurred in the Ringerike area during the last part of the Scandian deformation stage of the Caledonian orogeny. (Kleven, 2010) also observed four deformation phases; the first where tensile fractures resulting from sedimentary loading during burial. This was followed by bedding parallel shortening accommodated by thrust sub-parallel to the bedding as well as stylolites. The maximum compressive stress was oriented NNW-SSE to ENE-WSW. Subsequent foreland directed thrusting resulted in thrusts, ramps and folds on multiple scales (Kleven, 2010). Maximum stress was oriented NW-SE. The final deformation phase observed resulted in backthrusting, with a subdivision being made for low-angle and high-angle hinterland directed backthrusting. Kleven (2010) interprets the high angle back-thrusts as being younger than the low angle back-thrusts. The study is unclear as

to what the generation mechanisms for these back-thrust is, it does conclude that the back-thrusting is much more common than previously reported and has likely formed roughly simultaneous to the foreland directed thrusting.

The Tyrifjord area contains mainly Silurian strata and the deformation of the upper part, just below the Ringerike Sandstone, is characterized by fold trains with large wavelength-amplitude ratios (Vlieg, 2015). When going down in stratigraphy, the intensity of deformation increases as backthrusts are visible and folding increases in intensity. The area also contains a strongly deformed section at Ustranda where a pop-up structure cuts the Ringerike Sandstone Formation. This pop-up is characterized by strong deformation in the form of (ductile) folding, fault propagation folding and faulting (Vlieg, 2015).

Recent regional tectonic model

Bruton et al. (2010) organised the existing structural and paleontological data and provided new interpretations on the structures in the lower Palaeozoic succession of the region. They produced a general structural synthesis of the region and argued that the area be divided into four structural subareas/levels (Figure 1.6). The lowest level present is the basal thrust level, it is restricted to the Alum Shale Formation where it is characterised by duplexes and associated asymmetric folding on wavelengths of 100-300m (Bruton et al., 2010) (Figure 1.6). At several localities, the Alum shale has been intruded by mica syenite sills, which are dated at 310-298 Ma (B. Larrsen, *pers. Comm. 2014*). The middle thrust system is characterised by structures which vary in size by several orders of magnitude (Figure 1.6). Bruton et al. (2010) argued that this structural level consisted mainly of ramp flat ramp structures which transfer deformation up stratigraphy. Zones of almost undeformed strata are separated by small areas showing significant deformation. Wavelengths of first order structures are in the order of 100-500 m and amplitudes are around 50-100m (Bruton et al., 2010). Structures in the third structural level are dominated by the very competent Ringerike sandstone (Figure 1.6). Below

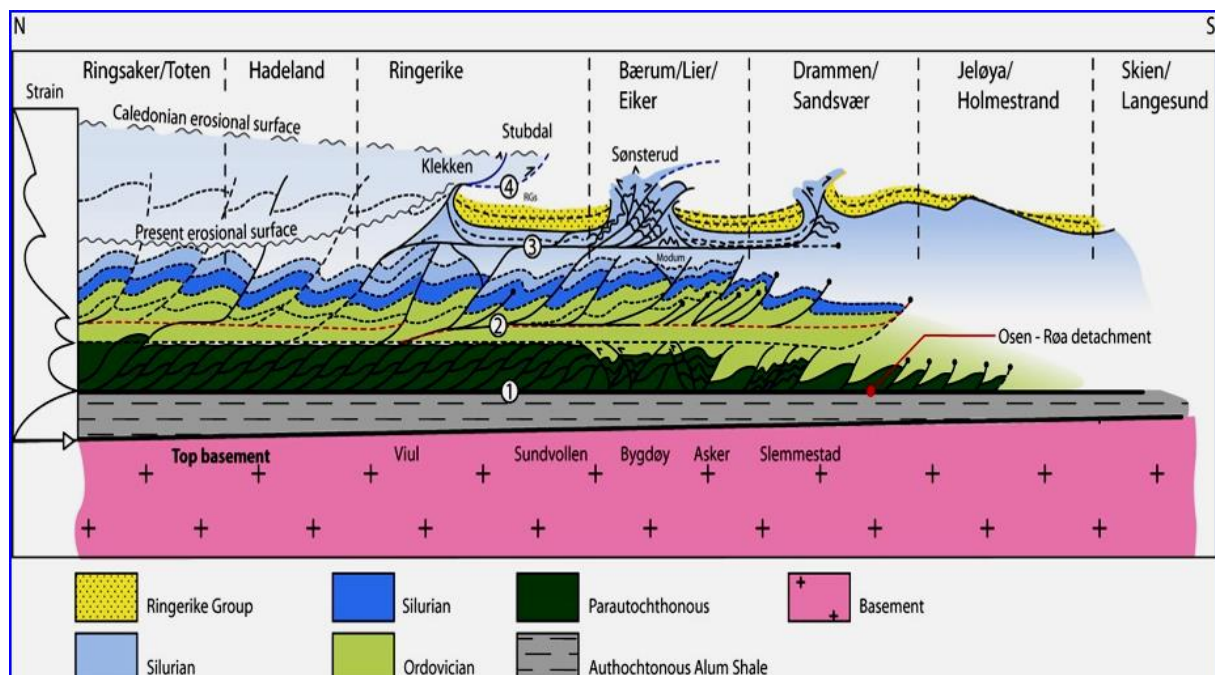


Figure 1.6: Regional structural model for the Oslo Region from Bruton et al. (2010). This tectonic model serves as a basis for the regional tectonic model constructed in this study. Note the 4 different structural levels and the decrease in strain when going up section (depicted in a strain curve on the left side of the figure). Figure from Bruton et al. (2010).

this unit, ramp flat ramp structures exist which most likely link below to the middle thrust system (Bruton et al., 2010), with the final flat just below the Ringerike sandstone. Below this Ringerike sandstone, the strata are very strongly deformed with sometimes a tectonic melange-like texture. The sandstone itself is relatively undeformed with folding on km scale with amplitudes of a few hundreds of meters. Locally the Ringerike sandstone contains very steep ramps (70-80°), at these localities faults have broken through the Ringerike sandstone into the overlying fourth structural level.

The master faults of the fourth structural level are closely related to structural level three (Bruton et al., 2010) (Figure 1.6). This level is constricted to structures cutting through the Ringerike Sandstone Formation as well as the formation itself. Decreasing strain up stratigraphy and erosion make outcrops of this level uncommon. Deformation of the Ringerike Sandstone Formation is characterised by very gentle buckle folding with very large wavelength-amplitude ratios. The deformation of the areas where faults cut the Ringerike Sandstone Formation are characterised by intense shortening and squeezing of the strata, leading to very complex outcrop patterns (Vlieg, 2015; Bruton et al., 2010).

1.2 Lithostratigraphy in the study area

Stratigraphy of the Oslo region was established by (Worsley et al., 1983) for the Silurian and (Owen et al., 1990) for the Ordovician strata. Both publications contain a very detailed description of the stratigraphy present in the study area (Figure 1.7) and are used in the following description. The following descriptions have been largely based on the descriptions of (Owen et al., 1990).

Alum Shale Formation

Deposited during Middle Cambrian to Lower Ordovician times, the 'Alum Shale' Formation is a shale present across large parts of the Baltoscandian shield with a thickness of roughly 30-100 m (Bruton et al., 2010). With a high organic content (TOC up to 15%) (Larsen and Olaussen, 2005), enriched in uranium and sulphur (Bruton et al., 2010; Larsen and Olaussen, 2005) and containing characteristic 'stinkstones' (limestone concretions). As mentioned before, the basal thrust unit is constricted to the

Alum shale formation. This means that at most localities, the Alum Shale is very strongly deformed to the point that it is no longer possible to see original structures. The uppermost part of the Alum Shale contains trilobites of the *Euloma-Niobe* fauna, which are dated to the latest Tremadoc (~488-479 Ma).

Bjørkåsholm and Tøyen Formation

Although technically two different formations, for this thesis the two formations are grouped together due to the fact that the two formations are often interweaved. The Bjørkåsholm Formation is a (nodular) limestone of roughly 1 m thick intercalated with thin shales. It also contains dark limestone concretions at its base as well as *Euloma-Niobe* trilobites, making it also latest Tremadoc.

The Tøyen Formation is a black/grey shale of <20 m thick. Transitioning from the Bjørkåsholm to Tøyen takes place in a gradual manner, the amount of limestone decreases and the shale content increases. The transition to the overlying Huk Formation is of a similar nature. Dating of the Tøyen Formation has proved difficult to the lack of fauna. (Spjeldnaes, 1957) concluded that it is equivalent to the entire British Arenig (~479-472 Ma).

Huk Formation

A nodular limestone containing three members, the Huk Formation has a thickness of ~9 m in the Ringerike region. Characteristic for the formation are the limestone members bounding a middle limestone-shale unit. It is thought to be of roughly Kunda age (468-464 Ma).

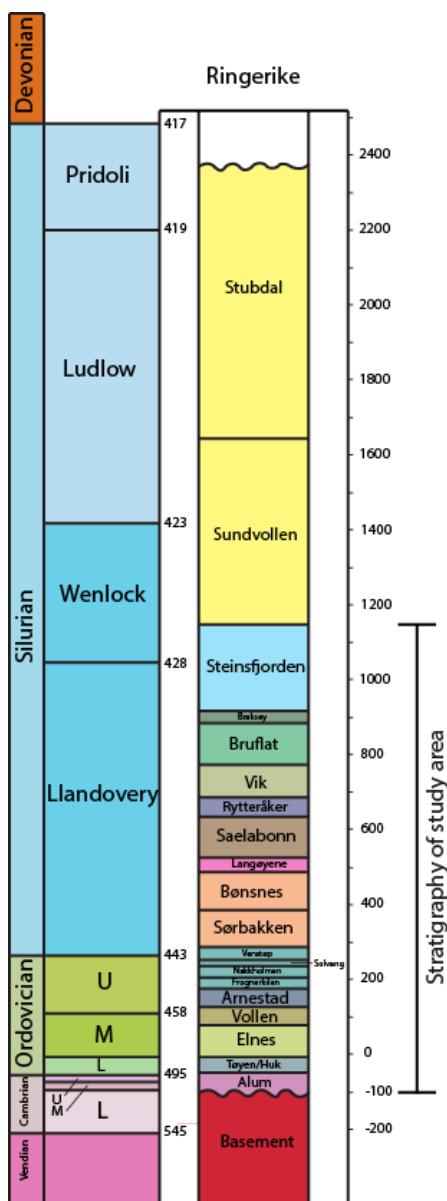


Figure 1.7: Lithostratigraphic column of the Ringerike district. Stratigraphy of the Hønefoss area is delineated. Figure from Larsen and Olaussen (2005).

Elnes Formation

The Elnes Formation is a black shale of unknown thickness, but estimates are around 60m. Because the black shale is very incompetent, the formation is heavily deformed, similar to the Alum shale. The shale contains limestone nodules present in bands of roughly 5 cm thick. Thickness of the shale layers are around 40 cm. Graptoliti fauna indicates that the formation is middle Llanvirn to early Llandeilo in age (~458-455 Ma).

Sørbakken Formation

No complete section exists of the Sørbakken Formation, however, its thickness is estimated to be around 100 m. It consists of a grey, nodular and bedded limestone intercalated with thinner calcareous shales. It contains diverse shelly fauna's, including trilobites, brachiopods, bivalves, cephalopods, gastropods and more. Age is estimated to be roughly 448-446 Ma.

Bønsnes Formation

A dark limestone with calcareous shale, the Bønsnes Formation has a thickness of around 1 m. The upper part contains shale layers of >45 cm thick with scattered limestone nodules. It contains lots of fauna, including, but not limited to algae, stromatoporoids, trilobites, brachiopods and cephalopods. Its age is estimated to be Rawtheyan (~446-445 Ma).

Langøyene Formation

With a thickness varying between 50 and 60 m, the Langøyene Formation is a sandstone interweaved with thin limestones. The formation is thought to have been deposited in a shallow water setting above the (storm)wave base. Many of the sandstone beds have been interpreted as storm deposits. Age indications from trilobites and brachiopods indicate a Hirnantian age (445 Ma-443 Ma).

The following descriptions have been largely based on (Worsley et al., 1983).

Sælabonn Formation

The Sælabonn Formation has a thickness of approximately 110 m. It is composed of sandstones, siltstones and shales in varying proportions. With the shale being dominant in the lower part of the formation, sandstone dominating the middle part and siltstone dominating the top. It is intercalated with minor limestones, which becomes more abundant towards the overlying Ryterråker Formation. Its age is determined to be roughly Rhuddanian to early Idwian (443-439 Ma) based on brachiopods (Thomas, 1981 via Worsley et al., 1983) and conodonts (R.J. Aldridge, *pers. comm.*, 1981 with Worsley et al., 1983)

Ryterråker Formation

A 50 m thick formation, the base of the Ryterråker Formation is similar to top of Sælabonn with thinly to medium bedded siltstones and shales with limestone intercalations. Limestone start to dominate upwards with thick beds and bioherms in the middle part of the formation. The upper part consists of planar limestone beds and calcareous nodules which are strongly bedded and interweaved with shales. Shale content increases into the overlying Vik Formation. In the Ringerike area, the age is determined to be middle to late Idwian (~438-437.5 Ma). Although ages vary for different locations in Norway, with some other locations being dated to early Fronian (~436 Ma).

Vik Formation

The Vik formation is approximately 80 m thick and consists of red and grey/ greenish shales, marls and (nodular) limestones. Its base consists of thinly bedded limestones and greenish grey shales transitioning into red mudstones and shales. The middle part contains thinly bedded limestones with calcareous nodules of grey marls. Going up, the upper part consists of grey to red shales interbedded with fine nodular limestone. Age constraints are provided by brachiopods and conodonts, giving an age of middle to late Telychian (~432-428 Ma)

Bruflat Formation

Having an estimated thickness of roughly 400-550 m, the Bruflat Formation has no type section due to the fact that it is very heavily deformed. It is characterised by varying proportions of sandstones, siltstones and silty shales. The lower part consists of medium to thickly bedded fine calcareous sandstones and silty shales. Going up stratigraphy the formation is made up of irregular and intergrading alternations of fine calcareous sandstones, siltstones and limestones. The latter are often present in thick beds. Age is determined to be late Telychian (~428 Ma).

Braksøy Formation

The Braksøy Formation has a thickness of 27 m. It consists of a complex carbonate development with minor marl and shale content. The carbonate is locally developed in small reefs which pass laterally and vertically into marls with variable thickness. It is overlain by a 3.5 m thick black, bituminous shale. At the top of the formation, the strata consist of well bedded limestone with some minor marl content. Its age is, based on dating of the overlying Steinsfjorden Formation, determined to be around low Sheinwoodian age (~428-427 Ma).

Steinsfjord Formation

The 260 m thick Steinsfjord Formation consists of irregularly varying proportions of greenish grey shales and marls, red dolomitic shales, dolomites and limestones. At its base, the Steinsfjord Formation is characterised by thinly interbedded limestones and shales. These strata transition into more thickly bedded dolomitic limestones and limestones interweaved with greenish grey shales and marls. At the top the interbedded limestones and greenish grey shales pass into red mud and sandstones. Age of the Steinsfjord Formation is somewhat complicated. The base of the formation has different ages at different localities, but it is generally accepted that it is of Wenlock age (~428-422 Ma).

2 The Hønefoss area, a field perspective

2.1 Field methodology

Fieldwork has been carried out in the area around the city of Hønefoss (Figure 2.1), where several key localities and sections have been studied. A suitable outcrop of the Osen-Røa thrust is located near the village of Viul in a dry riverbed (Figure 2.1). The locality consists of a wall section approximately 100 x 20 m in dimension and a section in the dry riverbed approximately 100 x 50 m. At this locality, the wall section is studied in detail and the riverbed section is mapped out. Located above the Viul wall and riverbed sections, the Viul railroad section contains exposures of the basal plane. It is located along a quiet railroad and is approximately 100 m in length. Here, additional structural data and information on the structural style of the Alum Shale was gathered. Further south and higher up in the stratigraphy, approximately 750 m south of the village of Klækken, a small road section is located along road 241. It is a small outcrop of approximately 15 x 4 m located as a local 'stump' in the landscape (Figure 2.19). The geographic position of this small outcrop makes it difficult to immediately place it in context. In the village of Klækken (Figure 2.1), the Ringkollveien road starts going up to the east. Along this road, a section up stratigraphy and across the Klækken fault has been studied in detail. The section is roughly 1500 m long (Figure 2.1).

For measuring structural data in the field, a Recta compass with an inclination needle and a spirit level was used. Bedding planes were measured using the strike-dip method (strike/dip general dip direction). Where possible, folds were measured directly on the fold hinge. Otherwise, two flanks of the fold were measured and a fold axis was constructed using a stereograph. Folds are described by their wavelength, amplitude and tightness. The classification of the tightness was done using criteria

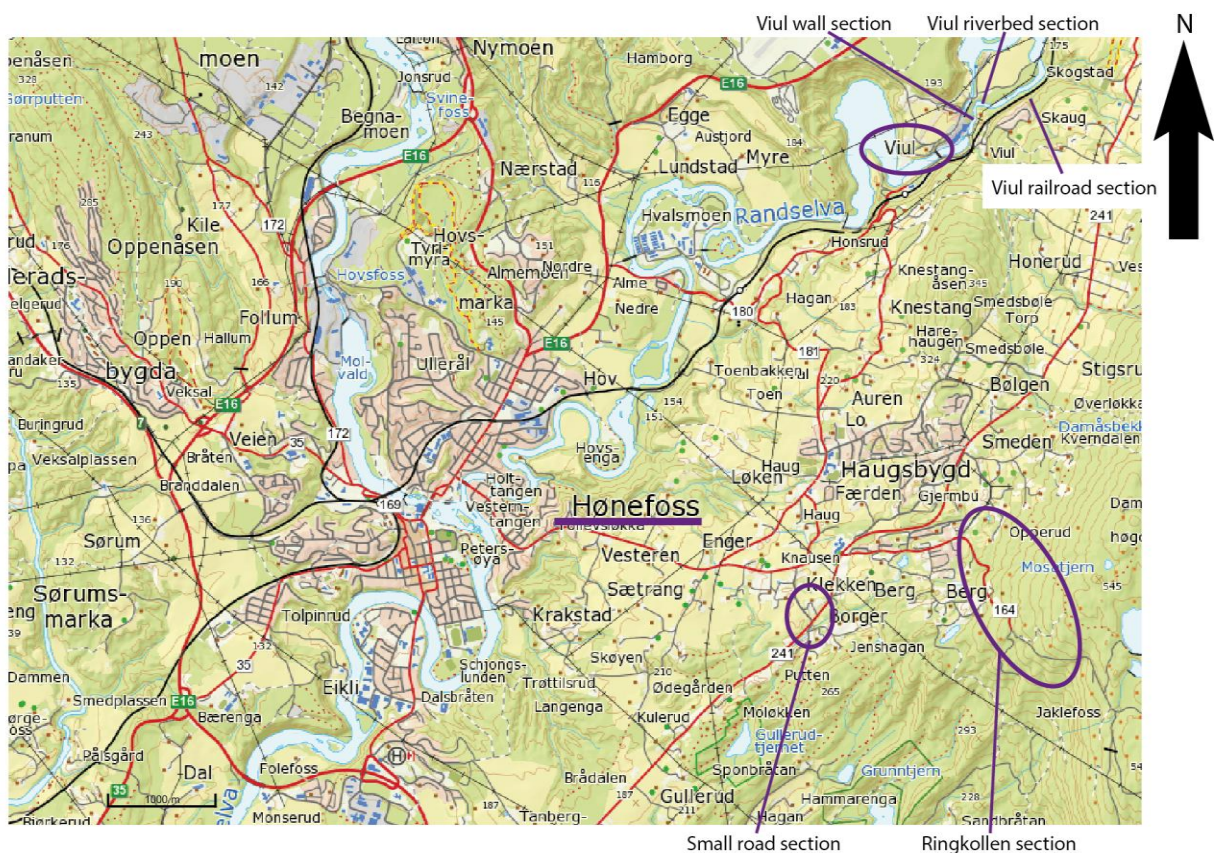


Figure 2.1: Map of the fieldwork area around the city of Hønefoss. Locations described in the text are highlighted on the map. Location of the Hønefoss area in the Oslo Region is presented in Figure 1.1.

Table 2.1: Fold tightness classification as used in field description.

Fold tightness	Interlimb angle (°)
<i>Isoclinal</i>	0 – 10
<i>Tight</i>	10 – 30
<i>Close</i>	30 – 70
<i>Open</i>	70 – 120
<i>Gentle</i>	120 – 180

presented in Table 2.1. Analysis of the structural data was done using the program ‘Stereonet’. The scientific algorithms used in this program are from (Allmendinger et al., 2013; Cardozo and Allmendinger, 2013).

2.2 Field observations

The strata in the fieldwork area are underlain by the strongly deformed Osen-Røa thrust, which is the basal decollement in the entire region. This basal decollement is characterised by complex duplex structures in the Alum Shale Formation. Observations on the basal plane were made at three outcrops, namely the Viul wall, Viul riverbed and Viul railroad sections (Figure 2.1). Up section, along the Klækken fault south of the village of Klækken (Figure 2.1), a local small road section is observed. Duplexes on the basal plane are inferred to be present below the entire Oslo Region based on similar observations made in Slemmestad, near the tip of the deformation (Weekenstroo, 2015). At the highest point in the section, following the Klækken fault, a partly overturned footwall syncline is observed along the Ringkollen road section. Here, the research area ends, as the area to the south has been extensively studied by (Vlieg, 2015).

Description of the field observations will be done per locality. The different localities in the region are indicated on Figure 2.1. Per locality, the geometry of the observed structures will be described first followed by any structural data.

2.2.1 Viul locality

Viul wall section

Located near the village of Viul, the Viul wall section (Figure 2.1) is a superb outcrop of the Osen-Røa basal thrust of the thin skinned fold and thrust belt situated in the Oslo Region. Spanning approximately 150 m, the outcrop contains numerous duplexes on multiple scales. The entire section consists of shale from the Cambrian Alum Shale Formation (Figure 1.7). A panoramic photo collage and the interpreted structures as well as a sketch of the interpreted structures are presented in Figure 2.2 & Figure 2.3. A larger, A3 sized print, of figure Viul wall is attached as Appendix A.

The largest structures visible are ~80 x 10 m duplexes (Figure 2.2) followed by slightly smaller, ~40 x 5 m, duplexes, observed at the tips of these largest structures. All structures are hinterland dipping (to the north).

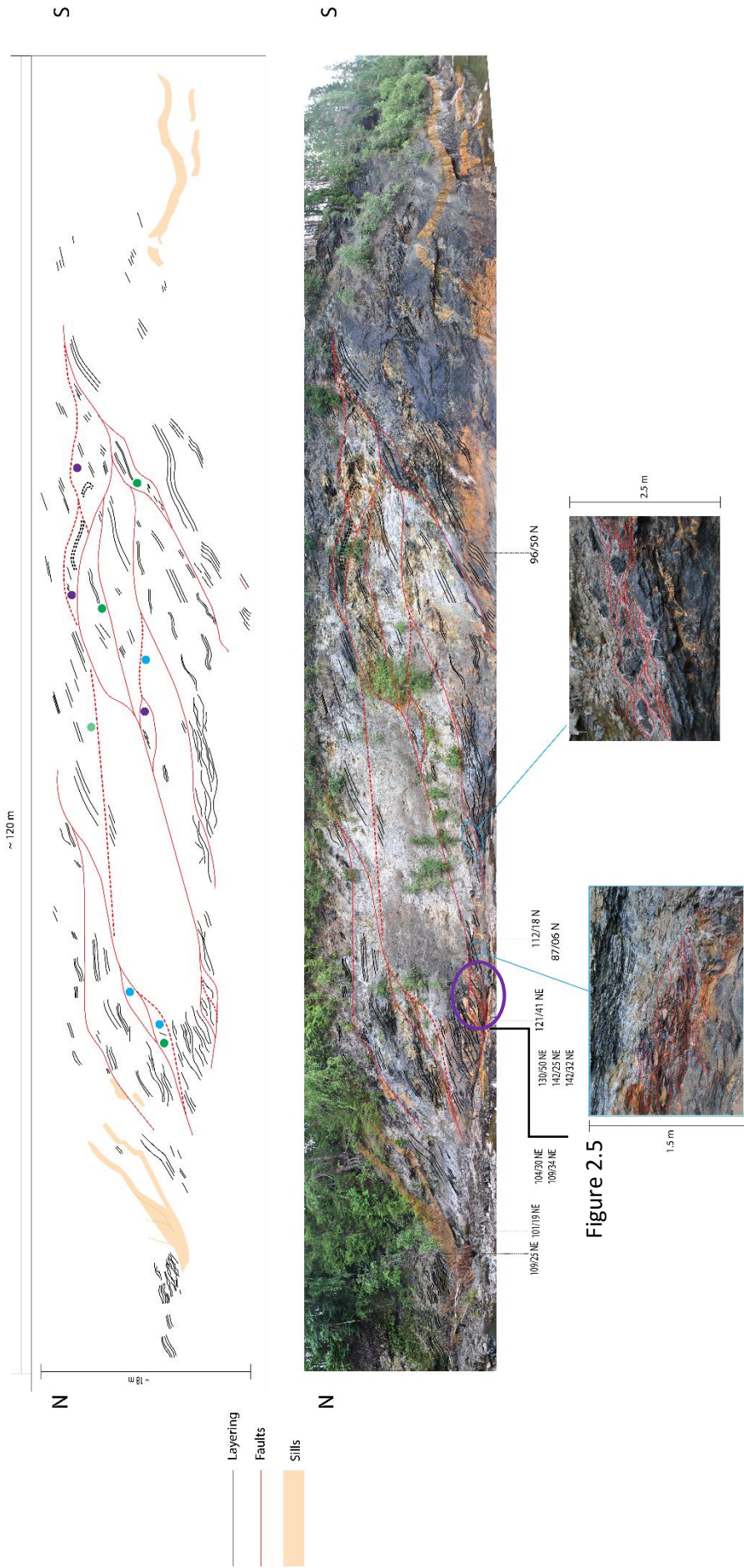


Figure 2.2: Photographic collage and sketch interpretation of the southern part of the Viul wall section. Note the numerous duplexes at multiple scales. The dots represent different classes of duplexes based on their suspected formation mechanism, for more detail see Figure 2.4. The photographs illustrate the intense deformation to which the section has been subjected. Also, several more close-up photographs of the section are presented below and their location is displayed on the photograph.

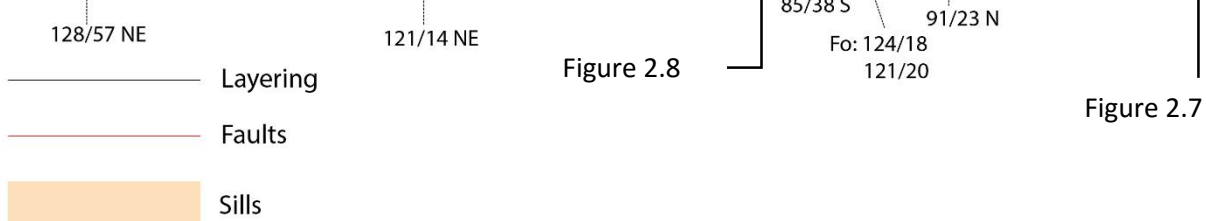
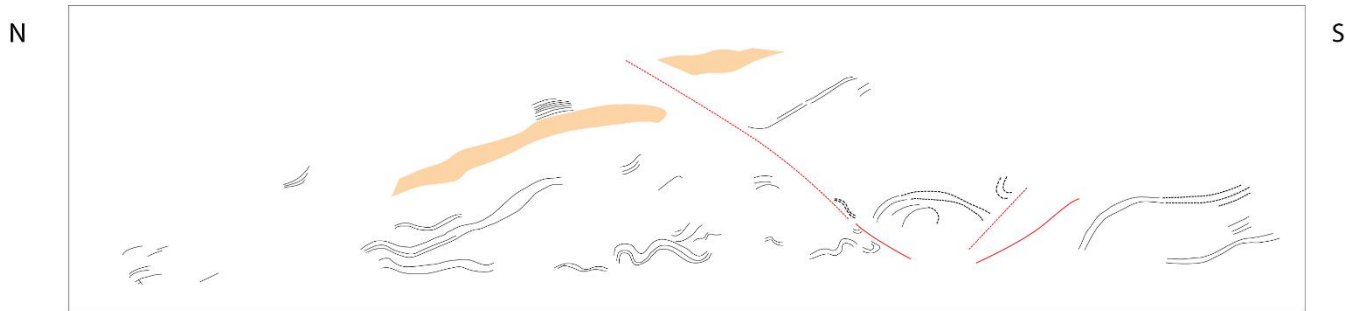


Figure 2.3: Photographic collage and sketch interpretation of the northern part of the Viul wall section. Note the backthrust offsetting the sill. Several close-up photographs of this part of the section are presented below, their locations are indicated on this figure.

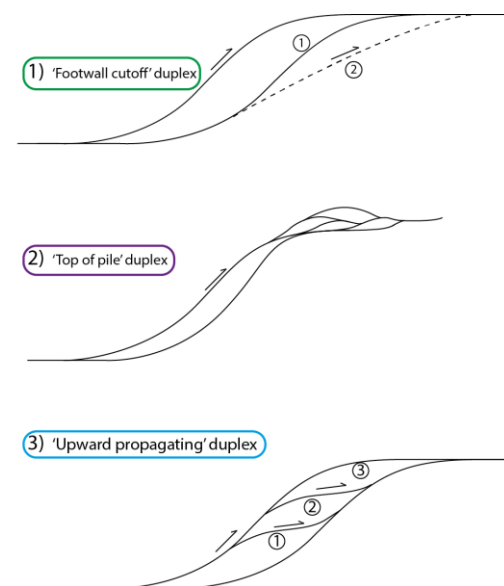


Figure 2.4: Schematic representation of the different classes of duplexes defined in the text. The colour around the name of the style corresponds to the dots which represent interpreted duplex styles in Figure 2.2.

Besides these large scale duplex structures, smaller scale duplexes and horses are also observed at multiple places along the section. All strata in the section is disharmonically folded. The most prominent example of these is located roughly in the centre of the wall section (Figure 2.5). Here, a small duplex with dimensions of $\sim 5 \times 1$ m is subdivided into 2-3 small horses with a roughly 1.5×1 m dimension. At present duplexes or horses are observed on $\sim 80 \times 10$ m, $\sim 40 \times 5$ m to $\sim 5 \times 1$ m-scale as well as horses of $\sim 1.5 \times 1$ m. These duplexes present at Viul are separated in four classes, based on their origin kinematics (Figure 2.4):



Figure 2.5: Horses inside a small duplex observed in the Viul wall section. Location of the photograph is indicated in Figure 2.2.

- The first type is 'normal' duplexes with no strange or complex kinematic origin.
- The second type of duplexes visible in the Viul wall section has been affected by footwall cutoff (Figure 2.4). Here, the angle of the duplex footwall has been lowered by a second fault forming at a lower angle, hence making it mechanically easier to shorten the stratigraphy.
- The third type of duplexes observed at the Viul wall section are duplexes formed at the top of a series of duplexes. These form in a very similar way to an antiformal stack (Figure 2.4).
- Finally, there are some duplexes which are thought to have formed by upward propagation of the hanging wall branch of the duplex (Figure 2.4).

When looking inside the smaller, m-scale, structures the strata are strongly deformed and have undergone very high strains. The faults bounding the duplexes are high strain zones with small cm to dm-scale lenses which could be considered small duplexes or horses. Inside these structures, the deformation style of the strata varies from obliterated to asymmetric tight to isoclinal folding of the bedding cleavage.

The dark, solid limestone concretions present in the Alum Shale Formation have a significant influence on the strain distribution, sometimes creating strain shadows, although this is more prominent in map view (Figure 2.11). In the shear zones these limestone concretions have often been deformed as well, becoming elongated and folded, sometimes with a σ -clast-like geometry (Figure 2.6), indicating that these zones have undergone high strains.

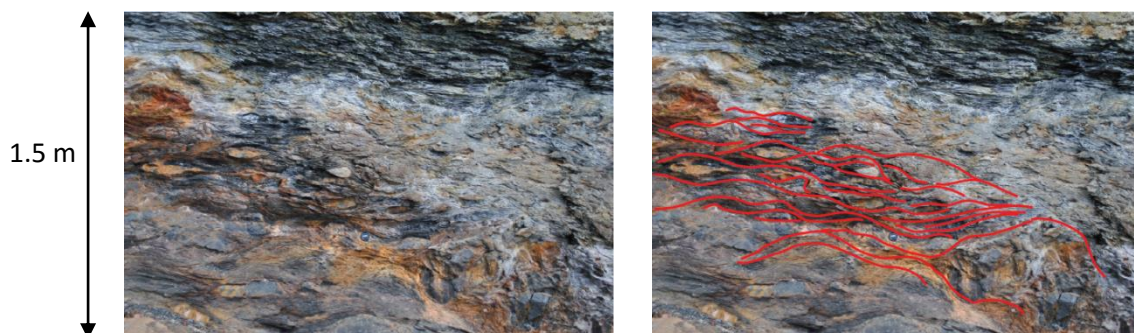


Figure 2.6: Sheared limestone concretions in the Viul wall section. Left is the un-interpreted section, right contains interpretations of fault/ glide planes. Pictures are larger versions of left close-up picture in Figure 2.2.



Figure 2.8: Small scale chevron folds in the Viul wall section. Position in larger section is indicated in Figure 2.3.



Figure 2.7: Disharmonic folding on m-scale with varying intensity. Figure location is indicated in Figure 2.3.

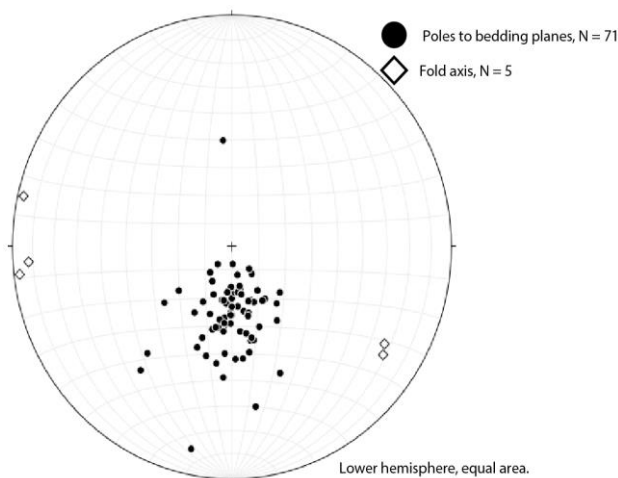


Figure 2.9: Structural data from the Viul wall section.

The Alum Shale in these areas is extremely deformed, almost to the point of cataclasis. This is most prominent in the shear zones, but present in the entire section, with the shale being reduced in size down to 1 cm slivers. Folding is present from mm-scale to 100 m scale. The prominent and varied colour scheme of the strata is a weathering result also; the strata is rich in pyrite. Although the outcrop itself is very colourful, the monomineralic content of the Alum Shale Formations prevented the measuring of stretching lineations. A second set of cleavages is overprinting the bedding cleavage, which is also sub horizontal and creating pencil cleavage.

Menaelite sills are also observed in the section (Figure 2.2 & Figure 2.3). There are in total two types of sills present in the Alum shale, the menaelite sills consist of pure feldspar and comptonite sills are mafic sills consisting of olivine and amphibole (Larsen, *pers. comm.*, 2014). The sills have a curved, s-shape geometry similar to that of the duplexes, dipping towards the north. Radiometric dating of these sills indicate an age of ~305-298 Ma (Larsen, *pers. comm.*, 2014). The riverbed in front of the wall section consists of one large menaelite sill, whereas when going north towards the Viul riverbed section, Alum shale crops out in the riverbed.

The most striking structure observed in the northern part (Figure 2.3) is a medium-large thrust with a transport direction towards the north, meaning it is a backthrust. It offsets a sill by ~3-5 m, giving a rough indication of the throw of the fault. Near the riverbed, drag structures of approximately 2-3 m in the hanging wall and 0.5-2 m in the footwall are observed. Inside these m-scale structures, small cm-scale structures such as chevron folds occur (Figure 2.8). Slightly north of the observed backthrust, some m-scale diachronous folding with varying intensities are observed (Figure 2.7).

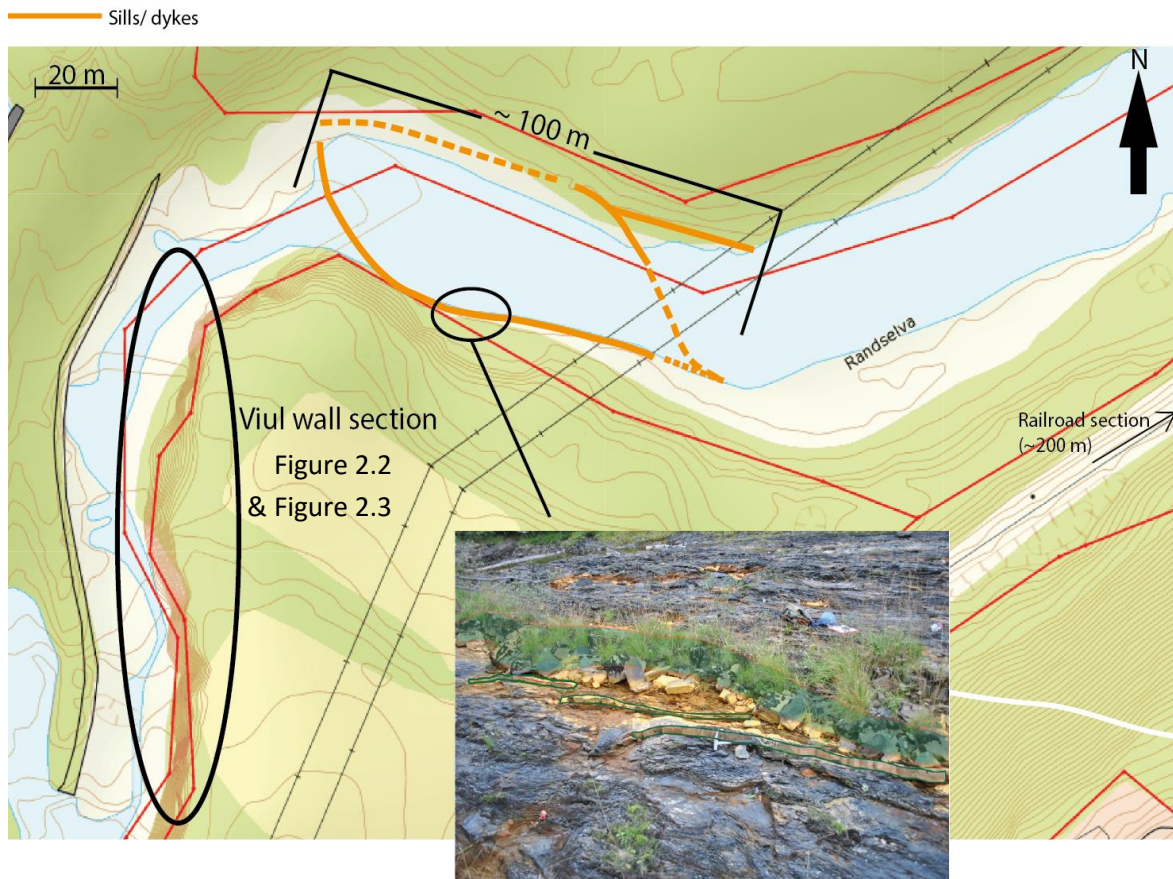


Figure 2.10: Map of Viul location with a focus on the riverbed section. The inferred large scale horse is traced with orange lines. The picture displays small scale duplexes on the southern limb.

The poles to the bedding planes from this section give a south dipping cluster with some spread and an anomalous measurement in the north (Figure 2.9). This indicates north dipping planes with a relatively shallow dip. The strike varies between NE-SW and NW-SE. The significant height of the section means that data sampling is local. Only in the lower 1.5 m of the section it is possible to measure structural data. Fold axis data is lacking from this section due to the fragile nature of the outcrop as well as the small slivers of shale which make measuring fold axis rather difficult. Five fold axes have been measured, which appear to have a SE-W orientation and very shallow dip (Figure 2.9).

Viul riverbed section

North of the Viul wall section, around the bend that defines the end of the wall section, the Alum Shale Formation of the Osen-Røa thrust crops out in the riverbed where it is not overlain by sills in an area of roughly 100 x 50 m (Figure 2.10). The outcrop is characterized by the presence of strongly, asymmetric folded Alum Shale and is bounded by an approximately 1 m thick menaenite sills on the northern side which coincides with the riverbank and is an abrupt topographic feature. On the eastern end of the outcrop, a large, 1 m thick sill runs out from the heavily overgrown riverbank into the river bed. On the south side, an approximately 0.3-1 m thick sill starts at the large sill which makes up the riverbed at the Viul wall section and runs towards the east (Figure 2.10). Approximately halfway along the length of the outcrop three smaller, sill of roughly 10-30 cm thickness, originate out of the thicker sill and form small 3 m long horses (close-up picture in Figure 2.10). South of this big southern sill, there is more alum shale outcropped in a 5-10 m wide strip.

In between these two sills, the Alum Shale Formation with its limestone concretions is strongly deformed. Furthermore, a high number of cm scale, asymmetric folds is observed (Figure 2.12). They have short overturned limbs dipping towards the north, and long limbs dipping shallow towards the north. Competence contrasts between the relatively weak shale and the strong limestone concretions result in strain shadows (Figure 2.11). All Alum shale outcropped in this riverbed is strongly deformed and has undergone significant amounts of strain.

Plotting the poles to bedding planes from the riverbed section (Figure 2.13), it becomes clear that the orientation is constant. There is a tight cluster of poles in the south, indicating a very tightly grouped cluster of north dipping bedding planes with a relatively shallow dip. Fold axes show an E-W trend, consisting of shallow dipping clusters in the east and west (Figure 2.13) with the most significant cluster dipping towards the east.

Viul railroad section

Located stratigraphically and topographically above the Viul wall and riverbed sections (Figure 2.1), the Alum Shale Formation is the only formation present in outcrops at the Viul railroad section. The section is approximately 100 m long and 8 m high (Figure 2.14). Intense deformation characterises the section with (part of) duplexes on multiple scales. Some parts of the section show a different structural style, with more cm to m-scale folding and more discrete faults.



Figure 2.11: Limestone concretion in the Alum Shale Formation. Note the strain shadow towards the south. Compass for scale and orientation. Top of picture is north.



Figure 2.12: Small, cm scale, asymmetric folding. Viewing direction is towards the west. Hammer for scale.

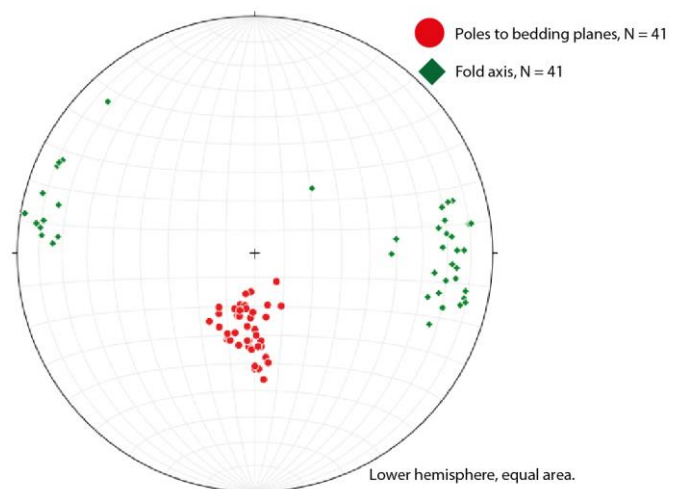


Figure 2.13: Structural data from the Viul Riverbed outcrop.

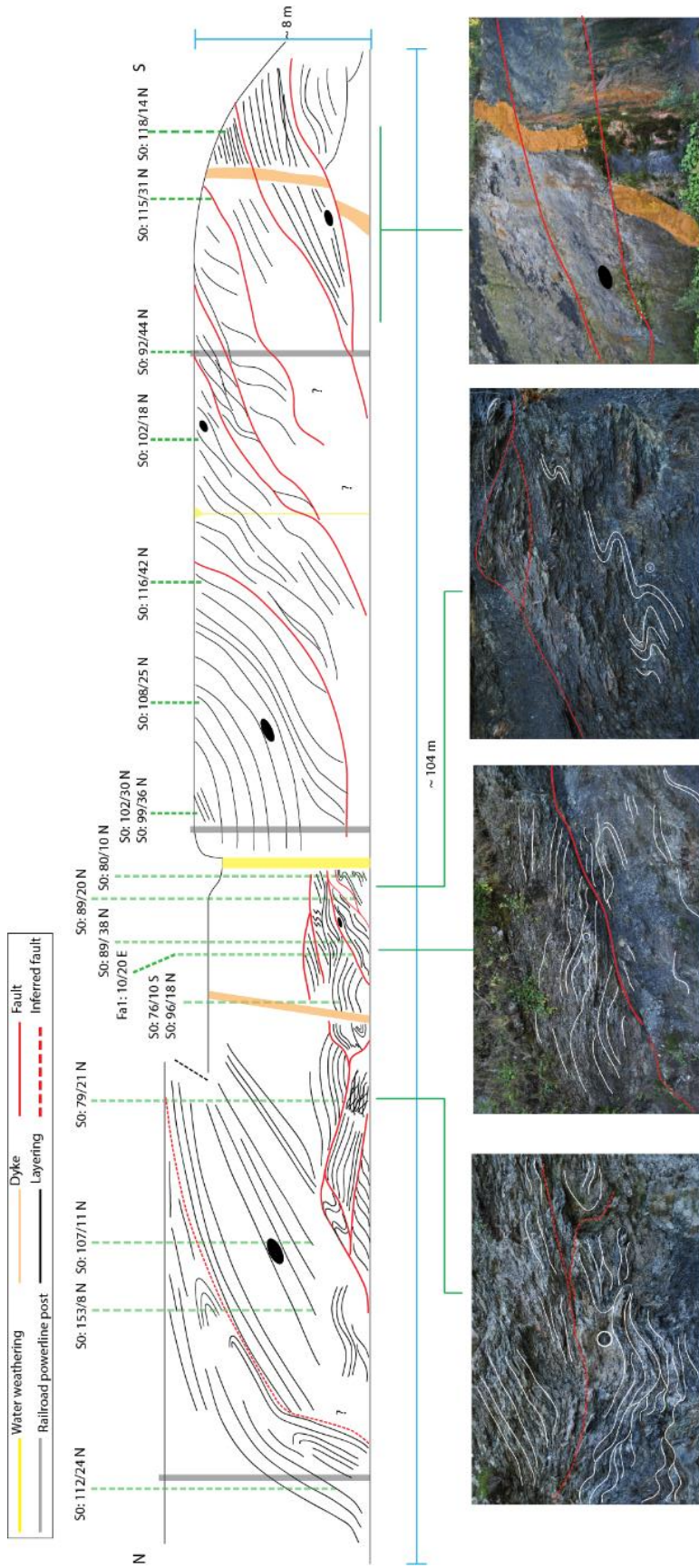


Figure 2.14: Sketch interpretation of the Viul railroad section with close-up field photographs of relevant details. Black ellipsoids in the sketch are limestone concretions. Note the different styles in the northern and southern parts of the section.

The section can be divided into two halves, a southern and a northern half (Figure 2.14). The southern half of the section is characterised by parts of large duplexes estimated to be of the same size as the duplexes in the Viul wall section, roughly 80 x 10 m. Because the section is not as high as the Viul wall section, only parts of these structures are visible and classification of duplexes is not possible. It can be observed that the shale has undergone significant amounts of strain, as slivers of shale down to 1 cm are observed. A menaëite dyke is also present in the southern tip of the section, where it is offset by a thrust fault (Figure 2.14).

A vertical strip of extremely weathered strata, due to a (semi)permanent waterfall, is dividing the section. North of this strip, part of the structural style changes dramatically, as the size of the structures decreases for about 40 m. Here it becomes even more clear that the strata is extremely deformed. The size of the horses decreases to m-scale and locally zones of very high strain are observed (Figure 2.14). One fault is clearly visible due to the abrupt change in the orientation of bedding cleavage across a fault. Folding in the strata is also observed, in the form of cm-dm-scale folds of tight to close nature. The most northern part of the section sees an increase in size of the structures. Here they are again on roughly the same scale as in the southern part, although decidedly less clear. Possible drag folding and contrast in layer orientations indicates the possible presence of a fault (first close-up picture from N in Figure 2.14).

Fold axes have not been measured at this location. The nature of the outcrop (severely weathered) and the strata prevented measurements of sufficient quality. Poles to bedding planes are shown in (Figure 2.15), it shows a cluster of N-S oriented poles in the south with a single anomalous pole in the NE. Planes of the Alum shale are here shallow north dipping with an E-W strike.

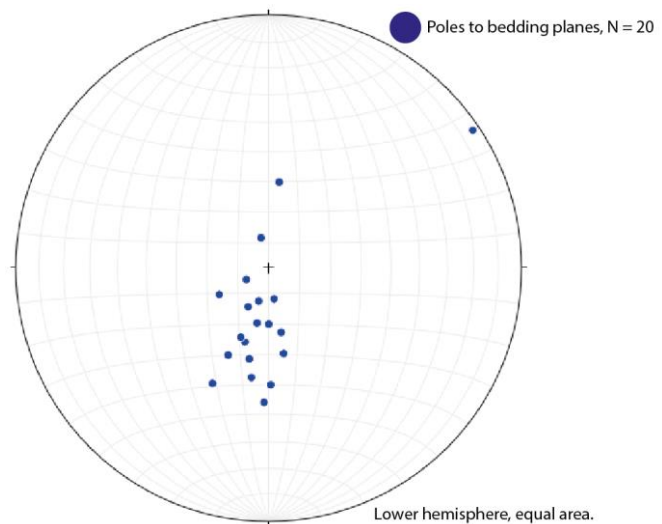


Figure 2.15: Structural data from the Viul Railroad section.

Combined structural data for Viul sections

The three combined sections near Viul resulted in 132 bedding planes and 46 fold axis measurements. Data from the three different locations show similar trends in the orientation of the poles to the bedding planes and the fold axis (Figure 2.9, Figure 2.13 and Figure 2.15). The data is therefore plotted together in a single stereograph displayed in Figure 2.16.

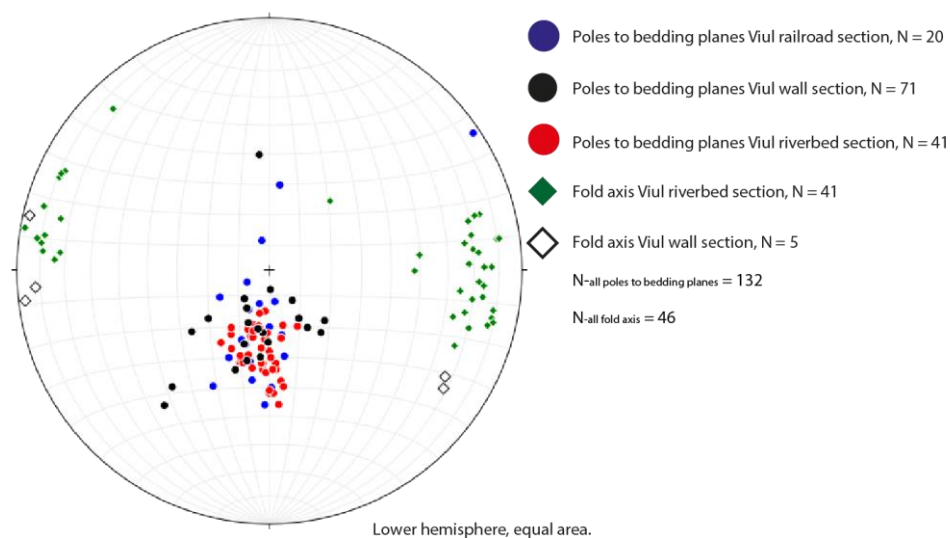


Figure 2.16: Structural data from the three different outcrops in the Viul location.

Analysis of Viul sections

Menaëite sills are intruded into the Alum Shale Formation at the Viul wall section (Figure 2.2 and Figure

2.3). On first glance, the geometry of these sills suggests that their intrusion was followed by deformation, as evidenced by their duplex-like geometry (Figure 2.2). However, radiometric dating indicates a late Carboniferous age of ~305-298 Ma for these sills (Larsen et al., 2008; Sundvoll et al., 1992; Sundvoll and Larsen, 1994), implying that their intrusion occurred after the main deformation phase deforming this section, which took place during Early to Middle-Devonian time (415-390 Ma). The age of the sills indicated that they are the result of magmatic activity related to the Oslo Rift, which was initiated in the Late Carboniferous (Larsen et al., 2008; Sundvoll et al., 1992; Sundvoll and Larsen, 1994). This suggests the intrusion of the sills exploited pre-existing weak zones in the strata. Therefore, it is concluded that the sills were intruded along the thrust faults and shear zones of the duplexes, as these are the most obvious weak zones in the strata.

Strain shadows due south of limestone concretions (Figure 2.11), asymmetric folding with overturned limbs and north dipping axial planes (Figure 2.12), north dipping duplexes on all scales (Figure 2.2) and the stereo plot of the poles to bedding planes for the Viul location, all point to a southward transport direction. This is in general accordance with previously published work in Ringerike, Slemmestad, the Mjøsa district and Hadeland (Bruton et al., 2010; Morley, 1994, 1987a, 1986b, 1986b; Nystuen, 1981).

2.2.2 Road section, south of Klækken

Located along road 241 from Klækken to Hønefoss (Figure 2.1), this road section is approximately 15 x 4 m in size (Figure 2.17). The outcrop consists of very massive limestone banks flanked by more nodular limestone banks and shale layers, the strata are part of the Huk Formation (Figure 1.7). A roughly 5 m wide fault zone with multiple duplexes on 2 m-scale cross cuts the outcrop, dividing it in two (Figure 2.17). This fault zone is made up of shale with nodular interweaved limestone layers. Towards the northeast, massive Huk limestone banks run into this fault zone. South of this fault zone, the strata becomes more shale dominated. These shale layers consist of cm-scale slivers. The thick Huk limestone banks are very local with a length of 3 m before the outcrop ends.

When observing the outcrop in a larger geomorphological or topographic setting, it becomes apparent that the outcrop is a very local feature (Figure 2.19). It only protrudes roughly 15 m into the landscape.

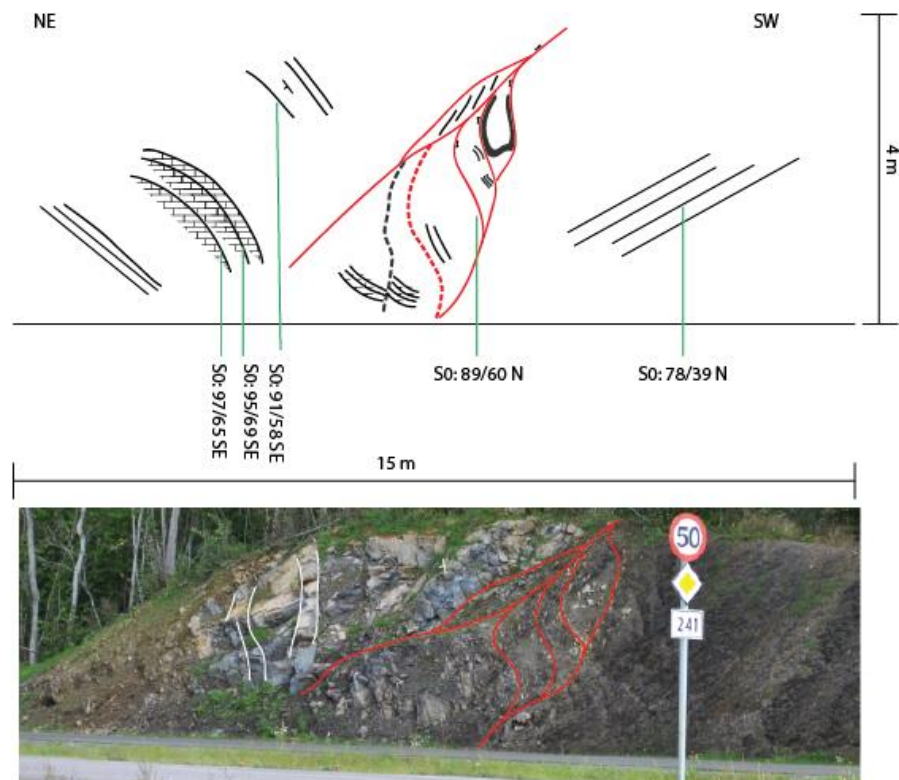


Figure 2.17: Photograph and sketch interpretation of the small road section.

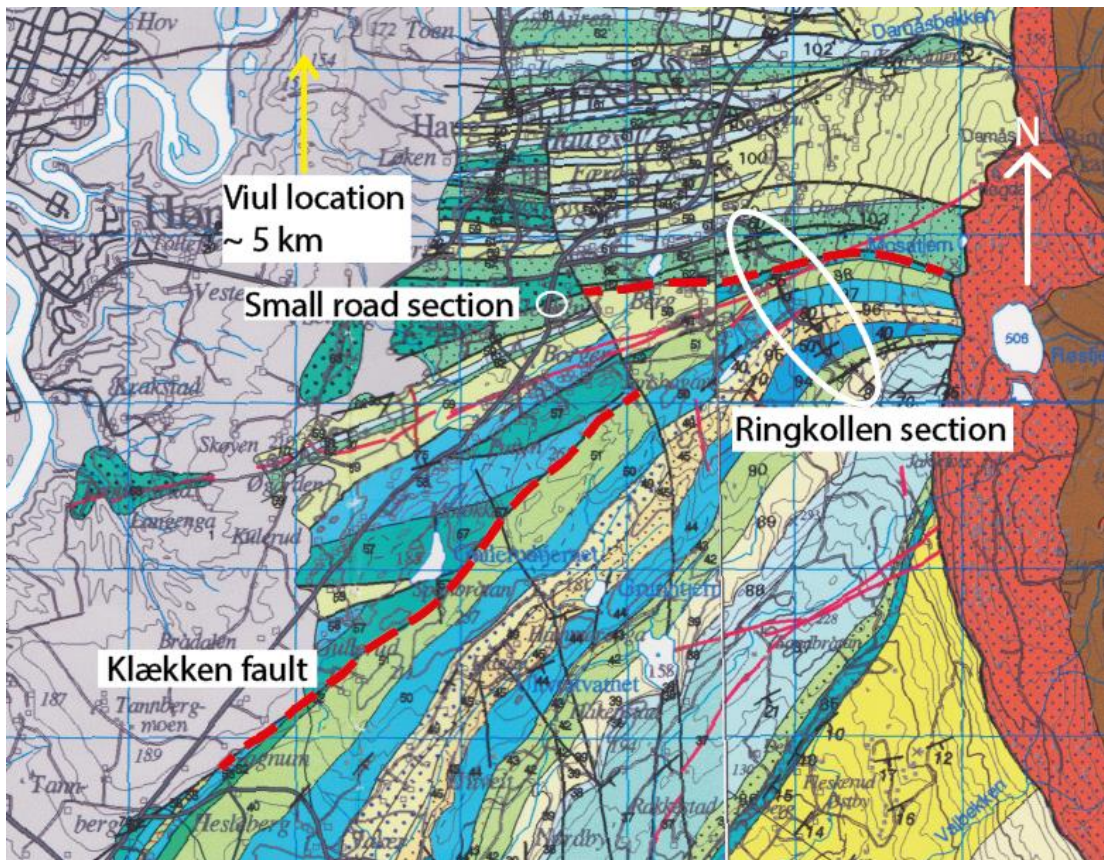


Figure 2.18: Modified blow-up of the geological maps of the Hønefoss (Zwaan and Larsen, 2003) and Oppkuven (Larsen et al., 2001) areas. The location of the Ringkollen and small road sections as well as the Klækken fault is indicated. Note the location of the Small road section with respect to the Klækken fault.



Small road section south of Klekken

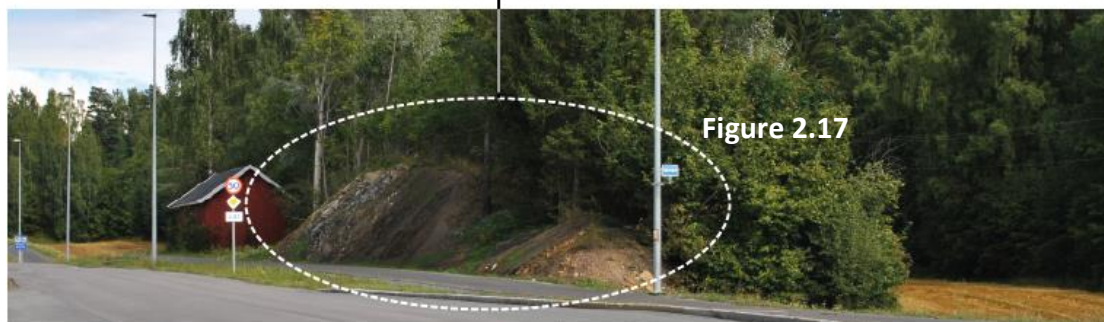


Figure 2.17

Figure 2.19: The position of the small road section in the landscape. Note that the section does not continue in any direction, exposed or unexposed.

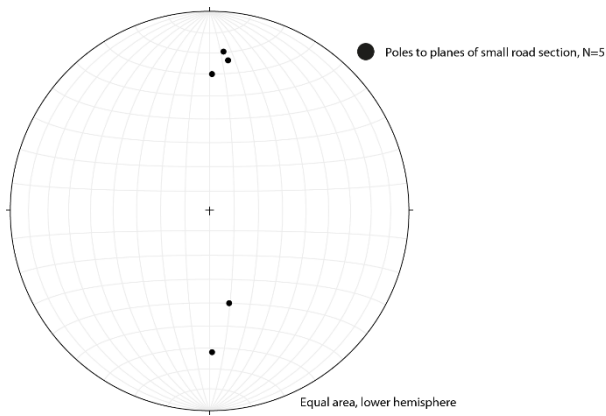


Figure 2.20: Structural data from the small road section.

When looking towards the north from a distance, it becomes clear that the outcrop is part of a small hill in the landscape and the strata present here are very local. The Huk limestone members dip around $60-70^\circ$ towards the SE, whereas the southern strata dip roughly 40° and the faults dip 60° towards the north (Figure 2.17). No fold axis was measured at this location. A total of 5 bedding planes have been measured at this location (Figure 2.20: Structural data from the small road section.)

Analysis of the road section

The road section south of Klækken is situated on or very close to the Klækken fault (Figure 2.18) (Zwaan and Larsen, 2003), which has a horizontal displacement of at least 5 km (Harper and Owen, 1983; Morley, 1987a; Størmer, 1934). Therefore, it is postulated that this road section is thrust up along the Klækken fault as a sliver inside the large shear zone. The section has been preserved due to the high competence of the strong limestone of the Huk Formation.

2.2.3 Ringkollen section

Running along the Ringkollveien from Klækken up towards the lava plateau, the Ringkollen road section cuts across the Klækken fault and through the entire sedimentary sequence up to the Steinsfjord formation (Figure 1.7). A profile roughly parallel to the road with a length of 1700 m was constructed to show the nature of this section (Figure 2.21). The map presented in Figure 2.22 is a

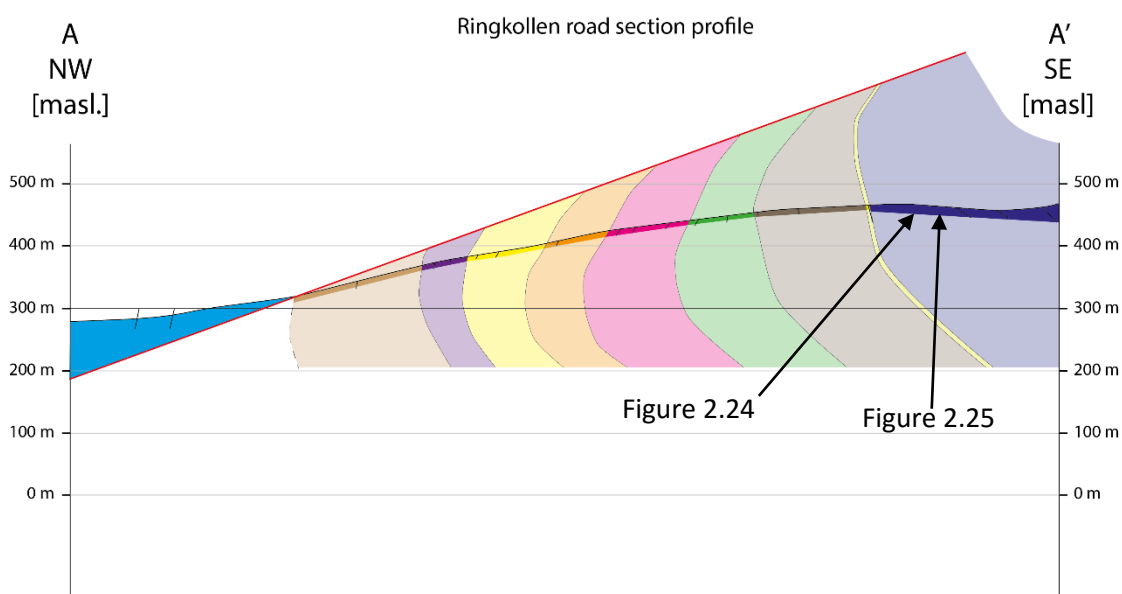


Figure 2.21: Cross section of the structure along the Ringkollen section. Note the partly overturned footwall syncline geometry. Map with the section is presented in Figure 2.22.

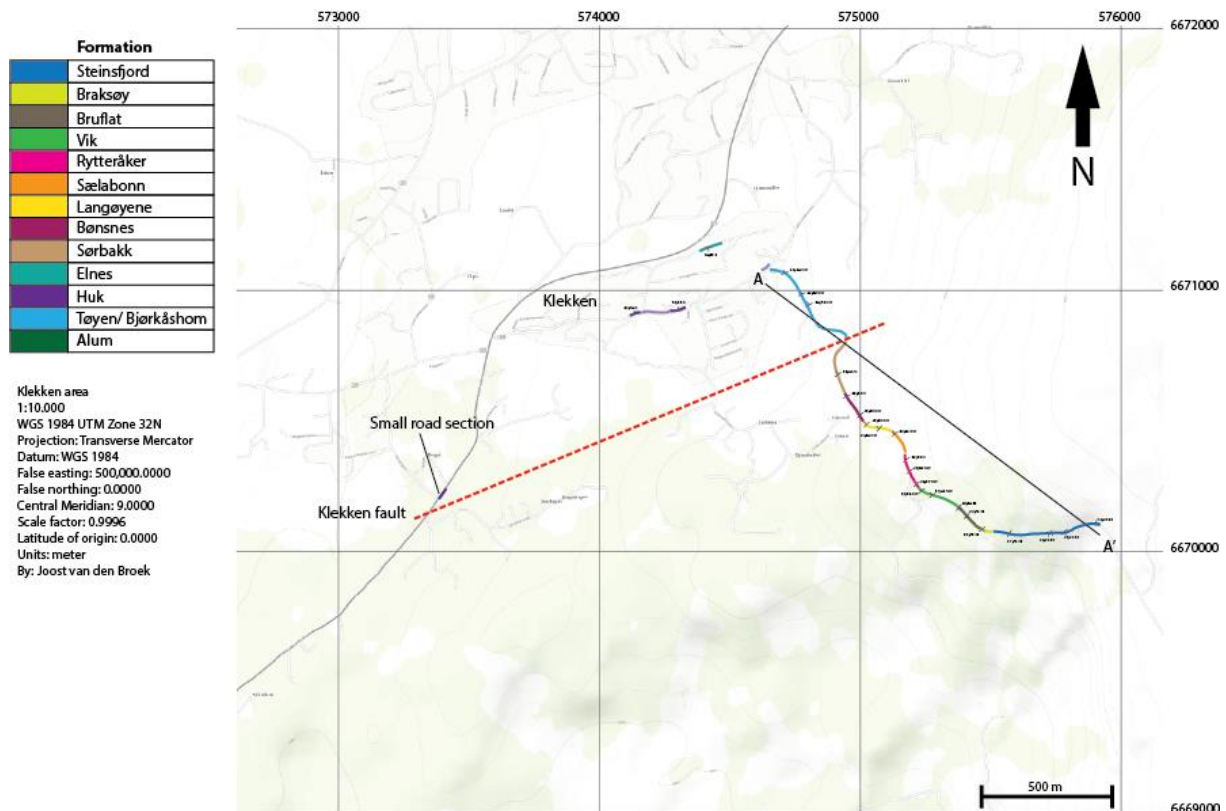


Figure 2.22: Map displaying the observations made along the Ringkollveien road, the location of the section displayed in Figure 2.21. The Klækken fault is inferred. See text for more details.

simplification of the geological by (Larsen et al., 2001) (Figure 2.18) in order to provide a better overview of the different kinds of strata at their respective location. It is by no means complete. A complete geological map of the section is available in Berggrunnskart Hønefoss 1815 III (Zwaan and Larsen, 2003) and Berggrunnskart Oppkuven (Larsen et al., 2001).

The first order structure visible in this profile is a syncline containing several sedimentary formations (Figure 2.21; Figure 1.7). It crosses the Klækken fault near the lower part of the section. Using a three point construction and the geological map by (Zwaan and Larsen, 2003), the dip of the Klækken fault is determined to be 13° . Starting in the north, the Tøyen Formation is exposed along the road. It is strongly deformed containing jointing along its bedding surface. Going up the road, the quality of the outcrop deteriorates as it becomes significantly looser and weathered. Igneous dykes of 1.5-2 m thickness are intruded into the Tøyen shale. Structurally, the formation has a steep, roughly 80° , north dipping orientation (Figure 2.22). The next formation that is outcropped is the Sørbakk Formation. It contains some gentle to open folds on dm-scale. Structurally, the strata have a very steep dip towards the north. Along the road the formation changes into the Bønsnes formation, which again contains very steep, $>80^{\circ}$, north dipping strata. Some minor thrust faults are also present here, with an offset on cm to dm scale. From the stratigraphy it is clear that there is an unconformity between the Tøyen Formation and the Sørbakk Formation (Figure 1.7), as the Huk and Elnes Formation are not outcropped along the road. The Langøyene Formation is outcropped above the Bønsnes formation. It again has north dipping strata, but the dip is decreasing to about 60° and contains open folds on m scale. However, it should be noted that the bedding is rather vague and unclear. The Sælabonn Formation is overlying the Langøyene Formation. Strata are north dipping by about 60° . Going further up section, the Rytteråker formation is present. It contains tight dm-scale folds as well as some local dm-scale fault propagation folds. The overlying Vik Formation is intruded by sills roughly parallel to the

bedding. Both the Ryteråker and the Vik Formation have north dipping strata with a dip around 60° . The Bruflat formation contains very steep dipping bedding planes with a dip around 70° as well as gentle m-scale folding with an approximately 20 cm amplitude. It is steeply south dipping by roughly 80° .

As the Braksøy formation is very thin, it is not readily observed in the section. The overlying Steinsfjord Formation however, is very thick in this section. It contains numerous structures such as low angle faults, roughly parallel to the Klækken fault, and layer parallel



Figure 2.23: Box fold in the Steinsfjord Formation along Ringkollveien.

gentle folding with a 1-2 m wavelength and 20 cm amplitude monoclines. At one locality, a box fold was observed (Figure 2.23). Small faults, with often unknown sense of movement, are also observed as well as fault propagation folds. The highest part of the Steinsfjord Formation in this section contains a lot of layer parallel sills due its proximity to the overlying lava's. A very interesting feature present in the Steinsfjord Formation is the presence of mud cracks (Figure 2.24), as it gives a younging direction, which in this case is towards the south. The strata of the Steinsfjord formation have a dip of around 70° to the south in its northern exposures (Figure 2.22). This dip decreases when going south along the section to about 35° at the southernmost part of the section (Figure 2.22).

In general, when looking at the poles to the bedding planes from the Ringkollen section, a NW-SE running band of poles is observed (Figure 2.25). Although fold axes are only measured in the Ryteråker and Steinsfjord Formations, there is distinct cluster in the NE. The average fold axis in the upper part of the section, above the Klækken fault, has an orientation of $040/20^\circ$.



Figure 2.24: Mudcracks in the Steinsfjord Formation along Ringkollveien indicating a younging direction towards the SE as evidenced by the compass in the left picture.

Analysis of Ringkollen section

The Klækken fault splays from the Osen-Røa thrust and is thus, according to (Morley, 1986b), a second order thrust. From the profile (Figure 2.21) it is clear that the Ringkollen road sections contain an overturned footwall syncline associated with the Klækken fault, which is very common for this region (Morley, 1987a). This is supported by the relationship between the stratigraphic age of the formations and their dip direction and magnitude, as well as the mudcracks present in the Steinsfjord Formation indicating a younging direction towards the south.

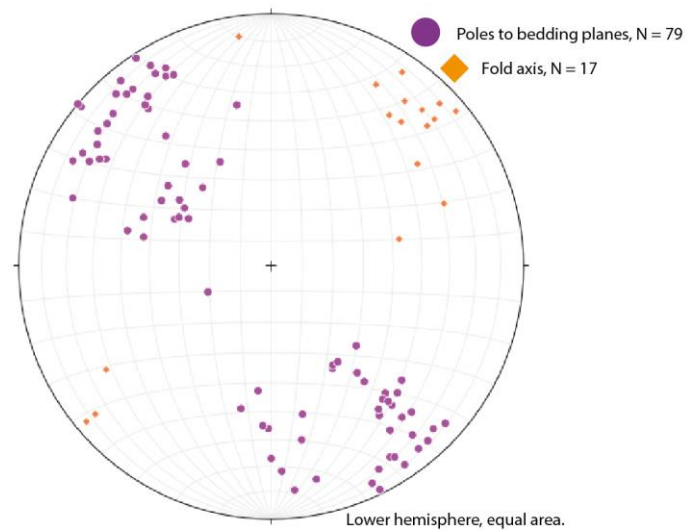


Figure 2.25: Structural data for the Ringkollen section.

3 Analogue modelling

3.1 Outstanding issues in the Oslo region

As noted by previous authors (Morley, 1987a, 1986a, 1986b; Vlieg, 2015) and is clear from the field observations in the Hønefoss area, there is a difference between the structural style of the lower (Cambrian to Middle-Ordovician) and the upper part (Middle-Ordovician to Silurian) of the stratigraphy. The weaker Cambrian to Lower-Ordovician strata are deformed mainly by imbrication and associated fault-propagation folding whereas the more competent Middle-Ordovician to Silurian strata is deformed primarily by buckle folding. These different styles are visible in outcrops north of Viul, in the Hønefoss area and in the Tyrifjord area (Vlieg, 2015). It is stated by Morley (1987, 1986a) that there is 'strong stratigraphic control on the deformation style' in the Oslo region with the more competent strata being deformed by buckle folding and the weaker strata being deformed by imbrication.

A major contrast in strain intensity has also been observed across the Klækken fault (Figure 4.9), with relatively undeformed strata being present in the footwall, except for the footwall syncline and associated structures. Deformation becomes suppressed below the Ringerike Sandstone Formation, as generally, folds, fault propagation folding and faults do not cut the Ringerike Formation. According to previous research, a major fault in north Asker, the Klækken fault, the pop-up at Ustranda (Vlieg, 2015) and a fault near Eiker (Morley, 1987a) are the only faults in the region to completely cut through the Silurian strata. These faults are thus responsible for significant strain transfer up section and possibly related to the bedding parallel detachment. The Klækken fault and the Ustranda pop-up also display a different style in their strain transfer up section.

The parameters controlling the style of this strain transfer (thrusting vs pop-up) as well as its location remains unclear. In order to investigate this issue analogue models were constructed and run. In these models rheological parameters will be varied and compared to the field observations. The aim of the modelling is thus not to recreate the Oslo Region in terms of geometry and exact distribution of deformation, but rather to investigate the geometric response of the system to mechanical/rheological variations. It is a purely mechanical study. This means that the models will not appear similar to the geometry of the Oslo Region nor the conceptual model presented in Bruton et al. (2010), but provide insight into the response on rheological variations, both spatially and stratigraphically.

Behaviour of weak basal planes is relatively well known. Therefore, the aim of these models is not to constrain the behaviour of the basal decollement, but the manner in which strain is transferred and accommodated up section. Therefore, the focus is on variations of strata higher up in the stratigraphic record. In nature, there are multiple weaker sedimentary layers present (mostly shales) higher up in the stratigraphy as well as local thickness variations of a single formation. This causes local competence variations which influence the structural style and strain transfer. Initial model setup is (mostly) based on the four fundamental characteristics of thin skinned fold and thrust belts (Chapple, 1978):

- The fold and thrust belt is thin skinned, thrusting only affects strata above a certain decollement. Strata below this horizon are not affected by any compressional deformation associated with thrusting.
- The basal decollement is generally composed of a weak rock, most often evaporate or shale.
- The sedimentary prism before, and fold and thrust belt after deformation are wedge shaped. Meaning they are thicker at the back than they are at the front in the direction where the deformation travels.
- The whole wedge, particularly its back end, has been strongly shortened and thickened.

To simulate this variable rheology, a model series of sand models was constructed with weaker ductile layers of varying sizes placed inside at various positions and heights.

3.2 Analogue modelling methodology

3.2.1 Aim and limitations

The complexity of nature means that comparing the results obtained from analogue modelling with the reality can only be done to a first order. This is due to the (significant) simplification of rheological and geometrical variations in the analogue models. Temperature dependent behaviour of the ductile material cannot be considered due to the uniform properties of the viscoelastic silicone putty's. Instead, it is assumed that the (scaled) bulk properties of the silicone putty are similar to the bulk properties of the ductile strata. The models are on crustal scale and constructed on a table, meaning flexural and isostatic variation due to external variables, such as (syn-tectonic) sedimentation, denudation or far field stresses, cannot be taken into account. Although as the first effects of nappe translation in the Oslo region were recorded around 430 Ma (Gradstein et al., 2004), so syntectonic sedimentation was not significant for the largest part of the stratigraphy. The 430 Ma age for the first (far field) effects of nappe translations observed in the Oslo Region suggest that the Osen-Røa thrust was established around this time. (Nystuen, 1983) also stated that 'initial detachment and movement of the Osen-Røa Nappe Complex started when the advancing nappe pile reached the cratonic 'Sparagmite basin' some 200-400 km NW of the present Sparagmite region', note that the Sparagmite region is the area around Mjøsa and Lillehammer.

Convergence velocity is also rarely constant, both in magnitude and direction. However, as the aim of the models is to investigate large scale structures this simplification is deemed acceptable. Combining this with the fact that the models are always a simplification of nature, it is clear that the results should always be compared to natural examples in order to prevent unrealistic conclusions. However, the main goal of these analogue models is to determine the influence of the mechanical and rheological properties of the strata on the geometry and distribution of the produced structures. Therefore, the results are not directly compared one to one with nature, but are used to provide further insights into the first order control of these mechanical and rheological properties on the geometry of the observed structures.

Figure 3.1 shows the definition of terms and directions used with respect to the models of this project. A backthrust is defined as a thrust where the overriding material moves towards the backstop. Similarly, a forethrust is defined as a thrust where the overriding material moves towards the foreland away from the backstop. In nature, the competence contrast of different strata is likely much smaller than the exaggerated situations used in this study. The rheological variations present represent smaller variations in nature. They can be a simulation of lateral changing of sedimentary facies or formation of small, local thickness variations in the strata. Both situations result in a local variation in strength and thus create a competence contrasts. The extreme differences in competence used in this study are purposely created in order to induce a strong reaction. This means that the initial setup is exaggerated, but this does give us clear control on the parameters responsible for the formed structures. As it is a purely mechanical study, the exaggerated nature of the models is noted and accepted.

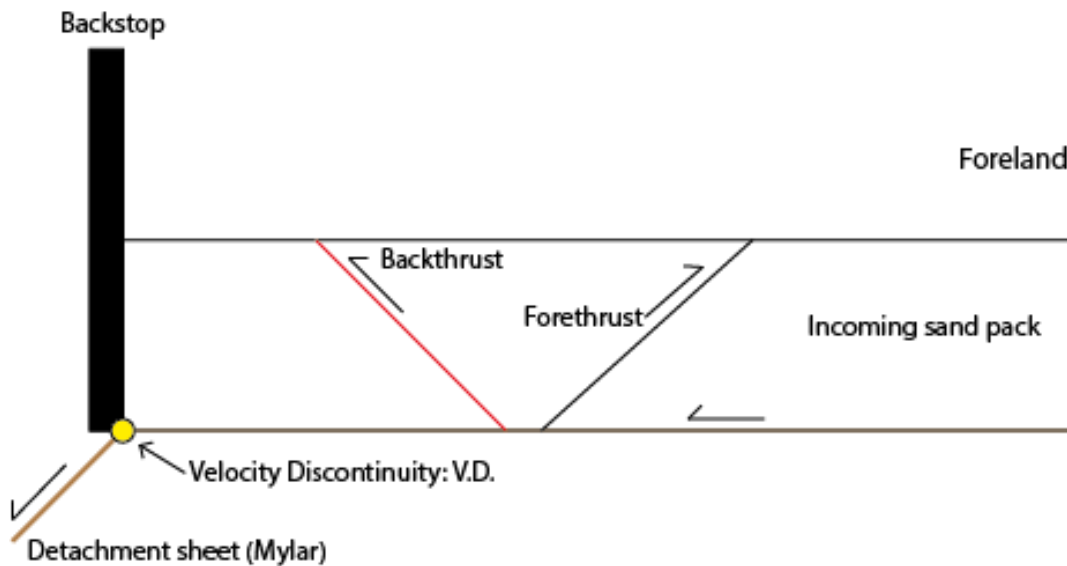


Figure 3.1: Schematic representation defining nomenclature used in treatment of analogue modelling results.

3.2.2 Experimental setup and procedure

The experiments were performed at the Teclab of the Department of Earth Sciences at Utrecht University. The experimental setup consisted of a backstop attached to an engine frame. Below this backstop, on the table, a 30 cm wide Mylar sheet was placed on which the models were constructed. Shortening of the models was accomplished by pulling the basal Mylar sheet underneath the backstop at a constant velocity of 5 cm/hour. This created the velocity discontinuity (V.D.) at the point where the sheet slides under the backstop (Figure 3.1). Small round glass beads were distributed below the basal Mylar sheet to reduce sliding friction and create smoother shortening. Metal bars with a width of 5 cm and varying thicknesses were used to provide lateral confinement. The models were shortened by 10-20% bulk shortening, which amounted to 10-15 cm of shortening. To record the evolution of the model, a Canon 1100D camera was positioned above the model, taking a picture every 60 seconds. To preserve the model for analysis, the surface structures were covered in black quartz sand and thoroughly wetted. Cross-sections were made by cutting the model orthogonally to the

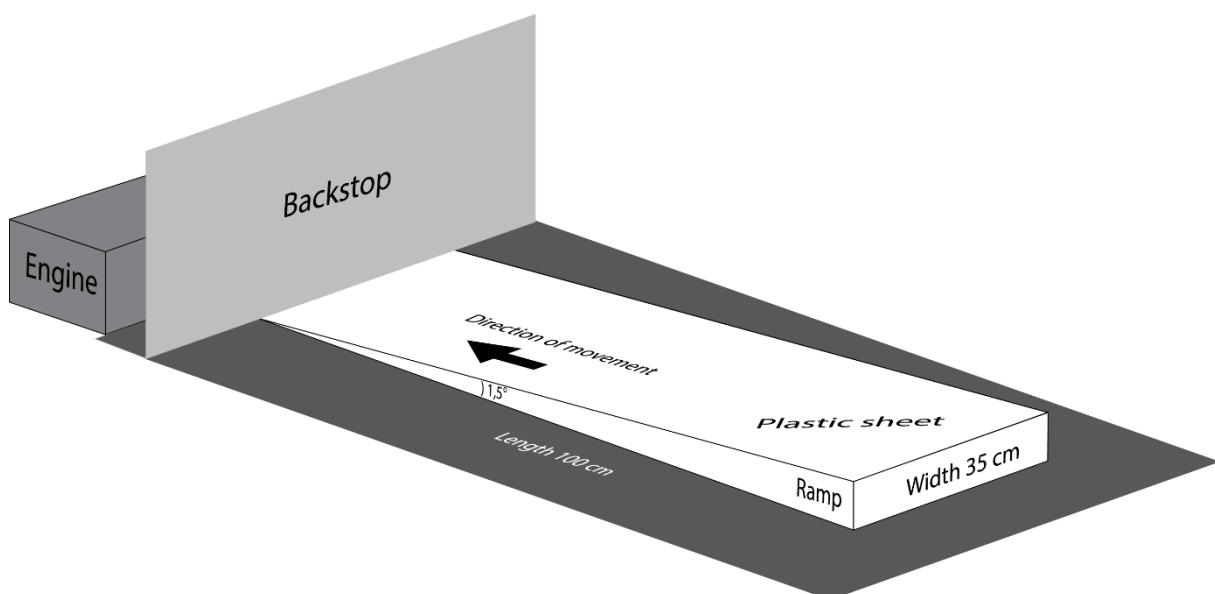


Figure 3.2: Schematic representation of the initial modelling setup. The basal inclination was varied between 0 and 1.5°.

Table 3.1: Properties of the materials used for analogue modelling.

<i>Material</i>	<i>Density ρ (g/cm³)</i>	<i>Viscosity η (s⁻¹)</i>	<i>n-value</i>	<i>A-value</i>	<i>Grain size (μm)</i>
<i>Quartz sand</i>	1.5	-	-	-	100- 355
<i>Weak silicone</i>	1.0	$1.98 \cdot 10^4$	1.2	$1 \cdot 10^{-5}$	-
<i>Strong silicone</i>	1.8	$2.88 \cdot 10^5$	1.6	$2 \cdot 10^{-8}$	-

strike of the structures and the backstop, after which these sections were photographed. Structures visible on top view and cross section photographs were traced using Adobe Illustrator software in order to accentuate the developing structures.

3.2.3 Materials and scaling

In order to produce a model that is realistically scaled, several scaled analogue materials were used. Dry quartz sand was used as a brittle material, as its properties make it a suitable analogue material for brittle behaviour (Graveleau et al., 2012) and references therein). The grain size of the used material was between 100 and 355 μm and it had a density of 1.5 g/cm³ (Table 3.1). The coefficient of internal friction of the quartz sand was 0.57 and it had a negligible cohesion. Ductile decollements in the crust (e.g. Salt or (over pressured) shale) were simulated using two silicone putty's. These putty's exhibit viscoelastic/ductile behaviour, with one material being very weak and the other material being very strong (Table 3.1). The weak material is a pure silicone (PDMS-SG36) and the strong material is based on rhodopile and contains fillers of BaSO₄, it was mixed at Utrecht University's TecLab.

A valid comparison between models and natural examples can only be made if there is a rheological, dynamic, kinematic and geometric similarity (Hubbert, 1937; Ramberg, 1981). Rheological similarity requires that the analogue materials have similar rheological behaviour to natural materials. Geometric similarity requires proportionality between the natural and the experimental lengths. This is usually defined as:

$$L^* = \frac{L_m}{L_n} \quad (1)$$

Dynamic similarity is reached when the ratio between different forces act in the model and in nature is constant, in the equation of dynamics this:

$$\frac{\delta\sigma_{ij}}{\delta x_{ij}} + \rho \left(g - \left(\frac{\delta^2 \epsilon_{ij}}{\delta t^2} \right) \right) = 0 \text{ with } (i, j = 1, 2, 3) \quad (2)$$

σ_{ij} = Stress components [Pa]

ϵ_{ij} = Strain components [s⁻¹]

x_{ij} = Space coordinates

ρ = Density of the material [m³/kg]

g = gravitational acceleration [m/s²]

t = Time [s]

From equation 2 it can be determined that there is a relationship between the ratios of the stresses and the thickness of the ductile layers (equation 3) and between the strain and time (equation 4).

$$\sigma^* = \rho^* g^* D^* \quad (3)$$

$$\epsilon^* = g^* (t^*)^2 \quad (4)$$

σ^* = Ratio of stresses [–]

ρ^* = Ratio of densities [–]

g^* = Ratio of gravitational accelerations (= 1 for these experiments) [–]

D^* = Ratio of thicknesses of the ductile layers [–]

ϵ^* = Ratio of strains [–]

t^* = Ratio of time [–]

As inertial forces are neglectable in geological processes (Hubbert, 1937) and experiments are conducted under normal gravity, equation 3 simplifies in such a way that the ratios of stresses roughly equal the ratios in thickness (equation 5).

$$\sigma^* \approx D^* \quad (5)$$

This leaves only equation 4 for verification (Brun, 2002). For ductile materials, velocity and viscosity can be scaled from the following equations:

$$\epsilon^* = \frac{\sigma^*}{\eta^*} \quad (6)$$

$$\epsilon^* = \frac{v^*}{L^*} \quad (7)$$

Where ϵ^* , σ^* , η^* and L^* are the strain rate, stress, velocity, viscosity and length ratios respectively. When combining the stress ratio from equation 2 with equations 6 and 7 it is possible to take a fixed value for the viscosity ratio (η^*) from equation 6 and calculate the velocity ratio (v^*). Or it is possible to fix the velocity ratio (v^*) and calculate the viscosity ratio (η^*). Accounting for time is somewhat more complex, as the requirements for velocity in modelling are (Ramberg, 1981):

$$t^* = \frac{t_m}{t_n} = \frac{1}{\epsilon^*} = \frac{\eta^*}{\sigma^*} = \frac{v^*}{L^*} \quad (8)$$


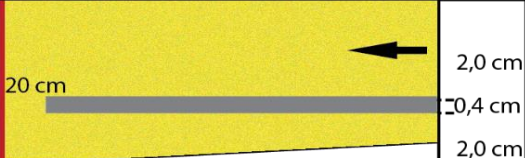
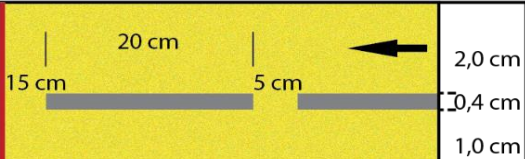
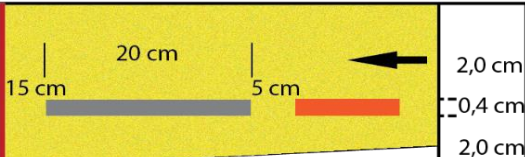
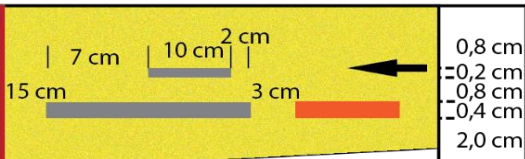
This means that for a thickness ratio of 10^{-5} (1km in nature equals 1 cm in the model) and a realistic natural timespan of 10^6 years, the model would take 3160 years, which is impractical (Ramberg, 1981). Kinematic similarity requires a similar evolution between the model and the natural prototype. These dynamic and kinematic similarities can be tested using dimensionless ratios of gravitational and viscous forces. For ductile layers the Ramberg number (R_m) is defined as (Ramberg, 1981):

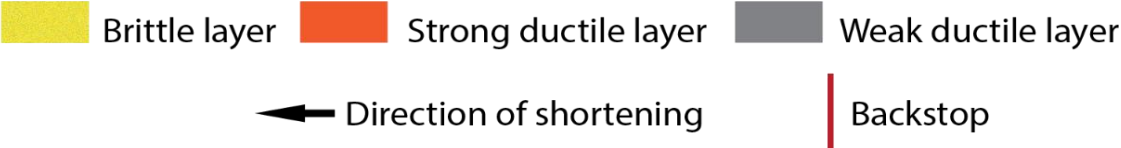
$$R_m = \frac{\rho g h}{(\sigma_1 - \sigma_3)_{viscous}} \quad (9)$$

Where ρ and h are density and thickness of the ductile layer respectively. $(\sigma_1 - \sigma_3)_{viscous}$ is the strength of the ductile material (equation 9). For brittle behaviour the similarity to be valid, the ratios between gravitational and frictional forces has to be similar. This is calculated using the Smoluchowsky number (S_m) (Ramberg, 1981):

$$S_m = \frac{\rho gh}{c + \mu \rho gh} \quad (10)$$

Where ρ , h , c and μ are defined as density, thickness, cohesion and coefficient of friction of the brittle layer. The models have a scale ratio of $D^* = 10^{-5}$, which gives a negligible scaled cohesion. The quartz sand used in the experiments had a density of 1.5 g/cm^3 and negligible cohesion and is therefore a suitable analogue material to natural rocks in the brittle domain. The scale ratio of $h^* = 10^{-5}$ implies that 1 cm in the model represents 1 km in nature.

Exp. #	Mechanical setup & stratigraphy (cross-section)	Mechanical conditions
1		Velocity: 5 cm/h Bulk shortening: 13% Inclination: 0°
2		Velocity: 5 cm/h Bulk shortening: 15,5% Inclination: 1.5°
3		Velocity: 5 cm/h Bulk shortening: 20% Inclination: 0°
4		Velocity: 5 cm/h Bulk shortening: 10% Inclination: 1.5°
5		Velocity: 5 cm/h Bulk shortening: 13% Inclination: 1.5°



Brittle layer
 Strong ductile layer
 Weak ductile layer
 Direction of shortening
 Backstop

Figure 3.3: The initial stratigraphic setup of the various models and details regarding the deformation velocity and bulk shortening applied as well as basal inclination. Note the increasing complexity of the initial setup. For more details the reader is referred to the text.

3.2.4 Variation of parameters

In order to investigate the role of the mechanical and rheological properties of the system on the geometry of the structures, 5 models were made. The varied parameters are the lateral extent of the weak ductile layer, basal inclination, the addition of a (very) competent ductile layer and the presence of a weak ductile layer higher up in the stratigraphy (Figure 3.3). The model series is divided into two groups; lateral homogeneous and lateral inhomogeneous models. The first category contains no lateral variations in stratigraphy whereas the second does contain lateral variation in the stratigraphy (Figure 3.3). Models 1 & 3 serve as starting models to provide a reference frame for other models with more rheological variations. Models 1 & 2 provide a good reference point to determine which structures are the result of basal inclination and which might be the result of lateral stratigraphic variation. Models 2, 4 and 5 have a lateral discontinuity in the ductile layers where it is separated by sand. This simulates the lateral and in the case of model 5 the stratigraphical variations present in nature. The very competent ductile material used in models 4 and 5 is used to simulate the Ringerike Formation. Its position, with weak ductile material and sand present at the same stratigraphic level simulates the local competence variations in the Ringerike Formation.

3.2.5 Construction and strength profiles

All models were 30 cm wide, 100 cm long and 2.4 cm thick (Figure 3.2; Figure 3.3). The brittle part of the stratigraphy was constructed by sieving quartz sand through a 355 μm mesh onto the Mylar sheet, underlying layers or the silicone putty. The viscoelastic silicone putty's were prepared with a 0.4 or 0.2 cm thickness and subsequently placed inside the stratigraphy (Figure 3.3). A grid with a spacing of approximately 5 cm was constructed on top of the model to create a reference frame.

In order to determine the amount of coupling between the brittle and ductile layers as well as presenting the strength of the models for verification of the scaling, strength profiles were constructed for the initial setup of all models on multiple localities and are included in Appendix B. The strain rate $\dot{\epsilon}$ is calculated by $\dot{\epsilon} = v/l_0$, with v being the velocity in m/s and l_0 being the initial thickness of the ductile layer in m . To calculate the differential stress for the brittle part of the stratigraphy, equation 11 (Weijermars, 1997) equation (6-5a), page 99, modified) is used.

$$(\sigma_1 - \sigma_3) = 2 \frac{\mu \rho g z}{\sqrt{(\mu^2 + 1) - \mu}} \quad (11)$$

With differential stress: $(\sigma_1 - \sigma_3)$ in Pa, coefficient of internal friction: μ , density: ρ in kg/m^3 , gravitational acceleration: g in m/s^2 and depth z in m . Ductile strength is calculated using equation 12, which is a non-Newtonian flow equation (Weijermars, 1997).

$$(\sigma_1 - \sigma_3) = 2 \left(\frac{\dot{\epsilon}}{A} \right)^{1/n} \quad (12)$$

With differential stress: $(\sigma_1 - \sigma_3)$ in Pa, the strain rate: $\dot{\epsilon}$ in s^{-1} , the material parameter, which is a function of temperature, pressure and material properties: A and the stress exponent: n .

3.3 Modelling results

For an overview of the different initial, stratigraphic setup, the reader is referred to Figure 3.3. Top view photographs are displayed for each 5% bulk shortening increment. The final top view photograph

is also shown. When looking at the top views, curved geometry of the structures is observed near the confining sidebars in each experiment. This is the result of friction with these side bars and is therefore a boundary/side effect. It has little to no impact on the structures. A legend explaining the different symbols used in the tracing of the structures is displayed in Figure 3.4.

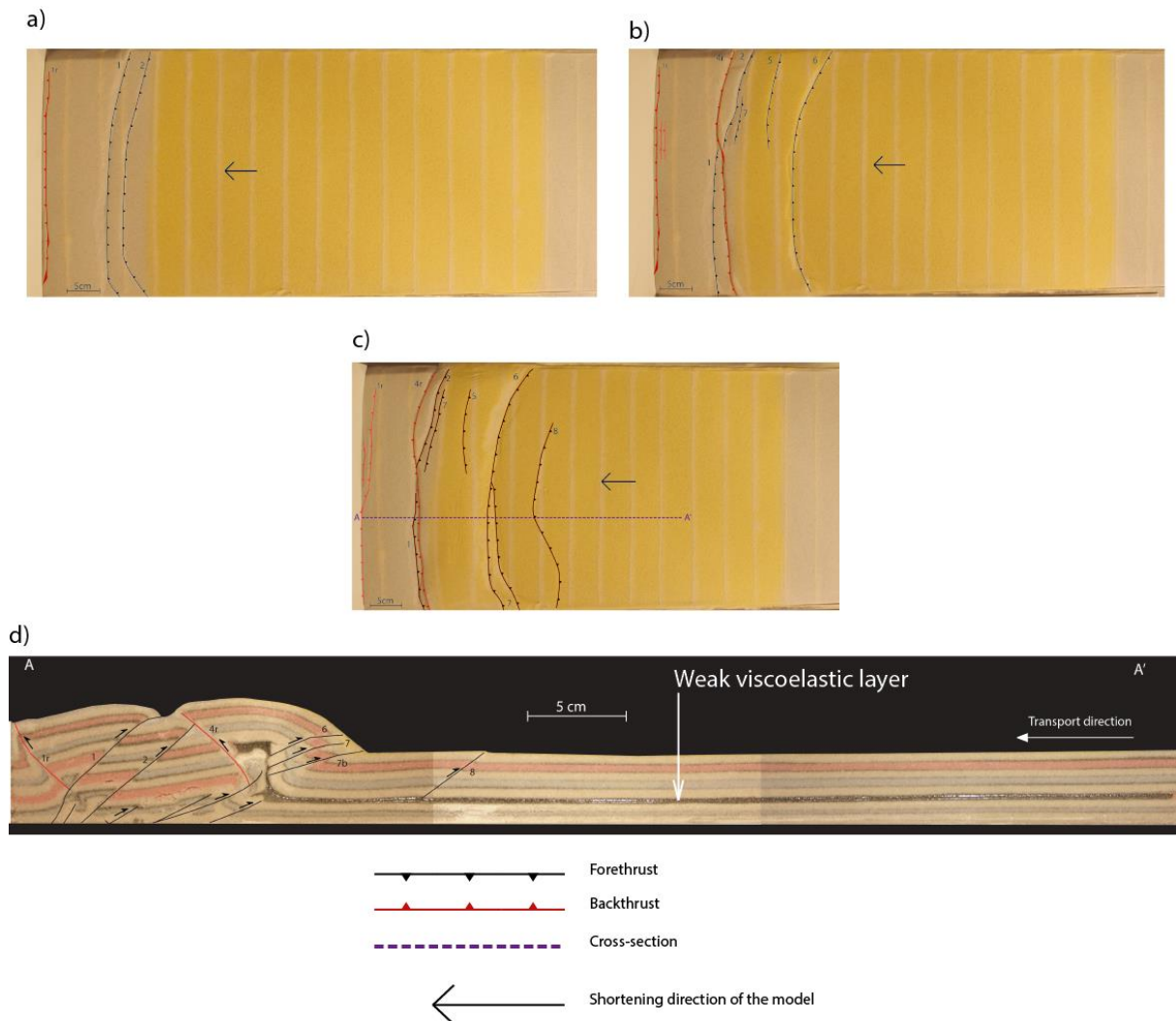


Figure 3.4: Modelling results for model 1. Note the weak viscoelastic material. All other layers consist of quartz sand. a) Top view after 5% bulk shortening. b) Top view after 10% bulk shortening. c) Final top view after 13% bulk shortening. d) Cross section A-A', section location in final top view. Note the legend for the symbols is the same for all model presented and will only be displayed here.

3.3.1 Model 1 (Figure 3.4)

After 5% bulk shortening, a first pop-up structure is formed directly in front of the backstop, nucleating slightly in front of the V.D. (Figure 3.4a). This first pop-up is approximately 8 cm wide. Deformation propagated almost immediately slightly forward in the form of a second forethrust. Moving on to 10% bulk shortening (Figure 3.4b), the second forethrust is overprinted by a backthrust. Several small forethrusts then develop, with the 6th one spanning the entire width of the model. Deformation has propagated roughly 8 cm forward. Also note the formation of multiple local backthrust near the backthrust. At 13% bulk shortening (Figure 3.4c), a forethrust nucleating in the centre of the 6th forethrust is formed. Movement on the 6th fault continued, as is apparent from the increased relief.

Deformation propagated finally propagated forward, as indicated by the formation of an 8th thrust fault. However, movement along this 8th thrust faults was slight.

The position of the section is displayed on the final top view (Figure 3.4c). Some small faults near the base of the model are visible on the cross section (Figure 3.4d). These are not numbered as it is unclear when each one was formed, except for the 3rd forethrust which ends as a blind thrust due to the viscoelastic layer (Figure 3.4d). The viscoelastic layer becomes active, squeezing up along the 4th backthrust. It is the source of the 6th and 7th forethrust as well as the final fault (No. 8). Some slight disturbances in the viscoelastic material are visible below the nucleation point of the 4rd backthrust. These are related to movement on these small faults.

3.3.2 Model 2 (Figure 3.5)

As with the other models, the first structure to nucleate and develop is a pop-up directly in front of the backstop with the backthrust against it. It is approximately 15 cm wide after 5% bulk shortening (Figure 3.5a). Some small thrust nucleate near the top half of the model at 10% bulk shortening (Figure 3.5b), however the most significant deformation propagates further in the form of a pop-up with a forethrust made up of several branches. The backthrust of this structure overprints most of the 1st forethrust (Figure 3.5b). Continuing to 15.5% bulk shortening (Figure 3.5c), deformation has propagated forward, past the viscoelastic layer. The 6th forethrust is again a branch of the 5th. Jumping forward ~8 cm, the 7th forethrust nucleates at the end of the viscoelastic layer (Figure 3.5d). Subsequent deformation is out of sequence as it jumps back in the direction of the backstop where a final pop-up structure is formed.

In cross section it becomes apparent that the viscoelastic layer is active, as evidenced by the low amplitude, long wavelength folding as well as the rising of small volumes of ductile material resembling a diapir geometry (Figure 3.5d). Ductile material is squeezed up and brittle faults nucleate from the tips of this ductile material. Further towards the backstop, the ductile material is folded upwards due to the formation of a deep fault (Figure 3.5d). This fault is not numbered as the exact timing of its movement is unclear. The backthrusting above this fault, near the backstop, is responsible for the rotation of the first initial pop-up. Also note the offset of the 1st thrust by the 5th backthrust. Deformation is thus slightly more spread out than in model 2, with a focus on the area near the backstop. Propagation is however of a similar magnitude as evidenced by the frontal thrust (thrust 7, Figure 3.5d).

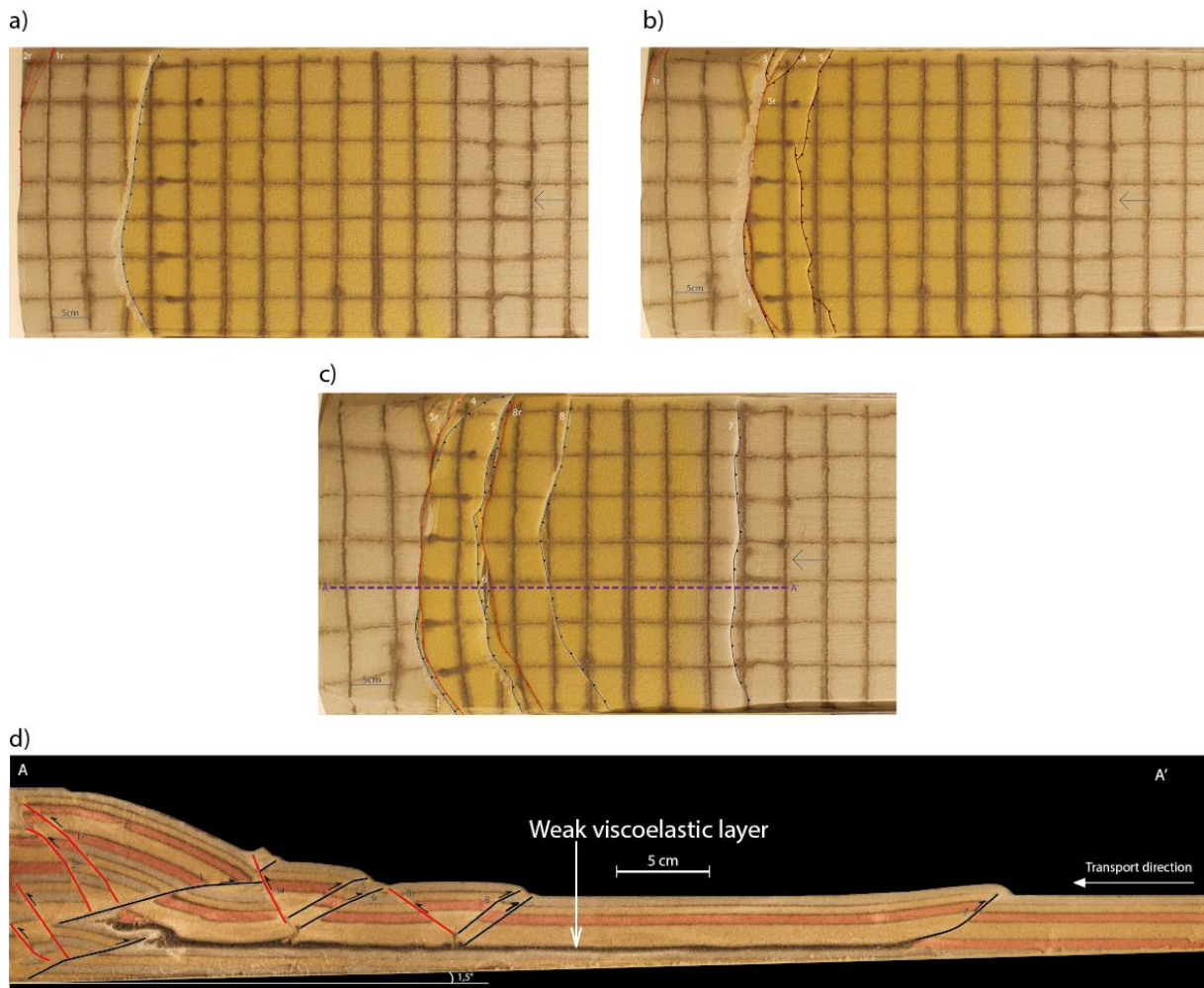


Figure 3.5: Modelling results of model 2, same setup as model 1 with the addition of 1.5° of basal inclination. Note the weak viscoelastic material, all other layers consist of quartz sand. a) Top view after 5% bulk shortening. b) Top view after 10% bulk shortening. c) Final top view after 15.5% bulk shortening. d) Cross section A-A', section location in final top view. Legend as in Figure 3.4.

3.3.3 Model 3 (Figure 3.6)

Nucleating slightly in front of the V.D., a first pop-up structure nucleates and increases its relief before the backstop at 5% bulk shortening (Figure 3.6a). Subsequent deformation propagates rapidly towards the foreland, with 4 extra forethrusts followed by a second pop-up having formed at 10% bulk shortening (Figure 3.6b). Although the majority of these faults are located in the top half of the top view and do not span the entire width of the model (Figure 3.6b). Whilst the 5%-10% bulk shortening interval contained significant amounts of propagation and deformation, at 15% bulk shortening the amount of additional deformation is less. Deformation has propagated towards the second viscoelastic layer by means of a single forethrust and multiple small backthrusts (Figure 3.6c). Continuing movement on the older structures is also observed as is apparent from the increased relief. At 20% bulk shortening deformation has propagated towards the end of the second viscoelastic layer by means of a final pop-up structure. Movement on older structures also led to an increased relief near the backstop (Figure 3.6d).

When looking in cross section, this model contains interesting geometries. The final pop-up nucleates at the exact end of the second viscoelastic layer and movement on these faults is not very significant (Figure 3.6e). Going towards the backstop, the entire stratigraphic column is undisturbed until the beginning of the second viscoelastic layer. At the start of this layer a small thinned structure

is visible in the viscoelastic material (Figure 3.6e). Above this structure is a ramp flat ramp system containing a single forethrust and multiple small backthrusts, all nucleating in the first viscoelastic layer. The forethrust is relatively steep, at $\sim 38^\circ$. Geometries become complex near the backstop, with structures overprinting each other (Figure 3.6e). A lens like structure nucleates from the first viscoelastic layer and meets a branch of the 4th/5th forethrust. This 4th/5th nucleates from what appears an antiformal stack like geometry with the ductile material being folded and squeezed along the faults (Figure 3.6e). Movement on the 4th thrust was followed by movement/ nucleating of the 5th thrust. This was shortly followed by nucleation of the 5th backthrust, cutting of the 4th forethrust (Figure 3.6e). The first pop-up is squeezed up against the backstop and rotated towards the foreland as a result. Deformation is localised mainly on the tips of the viscoelastic layers (Figure 3.6d/e).

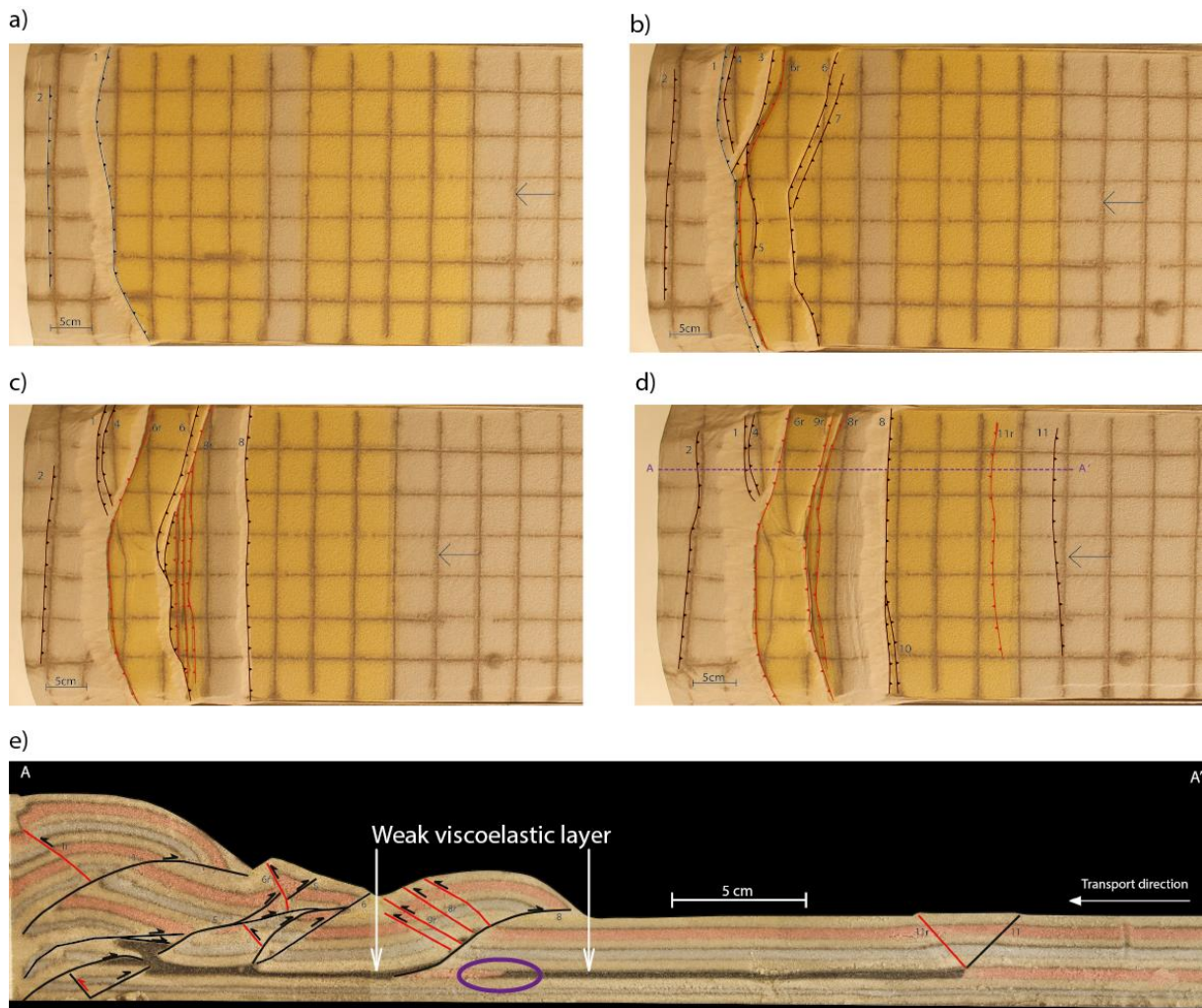


Figure 3.6: Modelling results of model 3, no basal inclination. Contains a lateral competence difference in the form of brittle sand between two weak viscoelastic layers (pointed out). All other layers consist of quartz sand. a) Top view after 5% bulk shortening. b) Top view after 10% bulk shortening. c) Top view after 15% of bulk shortening. d) Final top view after 20% bulk shortening. e) Cross section A-A', section location in final top view. Legend as in Figure 3.4.

3.3.4 Model 4 (Figure 3.7)

After 5% bulk shortening a large pop-up has developed in front of the backstop (Figure 3.7a). This pop-up is roughly 20 cm wide and contains a second backthrust. Branching the first forethrust is a second thrust, this creates a situation where the main part of this thrust is active during both the formation/movement on the first thrust as well as during the formation/movement of the second

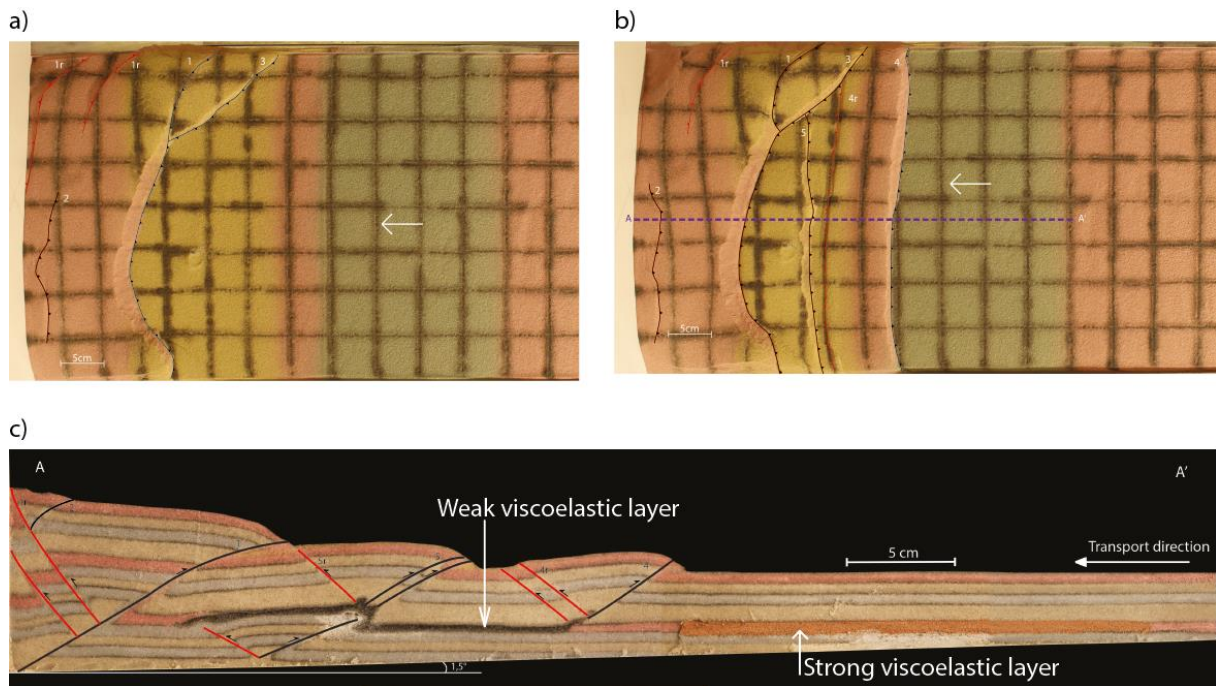


Figure 3.7: Modelling result of model 4, basal inclination of 1.5° and two different viscoelastic layers (weak and strong) for lateral competence differences. All other layers consist of quartz sand. a) Top view after 5% bulk shortening. b) Final top view after 10% bulk shortening. c) Cross section A-A', section location in final top view. Legend as in Figure 3.4.

thrust (Figure 3.7a). Deformation then propagates forward and by 10% bulk shortening a second, 8-10 cm wide, pop-up has formed just before the start of the very competent viscoelastic layer (Figure 3.7b). Subsequent deformation then becomes out of sequence as deformation moves back in the direction of the backstop with the formation of the 4th forethrust (Figure 3.7b).

In cross-section it is observed that the weak viscoelastic layer becomes active (Figure 3.7c), both near the backstop where it is thinned as at other spots. The 3rd fore- and backthrusts nucleate from the tip of the weak viscoelastic layer, which is also thinned and stretched at the nucleation point (Figure 3.7c). In the centre the weak layer is pushed up due to a pop-up structure with an unknown timing (Figure 3.7c). Above this structure the 4th pop-up nucleates. In-between these structures, there is little to no deformation visible.

3.3.5 Model 5 (Figure 3.8)

Unlike the previous models, model 5 does not have an initial pop-up structure spanning the entire width of the model after 5% bulk shortening (Figure 3.8a), it has a large wide forethrust spanning the entire width instead. But the backthrust is only present in the lower part of the model (Figure 3.8a). Subsequent deformation manifests itself in out of sequence forethrusts. Deformation then continues in an out of sequence manner. After 10% bulk shortening the deformation propagates towards the start of the strong viscoelastic layer (Figure 3.8b). After which it jumps back and forth as becomes clear from the timing of the faults. Multiple faults are reactivated and deformation jumps between foreland and hinterland verging (Figure 3.8b). The structures also curved along strike. After 13% bulk shortening, deformation has continued in its erratic out of sequence manner (Figure 3.8c). Deformation has propagated slightly forward, but reactivation of several older structures has also taken place.

In cross-section the structures are rather complex (Figure 3.8d). The strong viscoelastic layer is not deformed at all, a sand wedge is formed before it by forethrust 8. As mentioned above, this model has

two weak viscoelastic layers above each other (Figure 3.3). The lower weak layer has been strongly activated, with the tip closest to the backstop being stretched out (Figure 3.8d). Further forward, this weak layer becomes very mobile following faults both up and down in drag structures. Continuing forward, lens structures are observed ending in a blob of weak viscoelastic material (Figure 3.8d). Here the weak material has been stretched and folded and has undergone high strain. Going up in stratigraphy, above the first weak viscoelastic layer, a pop-up structure nucleates from this layer. This pop-up is cross-cut by subsequent backthrusting. The 10th forethrust originates in the lower weak layer and passes by the tip of the second weak layer (Figure 3.8d). Backthrust 6/13 mobilises the second weak layer as it is somewhat concentrated below this fault. In summary, this model shows significant deformation and strain just before the strong viscoelastic layer. Deformation is characterised by out of sequence thrusting and folding and activation of the weak viscoelastic layers.

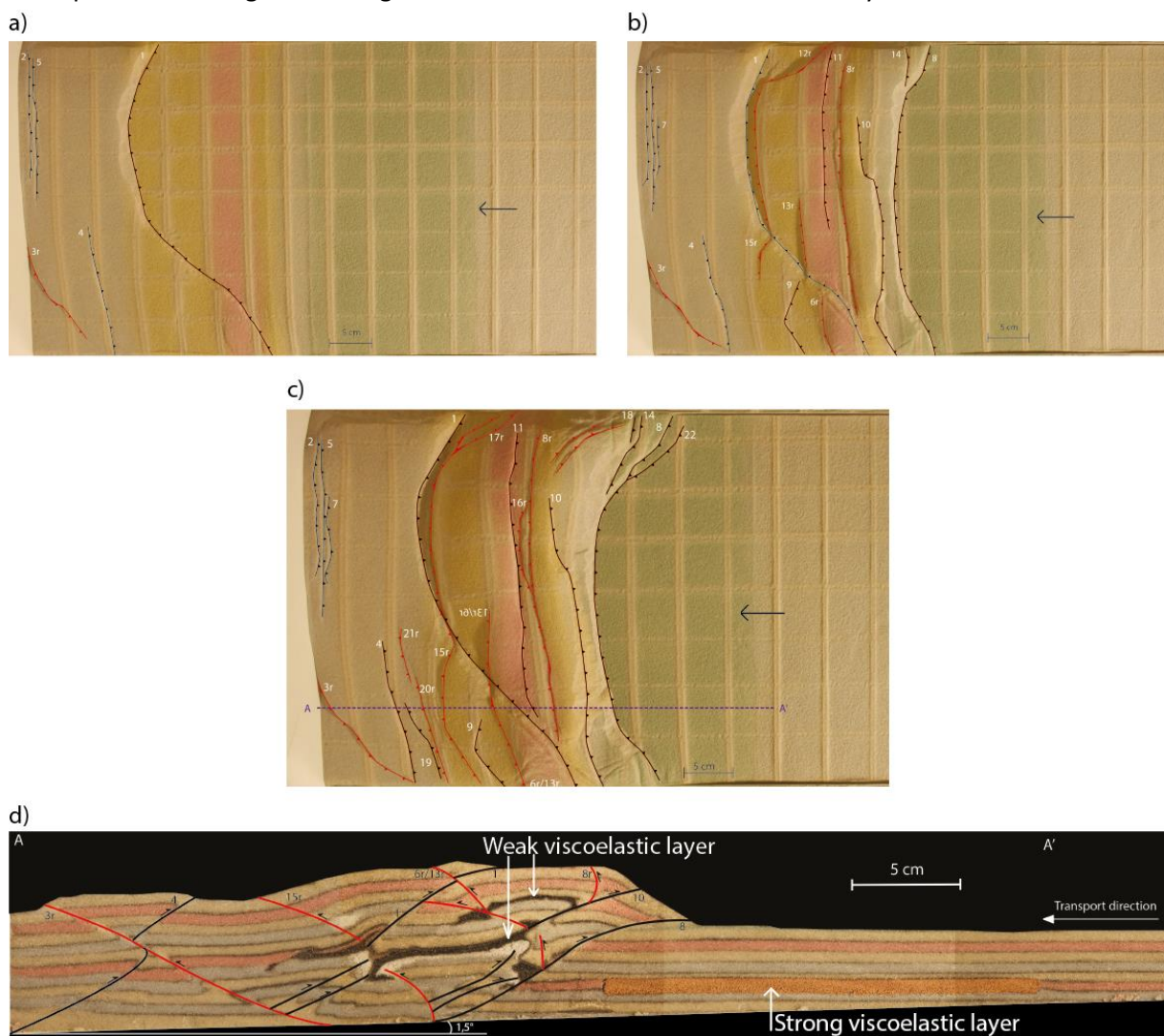


Figure 3.8: Modelling results of model 5, contains two weak and one strong viscoelastic layer all other layers consist of quartz sand. a) Top view after 5% bulk shortening. b) Top view after 10% of bulk shortening. c) Final top view after 13% of bulk shortening. d) Cross section A-A', section location in final top view. Legend as in Figure 3.4.

3.3.6 Summary of modelling results

A series of 5 models were run with varying rheological and geometrical parameters in order to determine what parameters control the style of strain transfer up section and how shortening discrepancies in vertical stratigraphy are accommodated.

The first model was laterally homogeneous with a weak viscoelastic layer one cm above the basal decollement (Mylar sheet) (Figure 3.3). Strain transfer up section was rather limited in the foreland with only a single small offset fault being present (Figure 3.4). There was no significant deformation below the viscoelastic layer. Model 2 consisted of the same setup as model 1 with the addition of a 1.5° basal inclination (Figure 3.3). Deformation in this model propagated much more towards the foreland and also contained more strain transfer up section in the form of two pop ups (Figure 3.5). There was no significant deformation below the viscoelastic layer. Model 3 was the first laterally heterogeneous model but with no basal inclination (Figure 3.3) resulting in much more pronounced strain transfer up section. It contained a very complex set of faults above the left viscoelastic layer as well as a ramp flat system with multiple small offset backthrusts at the end of the left viscoelastic layer (Figure 3.6). The second viscoelastic layer was activated and strain transferred laterally, as evidenced by layer parallel slip, to form faults no. 11 and 11r. There was no significant deformation below the viscoelastic layer. Model 4 contained a lateral heterogeneous setup of a weak viscoelastic layer in the back and a strong viscoelastic layer in the front and basal inclination was set at 1.5° (Figure 3.3). Deformation propagated towards the end of the weak viscoelastic layer in the form of a pop-up and was followed by a second, out of sequence, pop-up (Figure 3.7). This model did contain some deformation below the weak viscoelastic layer in the form of another pop-up. Model 5 had the same setup as model 4 with the addition of a second weak viscoelastic layer above the lower weak viscoelastic layer (Figure 3.3). Both weak viscoelastic layers were strongly activated, displaying folding as well as thrusts nucleating from their ends. Deformation below the lower weak layer was also present. The thrusting sequence was also strongly out of sequence (Figure 3.8) and a strongly deformed zone transferring strain upwards, much wider than in previous models, formed.

3.4 Initial discussion of modelling results – similarities with nature

Before starting the discussion on the modelling results it should be noted that all models contain boundary effects as a result of the backstop. The nature of the setup is such that the compressional structures are created due to shortening against a, for all practical considerations, infinitely high backstop creating a single vergent thrust wedge. Directly at the backstop, hinterland directed movement is not possible and material can only be transported forwards and upwards leading to unrealistic large displacements on these initial faults. Farther away from the backstop however, these effects are neglectable and results can be interpreted safely.

Although the modelling study is mechanical in nature, some of the structures formed in various models do show similarities with observed field structures. It is therefore possible that the mechanisms responsible for the formation of these structures in the field have been replicated in certain parts of the models. Model 1 contains a footwall syncline geometry very similar to the footwall syncline of the Klækken fault (Figure 3.9). However, that syncline contained an overturned limb (Figure 2.21) and the syncline in the model does not. This is because the movement along fault no. 6 was halted before it could overturn. The following faults (no. 7 & 7b) further accommodated the shortening.

This tendency of sand to break instead of fold is due to the homogeneous nature of the sand pack, which makes it impossible for layer parallel slip to occur and for folds to be accommodated (J. Smit, pers. comm. 2015). When strata are transported up a ramp and layer parallel slip between the layers is not possible rotation of the bedding is not possible and the strata will be transported up along the ramp in a passive manner. It is then cut by numerous small offset thrusts to accommodate the shortening creating a geometry hereafter referred to as a 'step geometry' (Figure 3.10). In nature layer parallel slip in the overriding strata would be possible due to stratigraphical heterogeneities present. This means the strata will fold as it is transported up-section. When this continues long enough a fault and associated hanging wall anticline – footwall syncline geometry will develop. This is observed at the Klækken fault, however the only slightly rotated strata making up de steps indicate that this has not happened. This geometry is also prevalent in a backthrusting situation, such as around fault no. 8 in model 3 (Figure 3.6). It is more clear than in the forward directed setting of model 1 as the strata is not rotated at all, clearly indicating that the closely spaced thrusts are a response to the forming of the ramp system. However, as observed in model 5 (Figure 3.8), the sand pack can display (limited intensity) folding but only if it is located directly above a weak viscoelastic layer which can activate in a simple shear manner. This effectively results in some layer parallel slip accommodating the folding.

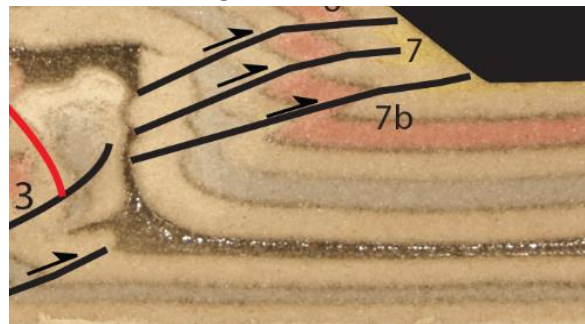


Figure 3.9: Geometry in model 1 similar to the overturned footwall syncline observed in the Ringkollen section. Note the three small offset faults. For more details the reader is referred to the text.

Although not at all developed, the most forward structure in model 3 is a slightly similar situation to the frontal part of the thrust system near Slemmestad (Figure 3.12). Model 3 only contains a single fault here, caused by strain transfer through the viscoelastic layer. Deformation propagates farther in this model (M3) than in model 1 due to the inclination. As the sand pack gets thinner near the front of the wedge the yielding strength decreases due to its linear relationship with the strata thickness (section 3.2.3). Similarities are more clear between the style of the Slemmestad area (Figure 3.12) and models from (Smit et al., 2003), especially his 1.5° inclined model deformed with 5 cm/h (Figure 3.11). The style of deformation changes towards the front of the wedge, with thrust transport directions being dominantly towards the front. This is explained by an increase in brittle – ductile coupling which is the result of decreasing brittle thickness towards the front (Smit et al., 2003). Both the model from Smit et al. (2003) (Figure 3.11) as well as field observations in the Oslo region (Figure 3.12) show that thrust vergence becomes dominantly foreland directed.

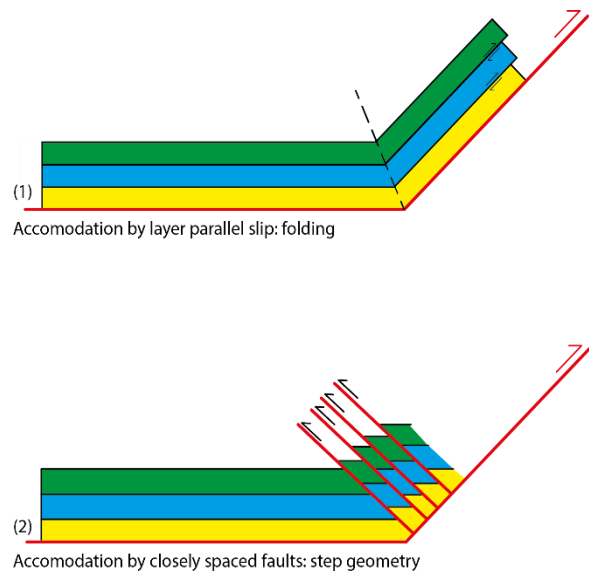


Figure 3.10: Schematic representation of a 'step geometry' as defined in the text. Situation 1 (top) displays the folded geometry achieved when a segment of strata is moved up along a ramp and layer parallel slip can occur between the layers.

-Situation 2 (bottom) displays the step geometry achieved when a segment of strata is moved up along a ramp and layer parallel slip **cannot** occur between layers. Note the lack of rotation in the bedding, segments are passively transported up along the ramp.

Model 5 contains very complex structures and significant out of sequence deformation. The model can be compared, to a first order, with structures observed in the Ustranda pop-up in the Tyrifjord area (Figure 3.8 vs Figure 3.13). Although the structures in the model are different from nature at first glance, the style shows some resemblance. There is significant out of sequence deformation as well as folding and activation of weak layers. All of these structures are, albeit on a smaller scale, observed in the Ustranda road section (Vlieg, 2015). Leading to the interpretation that the mechanism responsible for their formation in nature, is similar in the mechanism responsible for the formation of structures in the model.

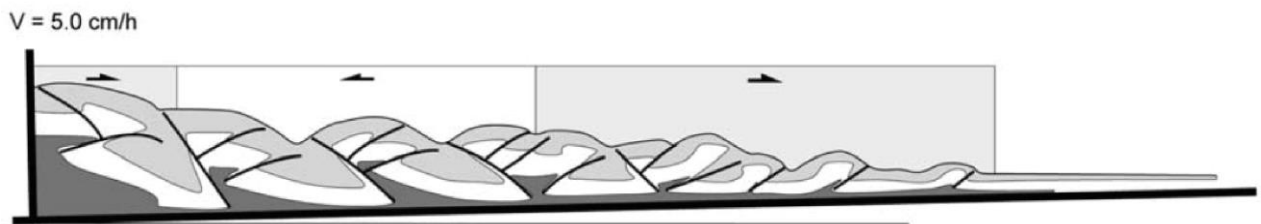


Figure 3.11: Model result from Smit et al. (2003) of a single vergent brittle-ductile thrust wedge. Basal inclination is $1,5^\circ$ and velocity was 5 cm/h. Note the different thrust vergence in different parts of the thrust wedge. For more details the reader is referred to the text and to Smit et al. (2003). Figure from Smit et al. (2003).

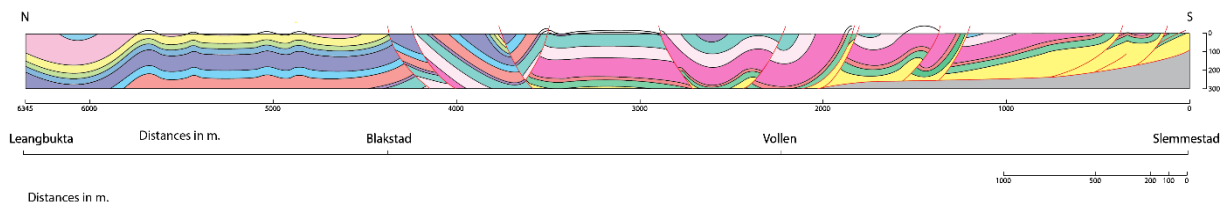


Figure 3.12: Section along the shore from Asker to Slemmestad, south of Oslo. Note the variation of structural style from north to south and the similarities with Figure 3.11 from Smit et al. (2013). This figure is presented in more detail in Figure from Weekenstroo (2015).

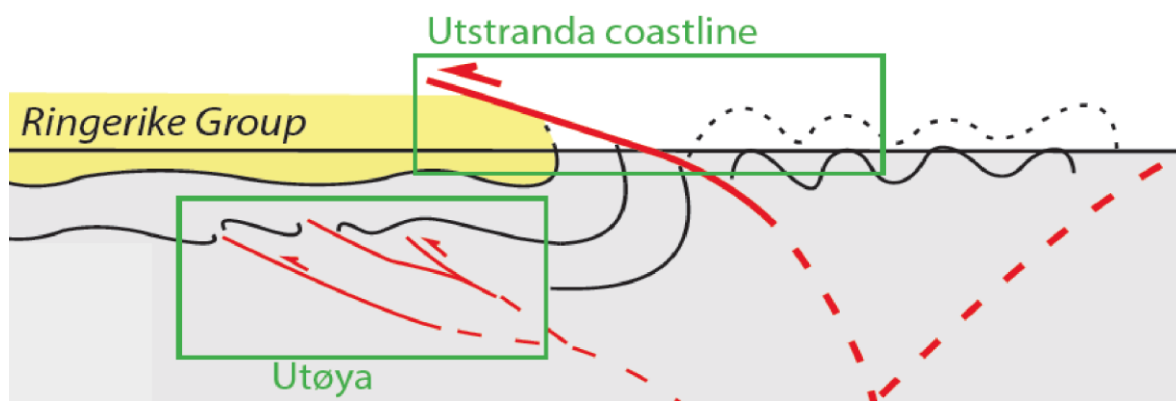


Figure 3.13: Part of the of regional model from Vlieg (2015) detailing the complex geometries observed at the Ustranda pop-up where faults and underlying strata are transported through the Ringerike Sandstone Formation. From: Vlieg (2015).

4 Discussion

Spanning a roughly 230 km long and 70 km wide region from Mjøsa in the north to Eikeren in the south (Figure 1.5), the Paleozoic sequence of the Oslo Region is exposed mainly in the downfaulted Permian graben on the shoulders of the Permian volcanics. The aim of this study is to better grasp the structural development of the Oslo Region with a focus on the Hønefoss area (Figure 1.5). Previous work from the region provides a good geological background on which to build this thesis (Bockelie and Nystuen, 1985; Bruton et al., 2010; Harper and Owen, 1983; Morley, 1986, 1986; 1987; Nystuen, 1983, 1981).

This discussion has several focus points; after a synthesis of field observations from the Hønefoss area the first aim is to provide a better description of the deformation style of the basal plane and speculate on its geometry in areas where it is not exposed. Using the model presented by Bruton et al. (2010) as a basis, a regional model for the Oslo region will be constructed. It will span the area from northern Ringerike to Asker and will utilise previously published and unpublished relevant literature. By utilizing the insights gained from the field, modelling and the construction of the regional model, possible reasons for lateral and vertical variations in shortening and structural style will be discussed. Combining all these points, the regional tectonic model from Bruton et al. (2010) will be updated to incorporate new insights.

Using field observations from the Hønefoss area, a general tectonic setting of the area can be constructed (Figure 4.1). It is the opinion of the author that the structural style of the Osen-Røa thrust continues in a generally similar sense southward as the exposure of the Osen-Røa thrust near Slemmestad has the same structural style (Weekenstroo, 2015). The Klækken fault, a second order thrust after the definitions of Morley (1986a), splays from the Osen-Røa thrust and cuts up section through the entire stratigraphy. The Ringkollen road section is located in the upper part of the stratigraphy and it displays the geometry of a footwall syncline associated with the Klækken fault (Figure 2.21). Although this section itself is rather strongly deformed with e.g. box folds, small scale folding and faulting, several authors noted that there is an abrupt drop in strain when crossing the Klækken fault from north to south (Figure 4.9) and attributed this strain shadow to the large horizontal displacement of the Klækken fault (~5 km) (Harper and Owen, 1983; Morley, 1987a, 1983; Størmer, 1934). The small road section, south of Klækken, is very local and contains a small outcrop of the very competent Huk Formation very close to the known position of the Klækken fault (Figure 2.18 & Figure 2.19). Based on these observations it is concluded that these Ordovician sediments were thrust up along the Klækken fault (Figure 4.1) into their present day position. The high mechanical strength of

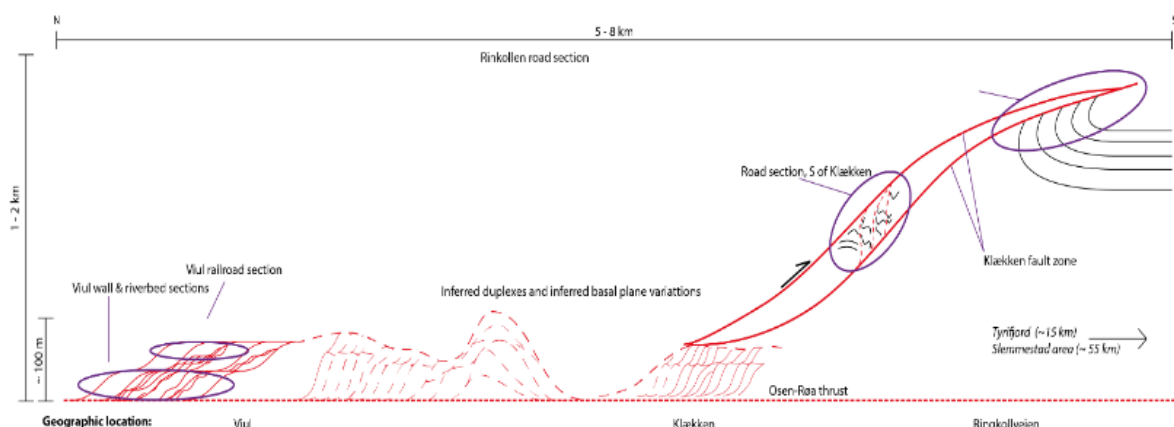


Figure 4.1: General structural outline of the Hønefoss area. Note the relative positions of the various field localities as discussed in chapter 2 as well as the basement involvement between Viul and Klækken. The size of the Osen-Røa and Klækken thrusts and the variation in basal thrust thickness are not to scale. Geographic locations are displayed at the bottom and correspond to Figure 2.1.

the Huk Limestone preserved the section from the destructive effects of the fault as well as subsequent erosion after it was exposed on the surface.

4.1 The Osen-Røa thrust

The Osen-Røa thrust underlies the entire Oslo Region and is the basal decollement (or soul thrust) over which the entire nappe slides. Near Slemmestad in the south (Morley, 1986b) observed numerous sub-horizontal slip planes in the Alum Shale Formation, all with small offsets. The surface of these slip planes were characterised by a smooth porcellaneous or shiny graphitic surfaces, as is also observed at Viul. A strong sub-bedding parallel cleavage has been strongly folded and on mesoscopic scale asymmetrical and disharmonic folds with wavelengths up to 4 m and amplitudes up to 3 m have been observed in the Alum Shale (Morley, 1986b). Concerning the mesoscopic folds, (Morley, 1986b) speculated that they were the result of flow in the Alum Shale from high stress synclines to areas with a lower stress regimes. These mesoscopic folds have been observed at Viul (Figure 2.7), however conclusive evidence for flow from high to low stress regimes have not been observed. Folded bedding parallel cleavage observed by Morley (1986b) in Slemmestad has also been observed at Viul in all three exposures (Figure 2.12). This structural style of intense folding, (folded) cleavage and numerous sub-horizontal slip planes indicate that the Osen-Røa thrust zone was a brittle, well constrained, high-strain shear zone. Previous authors determined that the maximum metamorphic grade present in the Oslo Region is of sub-greenschist facies (Bruton et al., 2010; Morley, 1994; Nystuen, 1981) and it is therefore likely that fluid content played a significant role in the deformation of the Osen-Røa thrust. Such a high fluid content resulted in low friction on the slip planes and thus created a favourable regime for layer parallel slip. This would also explain the potential decoupling with the overlying strata and why the Osen-Røa thrust could act as a basal decollement for the Oslo Region.

At the Viul locality (Bruton et al., 2010) also studied field relationships of the Osen-Røa thrust in Alum Shale. They observed that the entire package is characterised by variable styles and intensities of deformation and that the style of deformation is very similar to the deformation style at Slemmestad (Bruton et al., 2010). Most notably, the authors observed four large horses of roughly 100 m wide separated by decimetre-wide thrust faults at intervals of 10-15 meters with internal chaotic structures, sheared lenses of shale and limestone and disharmonic folding on cm scale. Inside these large fault zones second order, dm-scale duplexes and folds are observed as well as intense folding with upright axial planes (Bruton et al., 2010).

The observations made on the Alum Shale in this study are in agreement with earlier observations from both (Bruton et al., 2010; Morley, 1986b), but this study provides a much more detailed picture of the Osen-Røa thrust than previously available. Detailed sections resulted in better constraints on the size of the duplexes both in section and in map view (Figure 2.2, Figure 2.3 and Figure 2.10). The

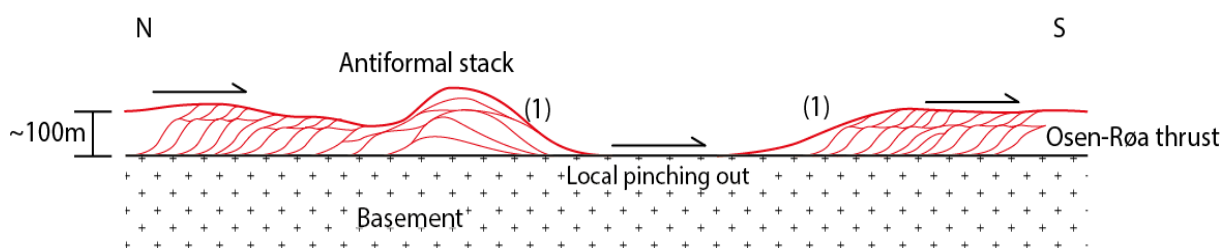


Figure 4.2: Schematic representation of the authors impression of the geometry of pinched out Alum Shale in the Osen-Røa thrust as a result of local friction variations. On the sides of the pinched out shale, indicated in the figure with (1), the presence of mesoscopic folds as observed at Viul is likely.

subdivision in different classes based on the hypothesised formation mechanics of different duplexes also provide more insight into the formation and behaviour of the Osen-Røa thrust (Figure 2.4). As the entire nappe glides over the Osen-Røa thrust and the deformation styles of the Alum Shale at Viul and Slemmestad are so similar, it seems logical to postulate that, at least in the southern Oslo Region (Ringerike and Oslo districts), the Alum Shale has a single dominant deformation style. More towards the north near lake Mjøsa, basement involvement changes the structural style (Nystuen, 1983). Lack of Alum Shale exposure between Viul and Slemmestad complicates the testing of this hypothesis of lateral constant structural style.

Although the Osen-Røa thrust is consequently positioned in the Alum Shale in the southern half of the Oslo Region and the deformation style of the shale is uniform, it is very unlikely that the basal thrust system as a whole maintains the same thickness over such a large distance. The observed exception near the Klækken fault where the Osen-Røa thrust cuts down into the basement seems to support this statement (F. Bockelie *pers. comm.*, 2007 via Bruton et al., 2010) (Figure 4.1). It is therefore postulated that while the deformation style of the Alum Shale is similar throughout the region, the basal decollement as a whole shows a variable geometry due to basement involvement as a result of thickness variations and local (secondary) pinching out of the shales (Figure 4.2). The sub-Cambrian peneplain on which the Alum Shale was deposited, has topographic variations in the order of 4-50 m (Gabrielsen et al., 2015). The formation itself has, in Norway, a thicknesses of between 30-100 m. The Alum Shale is very widespread throughout northern Europe and was deposited in an epicontinental sea. The widespread nature and the thickness of the Alum Shale in Norway, the sub-Cambrian peneplain topographic variations and the observed basement involvement near lake Mjøsa (Nystuen, 1983) and Klækken (Bruton et al., 2010) result in the statement that the pinching out of the Alum Shale is a secondary process due to tectonic activity. The pinching out can be related to local variations in basal friction due to local pore fluid pressure or content variations leading to 'rough gliding' (Nystuen, 1983) on slip planes or possibly a very high concentration of the limestone concretions present in the Alum Shale.

In the north, near Lillehammer and Mjøsa (the Sparagmite region), the Osen-Røa thrust is situated in/ on Cambrian shales and phyllites with some involvement of basement or Cambrian quartzites as it involves lower units (Nystuen, 1983). The friction along the basal decollement is locally increased by 'rough gliding' (Nystuen, 1983), resulting in basement involvement visible imbricated sheets of basement and pre-Alum Shale sediments adhering to the hangingwall of the Osen – Røa thrust as well as imbrication slicing into the footwall (Nystuen, 1983). This provides further support for the hypothesis that, although the deformation style of the Alum Shale is relatively similar throughout the (southern) half of the Oslo Region, local involvement of the basement is definitely a very likely, although difficult to prove, hypothesis. Due to the relatively close proximity of lake Mjøsa to the Oslo and Ringerike districts, basement involvement in the southern Oslo Region is a distinct possibility.

These variations in the thickness and geometry basal plane also means that strain rate was likely not constant through time and space as faults are created during tectonic activity and heal during tectonic inactivity. Combining this intermittent deformation with the strongly deformed nature of these shales, it is speculated that strain-hardening processes could take place. Such processes would further influence the localisation of subsequent deformation. It should be stressed that this is merely speculation and further rock mechanical testing and microstructural analysis of the Alum Shale is required. The hypothesis of Morley (1986b) on the origin of the mesoscopic m scale folds at Slemmestad, which are also observed at Viul in this study (Figure 2.7), supports this 'pinching out' hypothesis. However, it should be noted that there is no conclusive evidence to support this hypothesis

and it is, at this time, therefore speculation. Basement involvement due to pinching out of the Alum Shale would dramatically increase the basal friction, but it seems likely that the mechanically weak strata of the Lower-Ordovician will accommodate the resulting strain, possibly by layer parallel slip.

4.2 Regional synthesis

By combining data gathered in this study with data gathered by several other recent studies (Vlieg, 2015; Weekenstroo, 2015) as well as data from previously published literature (Bockelie and Nystuen, 1985; Bruton et al., 2010; Harper and Owen, 1983; Morley, 1994, 1987a, 1986a, 1986b), a structural synthesis for the southern part of the Oslo region is made (Figure 4.8). By incorporating new data, the regional tectonic model proposed by (Bruton et al., 2010) is also updated. The synthesis concerns districts of Ringerike and Oslo (Figure 1.7), districts more to the north are not incorporated as it was beyond the scope of this study. In order to be able to provide a sound synthesis of the Oslo Region it is important to analyse the available structural data so that interpretations of certain structures and styles can be placed in an appropriate context.

4.2.1 Structural data

Structural data gathered in the Hønefoss area is summarised in Figure 4.3. Overall the data shows a clear subdivision between the different locations, with the structural data from Viul (Figure 4.3a) and the small road section (Figure 4.3b) being oriented in a N-S manner. The fold axes for Viul are oriented E-W with a cluster in the east. The Ringkollen section shows a more NE-SW orientation of the bedding as the poles to the bedding planes are oriented NNW-SSE and the fold axes cluster in the NE with a shallow dip (Figure 4.3c). When comparing the data collected in this study (Figure 4.3) with the data from (Harper and Owen, 1983) (Figure 4.4), it is observed that the orientation is very similar to the orientation of the strata in the Ringkollen section with a rough NNW-SSE orientation of the poles to the bedding planes (Figure 4.3c). Structural data from (Morley, 1987b, 1986b) is summarised by (Morley, 1987a) (Figure 4.5). The orientations of these bedding and thrust planes and the fold hinges are very similar to the orientations of these features measured in the Hønefoss area and to the data from Harper and Owen (1983). Recent structural data gathered by in the Tyrifjord area (Figure 4.7a) (Vlieg, 2015) shows an almost exact match with the previously discussed data with a NNE-SSW trending band of poles to bedding planes and an average fold axis dipping shallowly towards the NE.

Structural data from the Alum Shale Formation near Slemmestad has a similar orientation as well (Figure 4.7b) (Weekenstroo, 2015). All structural data is thus very consistent with an ENE-WSW bedding orientation and a NE shallow dipping fold axis. The only deviations from these orientations are observed at Viul and the small road section (compare Figure 4.3a-b with Figure 4.3c, Figure 4.4, Figure 4.5 and Figure 4.7). Bedding and fold axis orientations at Viul and the small road section are oriented E-W. Both locations are north of, or inside of the Klækken fault. Figure 4.4 also displays structural data from north of the Klækken fault, however this data is oriented similarly to the rest of the region (ENE-WSW striking bedding orientation). The age of the measured strata in Figure 4.4 is Ordovician to Silurian strata (Harper and Owen, 1983) whereas the age of the strata measured at Viul and in the Klækken fault is Cambrian (Viul) to Lower-Ordovician (small road section), thus explaining the discrepancy. There is thus a difference in orientation and transport direction between the Alum Shales of the Osen-Røa thrust and the overlying Ordovician strata. This is likely due to some sort of local strain partitioning which is transferred up along the Klækken fault as the bedding planes in the

small road section are also oriented E-W. As a result of this it becomes clear that the Klækken fault has accommodated slip in an oblique manner.

This proposed strain partitioning is not only observed locally north of the Klækken fault (Figure 4.3 a-b). In Hadeland, north of the Hønefoss area (Figure 1.7), there is a similar difference in orientation between the Lower-Ordovician strata, which is strongly deformed by imbrication, and the Middle-Ordovician to Silurian strata (Figure 4.6). It is interesting to note that while in the Hønefoss area the lower units (Cambrium strata) had an anomalous orientation with respect to the rest of the region (Figure 4.3), in Hadeland the upper units (Middle-Ordovician to Silurian strata) are oriented in a N-S manner (Figure 4.6). When going south near Slemmestad the entire stratigraphy is deformed as a single unit (Morley, 1987a) and the data from the Osen-Røa thrust displays orientations similar to the observed elsewhere in the region (Figure 4.7b). It thus seems that there are multiple levels on which this strain partitioning takes place. This is in support of the previously proposed hypothesis that there are (ductile) layer parallel detachments accommodating the difference in structural styles.

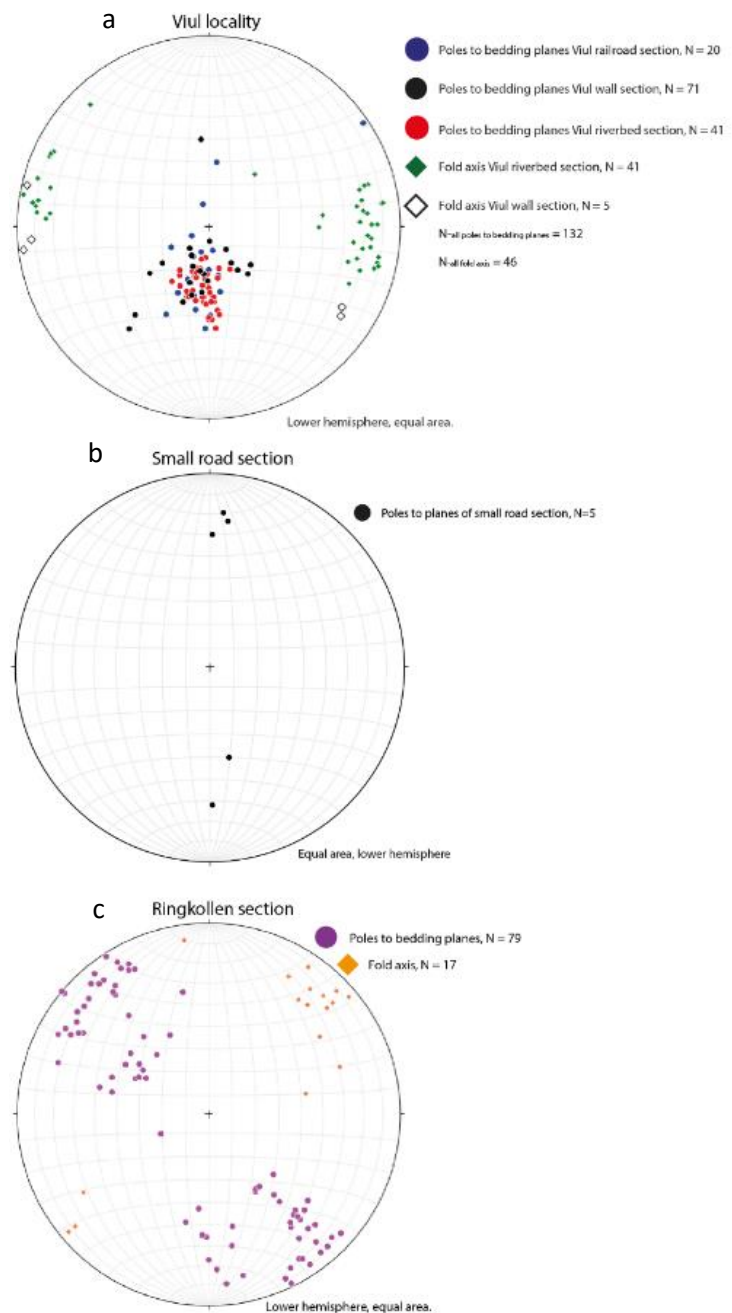


Figure 4.3: Summary of all structural data gathered in the Hønefoss area.

All structural data from the Oslo Region shows a remarkable consistency in its orientation for both (poles to) the bedding planes as well as the fold axes. Based on the data gathered in this study and by Vlieg (2015) and Weekenstroo (2015) it is determined that the average fold axis for the Oslo Region is roughly $060/10^\circ$. Structural data from both (ductile) folding as well as brittle faulting have the same orientation and the data scatter is very small (see also: Vlieg, 2015). This leads to the conclusion that the entire Oslo Region was deformed by a single progressive deformation event which is related to the Scandian deformation phase of the Caledonian Orogeny (Nystuen, 1981; Roberts, 2003) and it has not been overprinted by subsequent events. Orientation of the poles to bedding planes in combination with field observations at multiple locations by multiple other authors (e.g. Bruton et al., 2010; Morley, 1987a, 1986b; Vlieg, 2015; Weekenstroo, 2015) indicate a regional SSE directed transport direction with some variations on a smaller scale. This very consistent orientation of the observed structures is in contrast to recent studies in the Oslo Region, which indicated abnormal variations in the main transport direction (Bruton et al., 2010). It seems that these variations are restricted to local structural intervals.

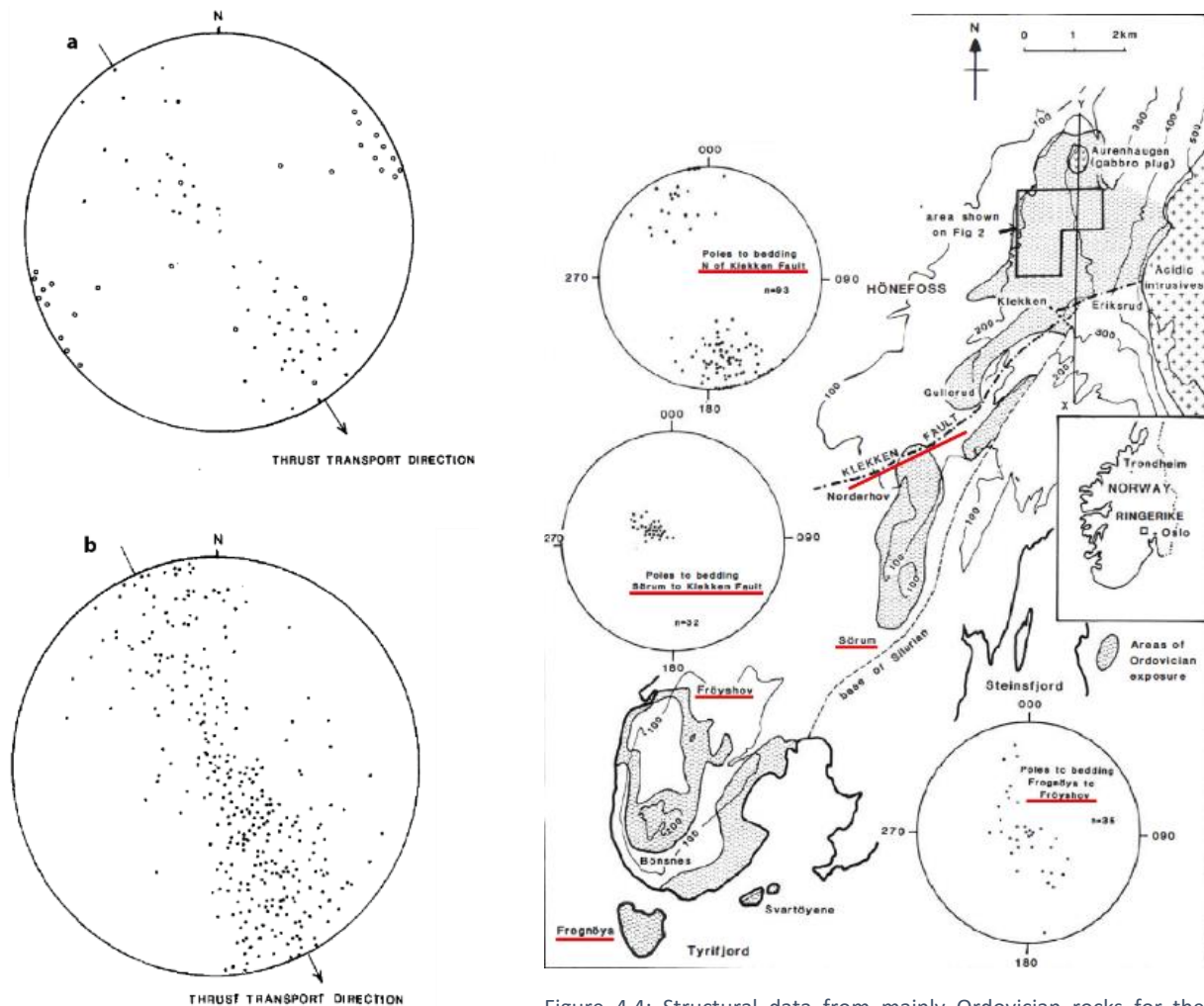


Figure 4.5: Structural data from the north Hadeland and Asker areas. a) Poles to minor thrust planes (dots) and minor fold hinge lineations (circles). b) Poles to bedding planes for the north Hadeland and Asker areas (N=326). Figure from Morley (1987a).

Figure 4.4: Structural data from mainly Ordovician rocks for the northern Ringerike area. Dots represent poles to bedding planes. Figure from Harpen and Owen (1983).

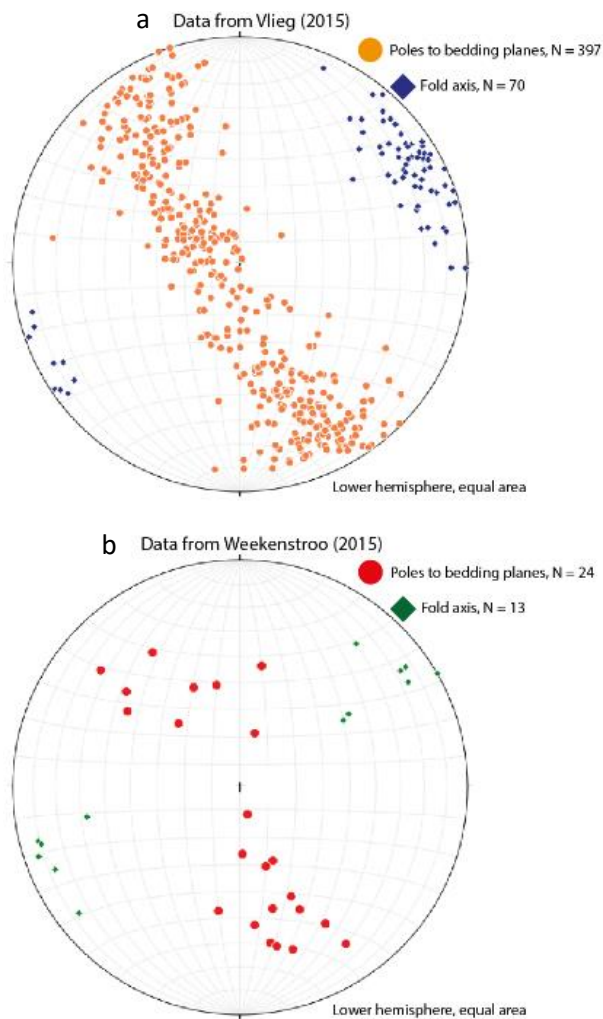


Figure 4.7: a) Structural data for the Tyrifjord area (Vlieg, 2015). b) Structural data for the Alum Shale Formation in Slemmestad (Weekenstroo, 2015).

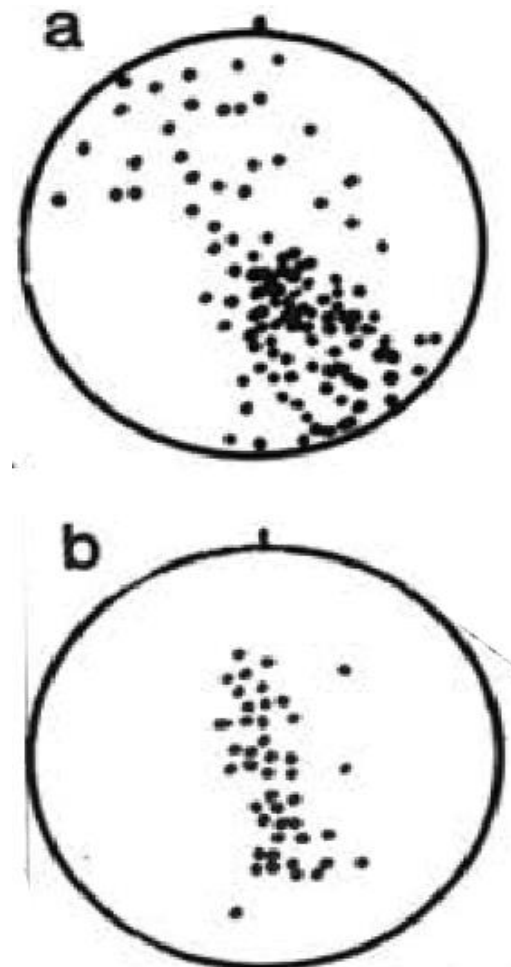


Figure 4.6: Structural data from Hadeland, north of the H. a) Poles to bedding planes for Lower-Ordovician strata. b) Poles to bedding planes in Middle-Ordovician – Silurian strata. Data from Morley (1987b).

4.2.2 Regional tectonic model

Analysis of the structural data shows that the entire region is deformed during a single progressive deformation event responsible for both the (ductile) folding and the brittle deformation. The difference in structural style is thus not the result of multiple deformation events. This makes it possible to construct a regional tectonic model for the Oslo Region (Figure 4.8). In the north, the exposed Lower to Middle-Ordovician strata is imbricated in numerous thrust slices with a southward transport direction (Morley, 1987a; Nystuen, 1983).

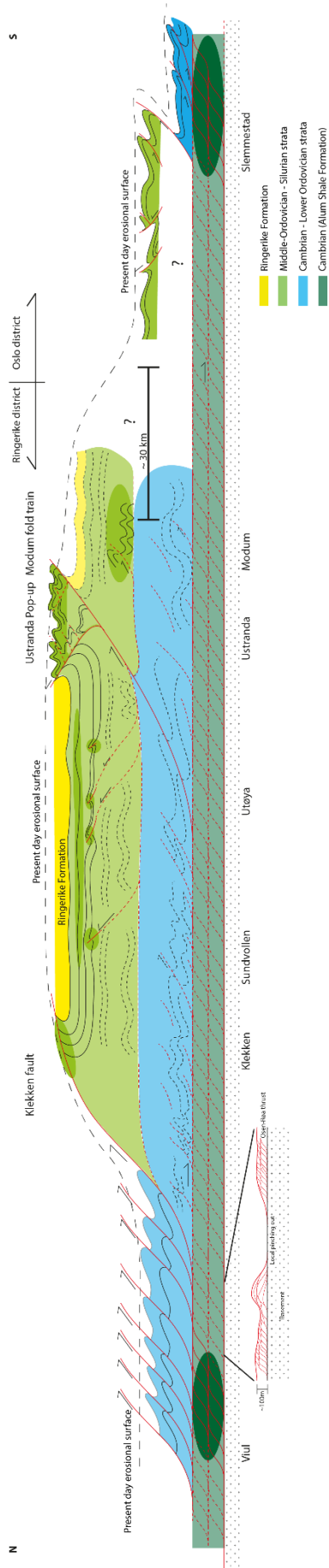


Figure 4.8: Schematic regional tectonic model for the southern Oslo Region (Oslo and Ringerike districts). The model is not to scale in both the horizontal and vertical directions. Structures are also schematic as they display the general structural style of deformation and are as such an oversimplification of reality. The position of the layer parallel detachment is schematic and its positions emphasises the separation of the two different structural styles based on stratigraphy. Lightly shaded areas and shaded lines represent inferred areas whilst darker shaded areas represent observed outcrops. The main data sets used in the construction of this tectonic model, besides this study, are from Weekenstroom (2015), Vlieg (2015) and Verdonk (2015). The insert just south of the Viul location represents a postulated geometry which could be responsible for the formation of the Klækken fault. For more information the reader is referred to the text. In the south near Slommestad, it is unclear how the Middle-Ordovician to Silurian strata is related to the Cambrian Osen – Røa thrust as the Lower-Middle Ordovician strata is not exposed. Geographic locations are displayed below the Osen – Røa basal decollement.

This strongly imbricated deformation style changes abruptly when crossing the Klækken fault (Figure 4.8) where Middle-Ordovician to Silurian strata is deformed by fold trains with large wavelength/amplitude ratio's (Vlieg, 2015). The Ringerike Formation which is present above the Steinsfjord Formation in the Ringkollen section (Larsen et al., 2001; Zwaan and Larsen, 2003) is also part of this structure. The footwall syncline in the Ringerike Formation is on the same stratigraphic level as the oppositely oriented footwall syncline at the Ustranda section of Vlieg (2015) (Figure 4.8) and the resulting geometry is dubbed a 'Viking ship geometry'. It is interpreted that the Ringerike Formation will continue in a similar manner south of the Ustranda pop-up.

Below the 'Viking ship' of the Ringerike Formation, buckle fold trains are present with the best examples being exposed on the Tyrifjord islands (Vlieg, 2015). When going west along these islands, which is equivalent to going down dip due to the general NE dip of the regional fold axis, the structural styles changes from broad buckle fold trains to more intensely folded strata (Vlieg, 2015). Also there are numerous backthrusts present, most of which die out below the Ringerike Formation. Recent studies have shown that this backthrusting in the Oslo region is more common and widespread than previously thought (Bruton et al, 2010; Kleven, 2010; Hjelsheth, 2010; Vlieg, 2015). These studies are mostly conducted in the Tyrifjord area, where exposed strata are mainly of Middle-Ordovician to Silurian in age. On the western side of the Tyrifjord in the Lower-Silurian strata, the Modum road section displays a fold train with higher strain intensities (Vlieg, 2015). Based on these observations it is concluded that although the structural style is markedly different between the upper and lower parts of the stratigraphy, inside these stratigraphic intervals the structural style is also variable. The Middle-Ordovician to Silurian strata displays a fold dominated structural style which increases in intensity when going down stratigraphy from the Ringerike Formation. Deformation is thus subdued below the competent Ringerike Formation. Late stage backthrusting deformed the folded, mainly Silurian, strata on the east coast of the Tyrifjord (Kleven, 2010; Vlieg, 2015).

The Lower-Ordovician strata positioned directly above the Osen-Røa basal decollement are not exposed in the Tyrifjord area and the structural style of this area depicted in Figure 4.8 are inferred based on the observations made in this as well as other studies (Verdonk, 2015; Vlieg, 2015; Weekenstroo, 2015). When going farther south there is a decrease in overall thickness and the entire stratigraphy is deformed as a single unit (Morley, 1987a). The nature of this decrease in thickness and how the discrepancies in shortening for the upper and lower parts of the stratigraphy are accommodated is unknown. The section by (Weekenstroo, 2015) in the Asker-Slemmestad area shows that the Middle-Ordovician to Silurian strata are mainly deformed by folding, a structural style similar to that observed in the Tyrifjord area by Vlieg (2015). The southernmost part of the section where lower part of the stratigraphy, including the Osen-Røa basal decollement, is exposed has a deformation style characterised by forethrusts. In between the folded style in the north and the forward directed imbricated style in the south a regime where backthrusting is common is observed.

The different structural styles of the Cambrian to Lower-Ordovician and the Middle-Ordovician to Silurian result in a shortening discrepancy between these two parts of the stratigraphy (**Fout! Verwijzingsbron niet gevonden.**) (Morley, 1987a). To accommodate for this, previous authors have postulated the existence of a layer parallel detachment somewhere in the Middle-Ordovician strata (Bruton et al., 2010; Morley, 1987a, 1986a), but due to poor exposure of Middle-Ordovician strata in the Tyrifjord area little evidence for such a structure exists. However, as this shortening discrepancy has to be accommodated, this study agrees with the existing hypothesis of a layer parallel detachment located somewhere in the Middle-Ordovician strata. This detachment is thought to have behaved in a ductile manner, taking up the missing shortening outlined in **Fout! Verwijzingsbron niet gevonden.**

originally presented in Morley (1986a). In Figure 4.8 this detachment is located exactly at the boundary between the Lower and Middle-Ordovician strata. It is stressed that this location is schematic. There is no evidence to support that the postulated detachment is indeed located exactly at this stratigraphic boundary. The main reason for its position in Figure 4.8 is that it is illustrative as the descriptions and observations of the different structural styles are generally separated in terms of Cambrian to Middle-Ordovician and Middle-Ordovician to Silurian strata.

4.3 Influence of lateral and stratigraphical shortening variations on structural style

Whilst lateral changes in the style of the Osen-Røa thrust itself are somewhat enigmatic, the observed variation in deformation styles when going up stratigraphy are very clear in the Oslo Region. The main contrasts in style of deformation when cutting through the entire stratigraphy are visible at the Klækken fault and at the Ustranda pop-up described by (Vlieg, 2015). The Klækken fault splays from the Osen-Røa thrust sheet and cuts through the entire stratigraphy where it creates a footwall syncline. Horizontal displacement along the Klækken fault was at least 5 km (Harper and Owen, 1983; Morley, 1987a; Størmer, 1934) and a significant drop in strain is observed across the fault (Figure 4.9). This leads to the interpretation that the Klækken fault is a ramp flat ramp style structure which is consistent with thin skinned fold and thrust belts.

The deformation cutting through the Ringerike Formation at Ustranda has a very different style in the form a pop-up geometry (Vlieg, 2015). Fore- and backthrusts cut the Ringerike Formation and inside the pop-up there are very complex deformation patterns e.g. fault propagation folds, small faults, and folding on different scale. The controlling parameters responsible for these two markedly different styles remain unclear. By utilizing the results obtained in the analogue modelling study the effect of initial mechanical stratigraphy on deformation styles at various levels is discussed. These newly obtained insights will then be utilized to discuss the influence of lateral and stratigraphical shortening variations on the structural style.

4.3.1 Insights from analogue models

Although, naturally, all models display strain transfer up section, in order to draw conclusion concerning the large faults at Klækken and Ustranda, the strain transfer up section in the model has to be distinct. For instance, fault no. 8 in model 1 (Figure 3.4) transfers some strain through the entire sand pack. However, it is a small offset fault and therefore a natural analogue would likely not be able to penetrate the Ringerike Sandstone Formation but die out below. Basal inclination does stimulate more pronounced deformation in the form of an out of sequence pop-up (Figure 3.5), the offset on the faults is still relatively small. Introducing lateral heterogeneity in model 3 results in the formation of a significant ramp flat ramp thrust (Figure 3.6), which does appear similar in nature to the Klækken fault. There is significant displacement up along this fault and it cuts and doubles the entire stratigraphy above the weak viscoelastic layer. More forward, the second weak layer is activated as a layer parallel detachment as evidenced by structures on both sides (Figure 3.6).

When comparing model 3 (Figure 3.6) with models 1 & 2 (Figure 3.4 & Figure 3.5), it seems that the lateral heterogeneity forced deformation up section. Both in models and in nature spacing of faults is controlled by the interplay between the shear stress along the decollement and the yield stress of the overlying strata. The introduced heterogeneity forced the creation of a fault at the tip of the viscoelastic layer as the stress required to transfer strain farther forward was much more as the stress required to create a new ramp flat ramp fold. The multiple backthrusts nucleating from this ramp flat

ram thrust (no. 8 in Figure 3.6) are interpreted as a step geometry. Stratigraphy above the weak viscoelastic layer was doubled due to the large displacement on fault no. 8. This created a strong sand pack and strain was thus transferred farther forward towards the second viscoelastic layer which transferred it to its end, resulting in pop-up no. 11 (Figure 3.6).

As lateral heterogeneity seems to play a role in the strain transfer up section, model 4 contained a second (too) strong viscoelastic layer in the foreland in order to localise deformation even further. A pop-up is created at the end of the weak viscoelastic layer, which is expected and similar to the evolution of model 4 (Figure 3.7), but the strong viscoelastic layer prohibits the deformation to propagate towards the end of the model (Figure 3.7). Subsequent shortening is accommodated in an out of sequence pop-up (faults no. 5 & 5r in Figure 3.7). The pop-up below the weak viscoelastic layer is interesting, but unfortunately the timing cannot be adequately constrained.

The addition of the second weak viscoelastic layer above the lower one in model 5 resulted in a more complex geometry as the layer was activated and the nucleation point of several thrusts and backthrusts (Figure 3.8). Significant out of sequence deformation resulted in a widely deformed zone and the final result does not resemble the typical single vergent thrust wedge geometry of the previous four models (Figure 3.8). It seems that the large lateral competence contrast resulted in the out of sequence deformation and complex final geometry of the model in section. As the foreland is basically to competent, shortening is accommodated by creating new out of sequence faults and/or reactivating older faults. Although the setup of model 5 might not be realistic, it represents a possible end member of a spectrum displaying the results if the lateral differences in mechanical strength increase.

From the modelling results discussed above it seems that the style of deformation up section is controlled by lateral competence differences. If there are no lateral changes in the mechanical strength, intensity of deformation up section is not very pronounced (e.g. fault no. 8 in Figure 3.4). The introduction of basal inclination does introduce some limited lateral heterogeneity with a linear gradient. In this setup strain transfer up section is more pronounced in the form of two pop-ups, one of which is out of sequence (Figure 3.6). When introducing a more distinct lateral competence difference in model 3, the intensity of deformation up section is much more pronounced and a distinctive style develops. Fault no. 8 in model 3 (Figure 3.6) starts as a pop-up but evolves in a ramp flat ramp type structure. Although strain transfer up section in model 4 is not very significant, this is most likely due to the low amount of bulk shortening applied to the model. When comparing the results of model 4 with model 5 (Figure 3.7 vs Figure 3.8), which has been subjected to 3% more bulk shortening (Figure 3.3), it becomes clear that strain is transported mainly up section and towards the backstop (hinterland) as it cannot propagate farther forward. Thus a pop-up style of strain transfers up section develops in models 4 & 5.

These observations lead to the conclusion that the style of strain transfer up section is controlled by lateral competence differences. In order for faults to be of sufficient magnitude to be able to cut through the Ringerike Sandstone Formation a significant lateral competence difference has to be present. The style will then in general be that of a pop-up evolving in a foreland directed ramp flat ramp system (Figure 3.6) similar to the style observed at the Klækken fault. If the lateral competence difference is larger deformation cannot propagate freely forward and thus a pop-up with a complex internal geometry will develop (Figure 3.8) similar to the style observed at the Ustranda section (Vlieg, 2015). In the models the exaggerated strength of the strong viscoelastic material in models 4 & 5 is an 'obstacle' for the propagation of strain towards the foreland. In nature the competence differences are unlikely to be of the same relative magnitude. However, differences in competence can be the result of (slight) thickness or compositional variations and thus mechanical properties of the strata.

This is possibly due to processes like lateral or vertical variation of sedimentary facies, sedimentation rate or a similar process. In nature, these (slight) local variations can add up to form a larger zone where the contrast between two areas becomes significant. If this is the case, the stronger zone will act as a sort of obstacle, and deform slightly or not at all.

While 'obstacles' as discussed above can definitely occur in nature in the form of local thickness variation or facies changes other mechanisms can also lead a similar outcome. For instance, if there is differential shortening along a single large fault it can lock and deformation will have to be accommodated by strain transfer up and/or backwards. A similar situation will develop if the ramp becomes too steep. Shear and normal stress orientations will resolve on the fault plane in such a manner that the fault will lock. Such processes are closely linked with friction on the fault plane(s). If the fluid content in a fault decreases the friction on the fault will increase resulting in a locked fault (Sibson, 2012, 1977).

All mechanisms mentioned above can result in a strain localisation and transfer up section, either in a ramp flat ramp system or in the case of significant resistance to propagation, a pop-up and/or out of sequence deformation up section. The exact reason for a fault to lock and strain to transfer up section depends on the complex interplay between stress orientation, fluid content and pressure, fault plane orientation and rheological parameters of the strata. A full discussion on these mechanisms is outside the scope of this thesis and the reader is referred to e.g. (Sibson, 2012, 1985, 1977) and references therein for more details.

4.3.2 Variable deformation style in the field

The abrupt drop in shortening (Figure 4.9b) and change in deformation style across the Klækken fault has been well established, with imbrication of Cambrian to Lower-Ordovician strata in the north and buckle folding of Middle-Ordovician to Silurian strata in the south. (Morley, 1987a) postulated that the imbrication north of the Klækken fault is possibly explained by high pore-fluid pressures leading to numerous thrusts attempting to ramp up through the strata creating the observed imbricate stack. Certain is that the Klækken fault had a large displacement and is thus responsible for the creation of a significant tectonic overburden. This could, according to (Morley, 1987a), inhibit deformation in the footwall as the vertical component of deformation would have to be larger than the tectonic overburden stress. Therefore, it seems logical that deformation was transferred further south where the overburden stress was lower. However, no explanation was provided for the initial formation of the Klækken fault. It has been previously postulated that pore-fluid pressure may have played a significant role in the deformation style of the lower half of the stratigraphy of the Oslo Region. F. Bockelie (2007) *pers. comm* via Bruton et al. (2010), indicated that near the Klækken fault the Osen-Røa thrust cuts down into the basement. Combining these observations with possible due to pore fluid variations, basal friction would locally increase, effectively resulting in an obstacle, which would influence the rapid closely spaced style of imbrication in the Lower-Ordovician strata. The resulting competence contrast could lead to nucleation of a thrust fault with relatively high friction after which the Klækken fault would form and cut up through the entire stratigraphy. Although this hypothesis is certainly plausible, it is unlikely that the formation of the Klækken fault was caused only by increased basal friction on the basal plane. Local pore fluid pressure variations and lateral facies changes are likely to have an influence as well.

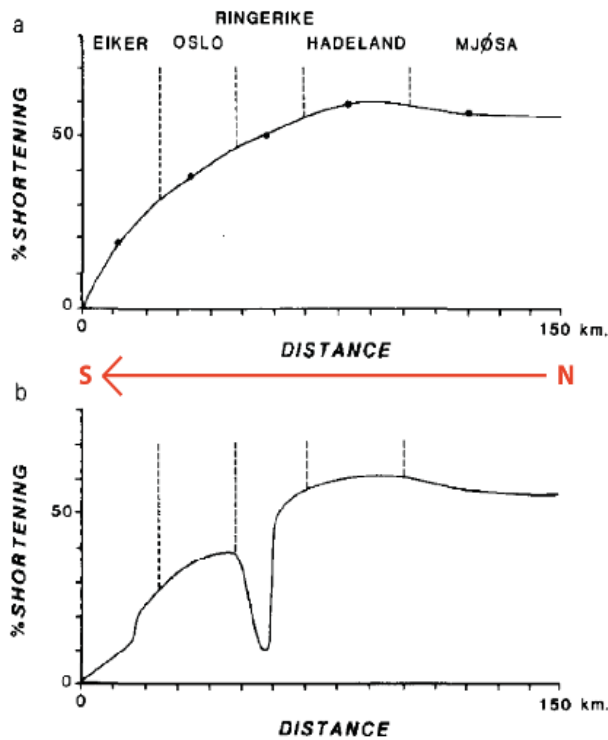


Figure 4.9: Relationship between distance from north to south and internal displacement inside the deformed strata. a) Average amount of shortening for each district. b) Estimated variations in shortening by folds and minor thrusts in each district. It illustrates the abrupt drop in shortening across the Klækken fault. Figure is from Morley (1987a).

The pop-up at Ustranda as described by (Vlieg, 2015) has a distinctly different deformation style when compared to the Klækken fault. It is interpreted that the pop-up geometry of a fore and backthrust does not continue down towards the basal decollement but the backthrust nucleates somewhat higher up in the stratigraphy from a 2nd order thrust fault (Vlieg, 2015). The relatively small width and the change in the mechanical properties of the stratigraphy in the Oslo Region also make it improbable that the pop-up would have nucleated in the basal plane. It is speculated that the Ustranda pop-up was initiated in a similar manner to the Klækken fault. However subsequent lateral differences higher up in the stratigraphy, such as local thickness variations, changing fluid content or steepening of the ramp possibly resulted in an out of sequence backthrust formation. Another possibility is that the large backthrust formed as a break thrust inside a folded competent lithology as described by (Morley, 1994). Although

these hypotheses are very interesting and the results of the modelling do shed light on this outstanding issue, the exact mechanism(s) responsible for the localisation of these large faults remain enigmatic. The differences in structural style present in the whole stratigraphy resulted in a discrepancy between shortening percentages of the upper (Middle-Ordovician to Silurian) and lower (Cambrian to Lower-Ordovician) parts of the stratigraphy (Table 4.1).

Shortening percentages for the entire Oslo region and parts of the Sparagmite region have been previously published (Morley, 1986a). Besides the lateral changes in shortening observed mainly in the Cambrian to Lower-Ordovician strata when going from north to south (Table 4.1); Figure 4.9) variation in shortening percentages when going up in stratigraphy are also observed (Morley, 1987a, 1986b) Table 4.1). In order to accommodate the difference in shortening due to the different structural styles, the existence of a bedding parallel has been postulated (Bruton et al., 2010; Morley, 1987a) and incorporated in the previously presented model (Figure 4.8). Unfortunately, the exact mechanism by which this is accommodated remains enigmatic in field observations. But based on observations made regarding the different structural styles and the work of (Morley, 1986a), such a detachment would

District	Eiker	Oslo	N. Ringerike	Hadeland	S. Mjøsa	N. Mjøsa
Average shortening						
Lower Ordovician	15%	37%	50%	60%	55%	60%
Lower Silurian	15%	27%	?	29%	28%	(Ecocambrian)

have be situated in one, or possibly more, of the weaker shale layers of the Middle-Ordovician. These could, when containing high fluid percentages, behave very similar to the Alum Shales of the Osen-Røa basal decollement.

Morley (1987a) did note that, in theory, it is possible to accommodate all the missing shortening by strong deformation in overlying Silurian strata which is now eroded. Such a theory cannot be disproven but the coincidence required for such a series of events is deemed unlikely, both by Morley and the present author as the exposed Silurian sequence is consistently shortened less than the underlying Cambrian to Lower-Ordovician strata.

Smit et al. (2003) conducted experiments on brittle-ductile thrust wedges to investigate the role of relative strength variations between ductile and brittle layers (brittle-ductile coupling). They compared their results to foreland thrust wedges with salt as a basal decollement. Result from their study indicate that for high brittle-ductile (BD) coupling (difference in yield strength between brittle and ductile material is small), thrust vergence is mostly towards the foreland. Low BD coupling (difference in yield strength between brittle and ductile material is large) results in mostly hinterland directed thrusting whereas intermediate BD coupling creates an oscillating pattern of foreland and hinterland directed thrusting.

Recent studies have shown that backthrusting in the Oslo Region is much more widespread than previously thought (Hjelseth, 2010; Kleven, 2010; Vlieg, 2015). These studies have been mainly conducted in the Tyrifjord area where exposed strata is mainly of Middle-Ordovician to Silurian in age (Hjelseth, 2010; Kleven, 2010; Vlieg, 2015). This large amount of backthrusting present in the Tyrifjord area of the Oslo region could thus be related to the brittle ductile coupling between the overlying strata and the proposed (ductile) layer parallel detachment from (Bruton et al., 2010; Morley, 1987a). Kleven (2010) and Hjelsheth (2010) both stated that backthrusting was an important process in the deformation of the Silurian sections and was most likely simultaneous with the main thrusting event as a secondary process. Combining these field observations with the study from Smit et al. (2003) it is postulated that the brittle ductile coupling between the detachment and the overlying strata was intermediate to low in the Ringerike district. Such a situation could explain the prevalence of backthrusting in the area as well as accounting for the discrepancies in shortening percentages between the lower and upper parts of the stratigraphy.

In section 4.3.1 it is stated that the large amount of backthrust created in the analogue models is not realistic and a mechanism for their formation is presented (Figure 3.10). It should be noted that the mechanism responsible for these unrealistic structures in the models can be, to some extent, realistic in a slightly different manner. The Middle-Ordovician to Silurian strata contains significantly more competent beds and is as such thus more homogeneous and competent. This means that, although not present on scales as seen in the models (figure model major backthrusting), backthrusting in the Tyrifjord area can also be the result of competent strata not being able to accommodate folding which results in the formation of backthrusts to accommodate the movement along a ramp fault. Besides these hypotheses to explain the backthrusts observed in the Oslo Region, the hypotheses presented at the beginning of section 4.3 on the possible mechanisms responsible for the difference in structural styles between the Klækken fault and the Ustranda pop-up can also be applied on a smaller scale to the prevalent backthrusting. Backthrusting could also be a result of local lateral competence difference due to either lateral thickness or facies variations, variations in fluid content or over steepening of a forward directed thrust resulting in subsequent out of sequence backthrusting. Whether the prevalence of backthrusting in the Tyrifjord area is due to low to intermediate BD coupling with a (ductile) layer parallel detachment or due to one of the other hypothesis presented remains

unclear and is a topic for further research. However, it is stated that backthrusting is likely not solely the result of one of these hypothesised mechanisms but that backthrusts formed due to a combination of these processes.

Weekenstroo (2015) also observed changing structural styles in the more southern areas near the city of Oslo only here the changes are mostly lateral instead of stratigraphical. When comparing the section from Weekenstroo (2015) near Slemmestad (Figure 3.12) to the results from Smit et al. (2003) (Figure 3.11), the similarities are evident. In the Oslo-Asker area the strata is not decoupled halfway by a layer parallel detachment, but is deformed as a single unit (Morley, 1987a, 1986b), but it is possible that below these Middle-Ordovician to Silurian strata the layer parallel detachment postulated for the Tyrifjord area is still present and dies out somewhere along this section. The Alum Shale Formation, which acts as the basal decollement, was activated as a ductile layer over which the wedge glided. Variations in the structural style from predominantly folding in the north to a more imbricated style with both back and forethrust in the middle part of the section, to a foreland directed thrust dominated style at the southern end of the section (Figure 3.12) indicate some variation in brittle-ductile coupling. This is explained by the overall thinning of the stratigraphy towards the south. The ratio of brittle to (assumed) ductile strata increases, which explains the changing deformation styles. As the brittle thickness decreases it becomes weaker, assuming the ductile strength of the Osen-Røa thrust remains the same, brittle-ductile coupling will increase. Going south along the profile from (Weekenstroo, 2015) (Figure 3.12), the BD coupling increases to intermediate levels as evidenced by the formation of backthrusts (Smit et al., 2003). The BD coupling is deemed intermediate as backthrusting is not the dominant style of thrusting. When going towards the most southern part of the section deformation is purely directed towards the foreland leading to the conclusion that this most southern part has very high BD coupling.

4.4 Updating the existing tectonic model

Using the data gathered in this study as well as by (Vlieg, 2015; Weekenstroo, 2015), it is possible to update the regional model from (Bruton et al., 2010) (Figure 1.6). Whilst this model presents a good recent synthesis of the Oslo Region based on modern literature, the author feels that there is potential for improvement. The structural style of the basal plane, especially in the north, is very schematic. In the discussion above the hypothesis is presented that the basal plane contains thickness and mesoscopic style variations and that the Osen-Røa thrust sometimes involves basement material (Figure 4.10) (F. Bockelie, Pers. comm., 2007 via Bruton et al., 2010). If basement is involved in thrusting along the Osen-Røa thrust this would have major implications for basal friction. It could then potentially be related to the localisation of deformation and nucleation of large thrust zones such as the Klækken thrust. Currently the model from Bruton et al. (2010) does not incorporate a bedding parallel detachment nor does it have a clear distinction between the imbricated style of the Cambrian to Lower-Ordovician strata and the more folded style of the Middle-Ordovician to Silurian strata. The main improvement suggested for the model of (Bruton et al., 2010) is thus the incorporation of such a bedding parallel detachment. Its location should be somewhere in the Ordovician stratigraphy as displayed in Figure 4.8 and previously postulated by several authors (Bruton et al., 2010; Morley, 1987a). Although no direct evidence for this detachment is observed in the field by any author, it is stated and deemed likely by several studies (Bruton et al., 2010; Morley, 1987a). Based on these arguments the present author feels that the bedding parallel detachment should be incorporated in the regional tectonic model (Figure 4.10). This bedding parallel detachment would also allow for a clearer representation of the difference in structural styles observed between the Cambrian to Lower-

Ordovician and the Middle-Ordovician to Silurian strata. The contrast between these two deformation styles is one of the principal observations of the Oslo Region and is closely tied to the aforementioned layer parallel detachment, discrepancies in shortening observed between the lower and upper parts of the stratigraphy and possibly also to the prevalent backthrusting in the Tyrifjord area. Finally, the backthrusting could also be better represented in the strata below the Ringerike Formation as the present author feels that this prevalent feature is underrepresented in the current model of Bruton et al. (2010).

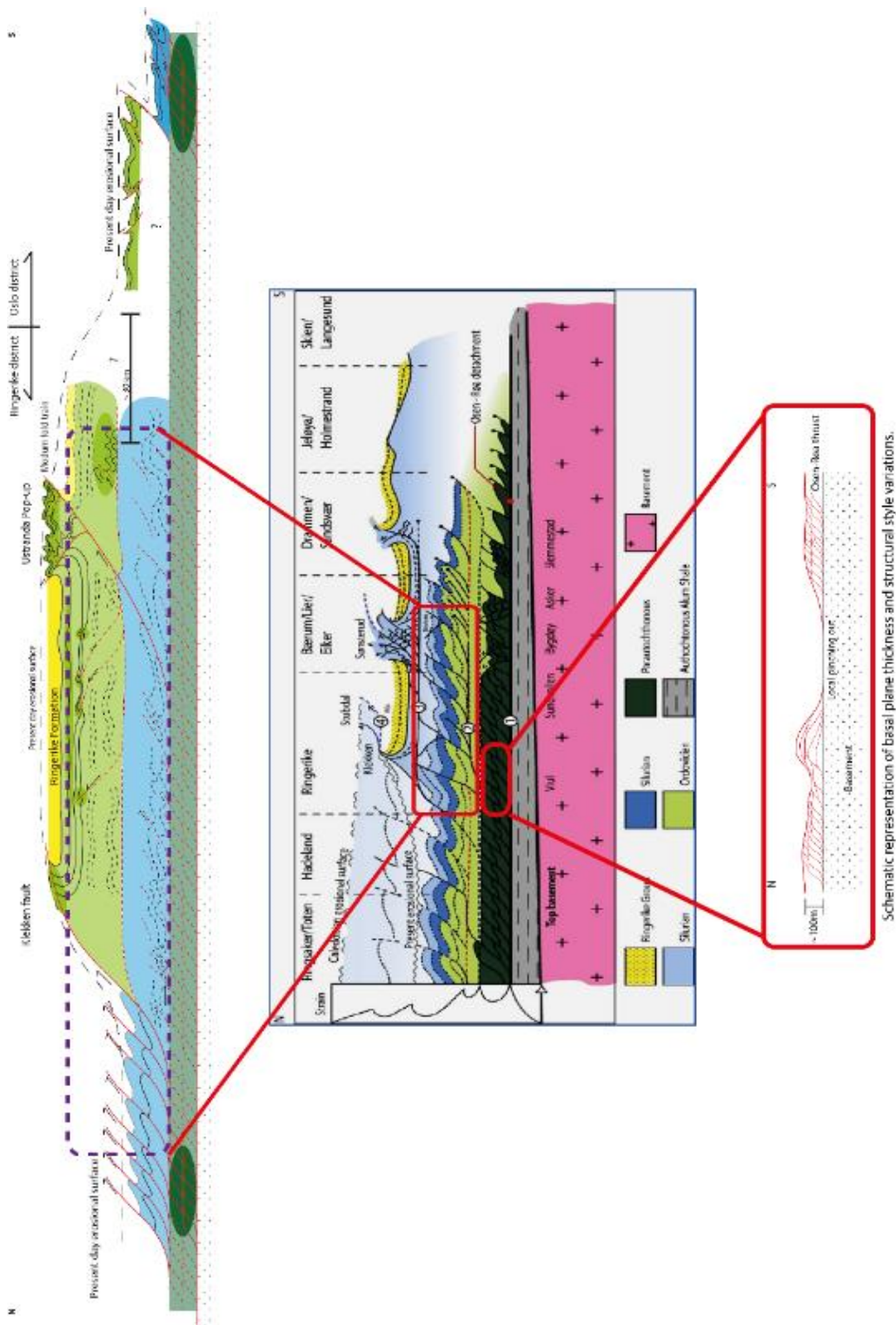


Figure 4.10: Comparison of regional tectonic model of this study with the model for Bruton et al. (2010). Note the absence of a layer parallel detachment in Ordovician strata and the lack of significant basal plane variations in the northern parts of the model from Bruton et al. (2010). For more details, the reader is referred to the main text.

5 Conclusions

The main goal of this study was to update the regional tectonic model of the Oslo Region which was recently published by Bruton et al. (2010). Based on the data and interpretations presented above several conclusions can be drawn and the regional model from Bruton et al. (2010) can be updated.

- Transport direction in the Oslo Region is more homogeneous than previously thought. This is supported by the homogeneous orientation of the large amount of structural data gathered throughout the Oslo Region by various authors. The small variations in transport direction are related to specific structural intervals. This is supported by the fact that the deviating transport direction in the Hønefoss area is constricted to the Osen-Røa basal thrust and the splaying Klækken thrust. And by the fact that in Hadeland the N-S deviating orientation is observed in the Middle-Ordovician to Silurian strata whilst the Cambrian to Lower-Ordovician strata are oriented parallel to the regional trend (Morley, 1987b).
- The layer parallel detachments postulated by Morley (1987a) are interpreted to be present somewhere in the Ordovician strata of the Oslo Region. These detachments accommodate differences in structural style, stratigraphical shortening discrepancies between the Cambrian to Lower-Ordovician and the Middle-Ordovician to Silurian strata, local strain partitioning (resulting in small deviations from the regional transport direction). Speculating that they could act as ductile detachments with low brittle-ductile coupling with the overlying Silurian strata could explain the prevalent backthrusting in the Silurian strata of the Tyrifjord area.
- Based on results from the analogue modelling study it is concluded that deformation style of the large faults cutting through the entire stratigraphy, including the very competent Ringerike Sandstone Formation, are controlled by (effective) lateral competence contrasts. Intermediate competence contrasts result in a ramp flat ramp structure whereas high competence contrasts result pop-up structures with a strongly deformed interior. Possible involvement of basement in the Osen-Røa thrust sheet can result in a local effective obstacle possibly related to the nucleation of these large faults. These lateral competence contrasts are also a possible backthrust formation mechanism.
- Crystalline basement might be involved in the Osen-Røa thrust of the Oslo Region, as evidenced by basement involvement in the Mjøsa district (Morley, 1987b) and near the Klækken fault (F. Bockelie *pers. comm.*, 2007 via Bruton et al., 2010). This leads to the tentative conclusion that involvement of basement is a realistic scenario.
- The regional tectonic model of Bruton et al. (2010) was updated (Figure 4.10) to include the postulated layer parallel detachment. By incorporating this detachment, the model can better represent the contrast in structural style between the imbricated Cambrian to Lower-Ordovician strata and the folded Middle-Ordovician to Silurian strata. Including a schematic representation of basement involvement in the Osen-Røa thrust sheet also increases the detail in the regional model. Finally, the prevalent backthrusting in the Silurian strata could also be better represented in the strata below the Ringerike Formation.

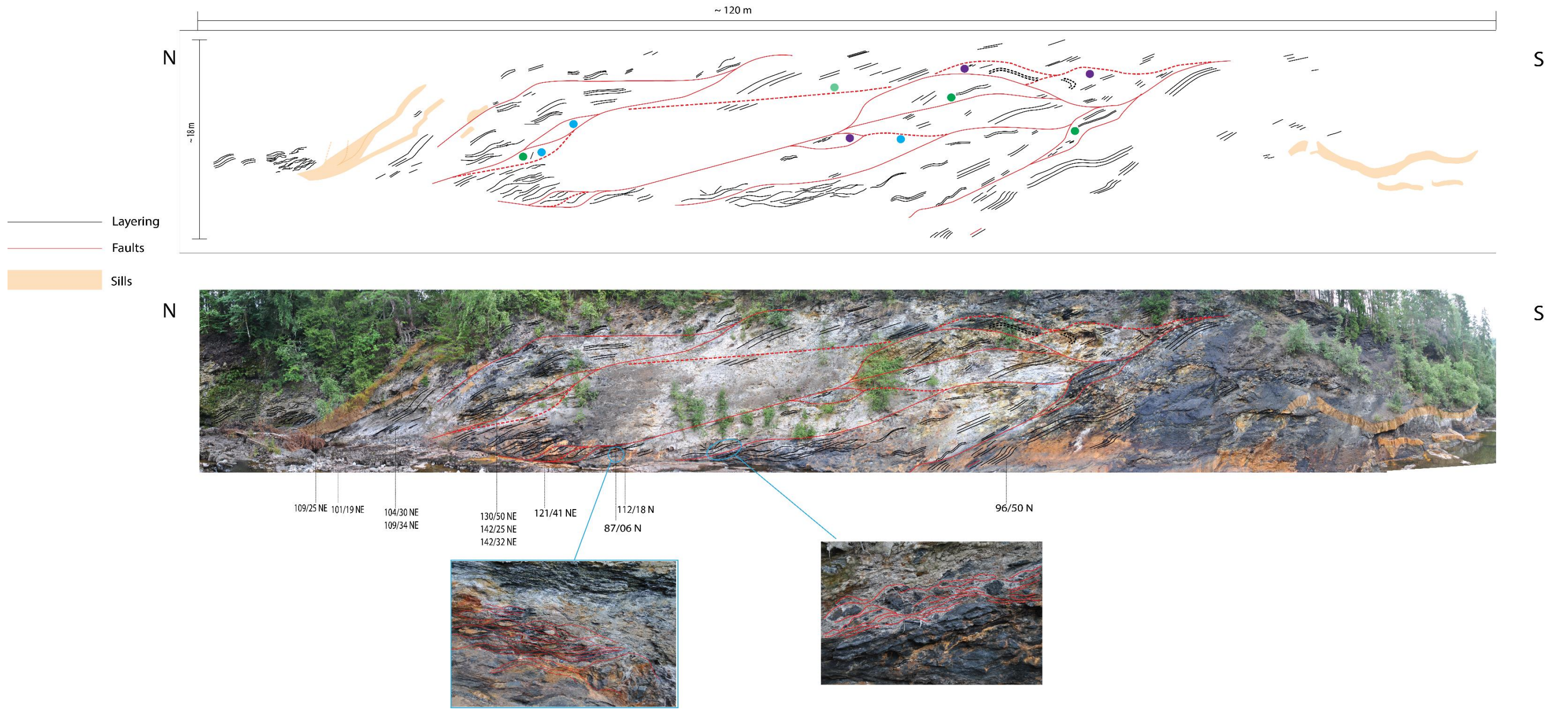
6 References

- Allmendinger, R.W., Cardozo, N.C., Fisher, D., 2013. *Structural Geology Algorithms: Vectors & Tensors*. Cambridge University Press, Cambridge, England.
- Bockelie, J.F., Nystuen, J.P., 1985. The southeastern part of the Scandinavian Caledonides. *The Caledonide Orogen - Scandinavia and Related Areas* 69–88.
- Brøgger, W.C., 1882. . Die Silurischen Etagen 2 and 3 im Kristianiagebiet und auf Eker, ihre Gliederung, Fossilien, Schichtenstörungen und Contactmetamorphosen.
- Brun, J.-P., 2002. *Deformation of the continental lithosphere: Insights from brittle-ductile models*, Geological Society Special Publication.
- Bruton, D.L., Gabrielsen, R.H., Larsen, B.T., 2010. The caledonides of the Oslo region, Norway - Stratigraphy and structural elements. *Norsk Geologisk Tidsskrift* 90, 93–121.
- Cardozo, N., Allmendinger, R.W., 2013. Spherical projections with OSXStereonet. *Computers & Geosciences* 51, 193–205. doi:10.1016/j.cageo.2012.07.021
- Chapple, W.M., 1978. Mechanics of thin-skinned fold-and-thrust belts. *Bulletin of the Geological Society of America* 89, 1189–1198. doi:10.1130/0016-7606(1978)89<1189:MOTFB>2.0.CO;2
- Cocks, L.R.M., Torsvik, T.H., 2005. Baltica from the late Precambrian to mid-Palaeozoic times: The gain and loss of a terrane's identity. *Earth-Science Reviews* 72, 39–66. doi:10.1016/j.earscirev.2005.04.001
- Cocks, L.R.M., Torsvik, T.H., 2002. Earth geography form 500 to 400 million years ago: A faunal and palaeomagnetic review. *Journal of the Geological Society* 159, 631–644. doi:10.1144/0016-764901-118
- Fossen, H., Dallmeyer, R.D., 1998. ⁴⁰Ar/³⁹Ar muscovite dates from the nappe region of southwestern Norway: Dating extensional deformation in the Scandinavian Caledonides. *Tectonophysics* 285, 119–133.
- Fossen, H., Dunlap, W.J., 1998. Timing and kinematics of Caledonian thrusting and extensional collapse, southern Norway: evidence from ⁴⁰Ar/³⁹Ar thermochronology. *Journal of Structural Geology* 20, 765–781. doi:10.1016/S0191-8141(98)00007-8
- Gabrielsen, R.H., Nystuen, J.P., Jarsve, E.M., Lundmark, A.M., 2015. The Sub-Cambrian Peneplain in southern Norway: Its geological significance and its implications for post-Caledonian faulting, uplift and denudation. *Journal of the Geological Society* 172, 777–791. doi:10.1144/jgs2014-154
- Gee, D.G., 1975. A tectonic model for the central part of the Scandinavian Caledonides. *American Journal of Science* 275, 468–515.
- Gradstein, F.M., Ogg, J.G., Smith, A.G. (Eds.), 2004. *A Geologic Timescale 2004*. Cambridge University Press, Cambridge, England.
- Graveleau, F., Malavieille, J., Dominguez, S., 2012. Experimental modelling of orogenic wedges: A review. *Tectonophysics* 538-540, 1–66. doi:10.1016/j.tecto.2012.01.027
- Harper, D. a. T., Owen, A.W., 1983. The structure of the Ordovician rocks of the Ringerike district: evidence of a thrust system within the Oslo region. *Norsk geologisk tidsskrift* 63, 111–115.
- Hjelseth, E. vd F., 2010. Caledonian structuring of teh Silurian succession at Sundvollen, Ringerike, southern Norway. (Msc. Thesis). University of Oslo, Oslo.
- Hossack, J.R., Cooper, M.A., 1986. Collision tectonics in the Scandinavian Caledonides. *Geological Society, London, Special Publications* 19, 285–304. doi:10.1144/GSL.SP.1986.019.01.16
- Hubbert, M.K., 1937. Theory of scale models as applied to the study of geologic structures. *Bulletin of the Geological Society of America* 48, 1459–1520. doi:10.1130/GSAB-48-1459

- Kjerulf, T., 1879. . Udsigt over Det Sydlige Norges Geologi 262.
- Kjerulf, T., 1873. . II.Sparagmittfjeldet.Universitetsprogram for andet Halvaar 85.
- Kjerulf, T., 1855. . Das Christiania-Silurbecken chemisch-geognostisch untersucht.
- Kleven, M.K.H., 2010. Caledonian (Silurian) out-of-sequence thrusting at Sønsterud, Holsfjorden, Ringerike. (Msc. Thesis). University of Oslo, Oslo.
- Larsen, B.T., Olaussen, S., 2005. The Oslo Region. A study in classical Palaeozoic geology. Field guide NGF's Centennial field trip. Norsk Geologisk Forening.
- Larsen, B.T., Olaussen, S., Sundvoll, B., Heeremans, M., 2008. The permo-carboniferous Oslo rift through six stages and 65 million years. Episodes 31, 52–58.
- Larsen, B.T., Sæther, E., Lutro, O., 2001. Oppkuven. Berggrunnskart; Oppkuven; 18152; Plottekart. Foreløpig utgave.
- Morley, C.K., 1994. Fold-generated imbricates: examples from the Caledonides of Southern Norway. Journal of Structural Geology 16, 619–631. doi:10.1016/0191-8141(94)90114-7
- Morley, C.K., 1987a. Lateral and vertical changes of deformation style in the osen-røa thrust sheet, Oslo region. Journal of Structural Geology 9, 331–343. doi:10.1016/0191-8141(87)90056-3
- Morley, C.K., 1987b. The structural geology of north Hadeland. NGT 67, 39–49.
- Morley, C.K., 1986a. The Caledonian thrust front and palinspastic restorations in the southern Norwegian Caledonides. J. Struct. Geol. 8, 753–765.
- Morley, C.K., 1986b. Vertical strain variations in the Osen-Røa thrust sheet, North-western Oslo Fjord, Norway. Journal of Structural Geology 8, 621–632. doi:10.1016/0191-8141(86)90068-4
- Morley, C.K., 1983. The structural geology of the Southern Norwegian Caledonides in the Oslo Graben and Sparagmite Region. (Phd Thesis). City of London Polytechnic, London.
- Murchison, R.I., 1847. . Anskuelse over Classificationen av de geologiske Lag i Overgangsformationen ved Christiania.
- Nystuen, J.P., 1983. Nappe and thrust structures in the Sparagmite region, southern Norway. Norges Geologiske Undersøkelse 380, 67–83.
- Nystuen, J.P., 1981. The Late Precambrian "sparagmites" of southern Norway: a major Caledonian allochthon - the Osen-Røa nappe complex. American Journal of Science 281, 69–94.
- Oftedahl, C., 1943. Oerskyvninger i den norsk fjellkjede. Naturen Oslo, 243–250.
- Owen, A.W., Bruton, D.L., Bockelie, J.F., 1990. The Ordovician successions of the Oslo region, Norway. Norges Geologiske Undersøkelse.
- Ramberg, H., 1981. Gravity, deformation, and the earth's crust: In theory, experiments, and geological application. Academic press.
- Ramberg, I.B., Bockelie, J.F., 1981. Geology and tectonics around Oslo. In: Larsen, B. T. (ed.): Guide to excursions B-4, 4th International Conference on Basement Tectonics, Oslo August 1981. Nytt fra Oslofeltgruppen 7, 81–100.
- Roberts, D., 2003. The Scandinavian Caledonides: Event chronology, palaeogeographic settings and likely modern analogues. Tectonophysics 365, 283–299. doi:10.1016/S0040-1951(03)00026-X
- Roberts, D., Gee, D., 1985. An introduction to the structure of the Scandinavian Caledonides., in: The Caledonide Orogen-Scandinavia and Related Areas. pp. 55–68.

- Sibson, R.H., 2012. Reverse fault rupturing: Competition between non-optimal and optimal fault orientations, Geological Society Special Publication.
- Sibson, R.H., 1985. A note on fault reactivation. *Journal of Structural Geology* 7, 751–754. doi:10.1016/0191-8141(85)90150-6
- Sibson, R.H., 1977. Fault rocks and fault mechanisms. *Journal of the Geological Society* v. 133:191–213.
- Smit, J.H.W., Brun, J.P., Sokoutis, D., 2003. Deformation of brittle-ductile thrust wedges in experiments and nature. *Journal of Geophysical Research B: Solid Earth* 108, ETG 9–1 – ETG 9–18.
- Spjeldnaes, N., 1957. The middle Ordovician of the Oslo Region, Norway. *Norsk Geologisk Tidsskrift* 37, 1–214.
- Størmer, L., 1934. Spor av Kledonisk overskyvning i Nordmarka. *NGT* 14, 115–128.
- Sundvoll, B., Larsen, B.T., 1994. Architecture and early evolution of the Oslo Rift. *Tectonophysics* 240, 173–189. doi:10.1016/0040-1951(94)90271-2
- Sundvoll, B., Larsen, B.T., Wandaas, B., 1992. Early magmatic phase in the Oslo Rift and its related stress regime. *Tectonophysics* 208, 37–54. doi:10.1016/0040-1951(92)90335-4
- Terry, M.P., Robinson, P., Hamilton, M.A., Jercinovic, M.J., 2000. Monazite geochronology of UHP and HP metamorphism, deformation, and exhumation Nordøyane, Western Gneiss Region, Norway. *American Mineralogist* 85, 1651–1664.
- Torsvik, T.H., Rehnström, E.F., 2001. Cambrian palaeomagnetic data from Baltica: Implications for true polar wander and Cambrian palaeogeography. *Journal of the Geological Society* 158, 321–330. doi:10.1144/jgs.158.2.321
- Verdonk, A., 2015. In Prep (Msc. Thesis). Universiteit Utrecht, Utrecht.
- Vlieg, M., 2015. Structural style and evolution of the Caledonian foreland, northeast Tyrifjorden, Oslo Region (Msc. Thesis). Universiteit Utrecht, Utrecht.
- Weekenstroom, M., 2015. The Caledonian structural development of the Oslo foreland basin. A field and analogue study into the mechanics of back thrusting in the Oslo-Asker section. (Msc. Thesis). Universiteit Utrecht, Utrecht.
- Weijermars, R., 1997. *Principles of Rock Mechanics*. Alboran Science Publishing.
- Worsley, D., Aarhus, N., Bassett, M.G., Howe, M.P.A., Mork, A., Olausson, S., 1983. The Silurian succession of the Oslo region. *Norges Geologiske Undersøkelse* 384, 1–57.
- Zwaan, K.B., Larsen, B.T., 2003. Hønefoss. Bergrunnskart; Hønefoss; 18153; foreløpig utgave plottkart.

Appendix A: Blow up of figure 2.2



Appendix B - Strength profiles for analogue models

